

**WL-TR-95-4084**

## **IMPROVED HYBRID BEARINGS**

**MICHAEL M. DEZZANI  
PHILIP K. PEARSON**

**THE TORRINGTON COMPANY  
ADVANCED TECHNOLOGY CENTER  
59 FIELD STREET, PO BOX 1008  
TORRINGTON CT 06790-1008**

**DECEMBER 1994**

**FINAL REPORT FOR 04/01/92 -- 11/01/94**



**Approved for public release; distribution unlimited**

**19961209 011**

**MATERIALS DIRECTORATE  
WRIGHT LABORATORY  
AIR FORCE MATERIEL COMMAND  
WRIGHT-PATTERSON AIR FORCE BASE, OH 45433-7734**

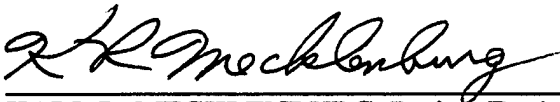
**DTIC QUALITY INSPECTED 3**

## NOTICE

When government drawings, specifications, or other data are used for any purpose other than in connection with a definitely related government procurement operation, the United States Government thereby incurs no responsibility nor any obligation whatsoever; and the fact that the government may have formulated, furnished, or in any way supplied the said drawings, specifications, or other data, is not to be regarded by implication or otherwise as in any manner licensing the holder or any other person or corporation, or conveying any rights or permission to manufacture, use, or sell any patented invention that may in any way be related thereto.

This report is releasable to the National Technical Information Service (NTIS). At NTIS, it will be available to the general public, including foreign nations.

This technical report has been reviewed and is approved for publication.

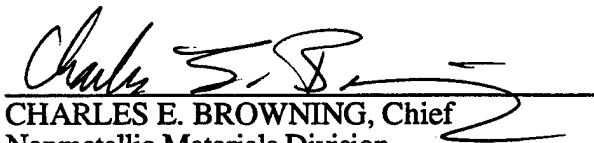


KARL R. MECKLENBURG, Project Engineer  
Nonstructural Materials Branch  
Nonmetallic Materials Division



KENT J. EISENTRAUT, Chief  
Nonstructural Materials Branch  
Nonmetallic Materials Division

FOR THE COMMANDER



CHARLES E. BROWNING, Chief  
Nonmetallic Materials Division  
Materials Directorate

If your address has changed, if you wish to be removed from our mailing list, or if the addressee is no longer employed by your organization, please notify WL/MLBT, Bldg 654, 2941 P Street, Suite 1, Wright-Patterson AFB OH 45433-7750 to help maintain a current mailing list.

Copies of this report should not be returned unless return is required by security considerations, contractual obligations, or notice on a specific document.

# REPORT DOCUMENTATION PAGE

Form Approved  
OMB No. 0704-0188

Public reporting burden for this collection of information is estimated to average 1 hour per response, including the time for reviewing instructions, searching existing data sources, gathering and maintaining the data needed, and completing and reviewing the collection of information. Send comments regarding this burden estimate or any other aspect of this collection of information, including suggestions for reducing this burden, to Washington Headquarters Services, Directorate for Information Operations and Reports, 1215 Jefferson Davis Highway, Suite 1204, Arlington, VA 22202-4302, and to the Office of Management and Budget, Paperwork Reduction Project (0704-0188), Washington, DC 20503.

1. AGENCY USE ONLY (Leave blank)		2. REPORT DATE DEC 1994	3. REPORT TYPE AND DATES COVERED FINAL 04/01/92--11/01/94	
4. TITLE AND SUBTITLE IMPROVED HYBRID BEARINGS			5. FUNDING NUMBERS C F33615-92-C-5922 PE 62712 PR 8355 TA 00 WU 05	
6. AUTHOR(S) MICHAEL M. DEZZANI PHILLIP K. PEARSON				
7. PERFORMING ORGANIZATION NAME(S) AND ADDRESS(ES) THE TORRINGTON COMPANY ADVANCED TECHNOLOGY CENTER 59 FIELD STREET TORRINGTON CT 06790			8. PERFORMING ORGANIZATION REPORT NUMBER  30940	
9. SPONSORING/MONITORING AGENCY NAME(S) AND ADDRESS(ES) MATERIALS DIRECTORATE WRIGHT LABORATORY AIR FORCE MATERIEL COMMAND WRIGHT PATTERSON AFB OH 45433-7734 POC: K. R. Mecklenburg, WL/MLBT, 937-255-2465			10. SPONSORING/MONITORING AGENCY REPORT NUMBER  WL-TR-95-4084	
11. SUPPLEMENTARY NOTES				
12a. DISTRIBUTION/AVAILABILITY STATEMENT  APPROVED FOR PUBLIC RELEASE; DISTRIBUTION IS UNLIMITED.			12b. DISTRIBUTION CODE	
13. ABSTRACT (Maximum 200 words) Nitriding technology was determined to significantly enhance the performance of steel bearing rings coupled with silicon nitride balls. NBD-200 silicon nitride was tested in two different sized full scale bearing tests with two nitrided steel ring materials, M50 and M50 NiL. Test bearing sizes were 35mm bore radial bearings and 40mm bore thrust bearings. Results showed truly superior rolling contact fatigue life under conditions of thin film and contaminated lubricant. Satisfactory results were obtained under full film lubrication conditions. Several silicon nitride ball failures were experienced during the high stress, full film lubrication test which prevented demonstrating truly superior fatigue life over all steel bearings under full film lubrication conditions. Three-ball-on-rod rolling contact fatigue tests were used to screen nitriding cycles before bearing raceways were nitrided.				
14. SUBJECT TERMS  hybrid bearings, nitriding, silicon nitride, NBD-200, fatigue testing, 35mm bore bearings, 40mm bore bearings, Weibull analysis			15. NUMBER OF PAGES 118	
			16. PRICE CODE	
17. SECURITY CLASSIFICATION OF REPORT UNCLASSIFIED	18. SECURITY CLASSIFICATION OF THIS PAGE UNCLASSIFIED	19. SECURITY CLASSIFICATION OF ABSTRACT UNCLASSIFIED	20. LIMITATION OF ABSTRACT  SAR	

## Table of Contents

	Page
1.0 SUMMARY .....	1
1.1 Purpose .....	1
1.2 Selection of Processes and Materials .....	1
1.3 Evaluation of Nitriding Procedures .....	2
1.4 Rolling Contact Fatigue Rig Tests .....	2
1.5 Bearing Manufacturing .....	3
1.6 Radial Bearings Fatigue Test .....	4
1.7 Thin Lubrication Test .....	4
1.8 Conclusion .....	4
2.0 BACKGROUND .....	5
2.1 Hybrid Bearings .....	5
2.2 Background Rig Test Results .....	5
2.3 Rolling Contact Fatigue Rig Test .....	5
2.4 Full Scale Bearing Tests .....	6
3.0 NOMENCLATURE .....	7
4.0 EXPERIMENTAL EVALUATION OF NITRIDING PROCESSES .....	9
4.1 Types of Nitriding .....	10
4.2 Discussion of Nitriding Experiments .....	11
4.2.1 Hardness .....	15
4.2.2 Residual Stress .....	16
4.2.3 Nitrided Case Microstructure .....	55
4.3 Experimental Nitriding Conclusions .....	58
5.0 ROLLING CONTACT FATIGUE RIG EVALUATION .....	59
5.1 Test Conditions .....	59
5.2 Baseline Data .....	60
5.3 Manufacturing Process, RCF Specimens .....	61
5.4 Summary of RCF Testing .....	63
5.4.1 Summary of RCF Testing, M50 Steel .....	63
5.4.2 Summary of RCF Testing, M50 NiL Steel .....	66
5.5 RCF Test Conclusions .....	66
6.0 PROCUREMENT OF SILICON NITRIDE BALLS .....	68
6.1 Discussion of Past Test Experience with Ceramic Balls .....	68
6.2 Norton Advanced Ceramics NBD-200 .....	69
7.0 MANUFACTURING PROCESSES, M50 AND M50 NiL STEEL RINGS .....	70
7.1 Heat Treatment of M50 Steel .....	70
7.2 Heat Treatment of M50 NiL Steel .....	72
7.3 Nitriding Process, Bearing Rings .....	73
7.4 Finishing and Assembly .....	83

## Table of Contents (con't)

	Page
8.0 ROLLING CONTACT FATIGUE EVALUATION, 35 MM BORE, 207 RADIAL BEARINGS .	85
8.1 Baseline Definition .....	85
8.2 Summary of Fatigue Testing, 207 Radial Bearings .....	87
8.2.1 Summary of Fatigue Testing, M50 Steel .....	87
8.2.2 Summary of 207 Fatigue Testing, M50 NiL Steel .....	88
8.3 Failure Analysis, 207 Bearings .....	89
8.4 207 Bearing Test Conclusions .....	96
9.0 ROLLING CONTACT EVALUATION, 40 MM BORE 208 THRUST BEARINGS .....	98
9.1 Baseline Tests and Contact Stressing .....	98
9.2 Summary of Fatigue Testing, 208 Bearings .....	99
9.2.1 Discussion of Equal Stress Testing .....	99
9.2.2 Discussion of Equal Load Testing .....	101
9.3 Failure Analysis, 208 Bearings .....	103
9.4 208 Bearing Test Conclusions and Discussion .....	116
10.0 REFERENCES .....	118

# List of Figures

Figure		Page
1.4-1	Histogram of FMC RCF L <sub>10</sub> Test .....	3
4.2.1-1	Experimental Nitriding Cycles, M50 Samples .....	17
4.2.1-2	Experimental Nitriding Cycles, M50 NiL Samples .....	18
4.2.1-3	M50 Nitrided 16 hours, Low Dissociation Rate, 975F in a Fluidized Bed Furnace .....	19
4.2.1-4	M50 Nitrided 32 hours, Low Dissociation Rate, 975F in a Fluidized Bed Furnace .....	20
4.2.1-5	M50 Nitrided 16 hours, High Dissociation Rate, 975F in a Fluidized Bed Furnace .....	21
4.2.1-6	M50 Nitrided 32 hours, High Dissociation Rate, 975F in a Fluidized Bed Furnace .....	22
4.2.1-7	M50 Nitrided 60 hours, 50% Dissociation Rate, in a Gas Retort Furnace .....	23
4.2.1-8	M50 Nitrided 16 hours, High Dissociation Rate then 16 hours at a Higher Dissociation Rate, 975F in a Fluidized Bed Furnace ....	24
4.2.1-9	M50 Nitrided per the Lindure Process, 975F in a Gas Retort Furnace .....	25
4.2.1-10	M50 Nitrided 32 Hours, Low Dissociation Rate, 1000F in a Fluidized Bed Furnace .....	26
4.2.1-11	M50 Nitrided 60 Hours, 50% Dissociation Rate, 1000F in a Gas Retort Furnace .....	27
4.2.1-12	M50 NiL Nitrided 16 Hours, Low Dissociation Rate, 975F in a Fluidized Bed Furnace .....	28
4.2.1-13	M50 NiL Nitrided 32 Hours, Low Dissociation Rate, 975F in a Fluidized Bed Furnace .....	29
4.2.1-14	M50 NiL Nitrided 16 Hours, High Dissociation Rate, 975F in a Fluidized Bed Furnace .....	30
4.2.1-15	M50 NiL Nitrided 32 Hours, High Dissociation Rate, 975F in a Fluidized Bed Furnace .....	31
4.2.1-16	M50 NiL Nitrided 60 Hours, 50% Dissociation Rate, in a Gas Retort Furnace .....	32
4.2.1-17	M50 NiL Nitrided 16 Hours High Dissociation Rate then 16 Hours at a Higher Dissociation Rate, 975F in a Fluidized Bed Furnace ..	33
4.2.1-18	M50 NiL Nitrided per the Lindure Process, 975F in a Gas Retort Furnace .....	34
4.2.1-19	M50 NiL Nitrided 32 Hours, Low Dissociation rate, 1000F in a Fluidized Bed Furnace .....	35
4.2.1-20	M50 NiL Nitrided 60 Hours, 50% Dissociation Rate, 1000F in a Gas Retort Furnace .....	36
4.2.2-1	M50 Nitrided 16 Hours, Low Dissociation Rate, 975F in a Fluidized Bed Furnace .....	37
4.2.2-2	M50 Nitrided 32 Hours, Low Dissociation Rate, 975F in a Fluidized Bed Furnace .....	38
4.2.2-3	M50 Nitrided 16 Hours, High Dissociation Rate, 975F in a Fluidized Bed Furnace .....	39
4.2.2-4	M50 Nitrided 32 Hours, High Dissociation Rate, 975F in a Fluidized Bed Furnace .....	40

# LIST OF FIGURES (con't)

Figure		Page
4.2.2-5	M50 Nitrided 60 Hours, 50% Dissociation Rate in a Gas Retort Furnace .....	41
4.2.2-6	M50 Nitrided 16 Hours, High Dissociation Rate, Then Another 16 Hours at Higher Dissociation Rate, 975F in a Fluidized Bed Furnace .....	42
4.2.2-7	M50 Nitrided per the Lindure Process, 975F in a Gas Retort Furnace .....	43
4.2.2-8	M50 Nitrided 32 Hours, Low Dissociation Rate, 1000F in a Fluidized Bed Furnace .....	44
4.2.2-9	M50 Nitrided 60 Hours, 50% Dissociation Rate, 1000F in a Gas Retort Furnace .....	45
4.2.2-10	M50 NiL Nitrided 16 Hours, Low Dissociation Rate, 975F in a Fluidized Bed Furnace .....	46
4.2.2-11	M50 NiL Nitrided 32 Hours, Low Dissociation Rate, 975F in a Fluidized Bed Furnace .....	47
4.2.2-12	M50 NiL Nitrided 16 Hours, High Dissociation Rate, 975F in a Fluidized Bed Furnace .....	48
4.2.2-13	M50 NiL Nitrided 32 Hours, High Dissociation Rate, 975F in a Fluidized Bed Furnace .....	49
4.2.2-14	M50 NiL Nitrided 60 Hours, 50% Dissociation Rate, in a Gas Retort Furnace .....	50
4.2.2-15	M50 NiL Nitrided 16 Hours, High Dissociation Rate, Then Another 16 Hours at a Higher Dissociation Rate, 975F in a Fluidized Bed Furnace .....	51
4.2.2-16	M50 NiL Nitrided per the Lindure Process, 975F in a Gas Retort Furnace .....	52
4.2.2-17	M50 NiL Nitrided 32 Hours, Low Dissociation Rate, 1000F in a Fluidized Bed Furnace .....	53
4.2.2-18	M50 NiL Nitrided 60 Hours, 50% Dissociation Rate, 1000F in a Gas Retort Furnace .....	54
4.2.3-1	Photomicrograph Showing Typical Nitrided Case, M50 Steel, 100X, Nital Etch .....	56
4.2.3-2	Photomicrograph Showing Typical Nitrided Case, M50 Steel, 400X, Nital Etch .....	56
4.2.3-3	Photomicrograph Showing Typical Nitrided Case, M50 NiL Steel, 100X, Nital Etch .....	57
4.2.3-4	Photomicrograph Showing Typical Nitrided Case, M50 NiL Steel, 400X, Nital Etch .....	57
5.1-1	Diagram Showing the RCF Test Rig, Glover (4) .....	60
5.3-1	Manufacturing Process for Nitrided Steel Bearing Components ....	61
5.3-2	Soft Machining Dimensions, RCF Test Specimen, M50 Steel .....	64
5.3-3	Soft Machining Dimensions, RCF Test Specimen, M50 NiL Steel ....	64
5.3-4	Pre-Nitriding Dimensions, RCF Test Specimen, M50 and M50 NiL Steels .....	65
5.3-5	Finish Grinding Dimensions, RCF Test Specimen, M50 and M50 NiL Steels .....	65

# LIST OF FIGURES (con't)

Figure		Page
7.3-1	Hardness Profiles, M50 and M50 NiL Steel Bearing Rings As Nitrided, 32 hour Ferritic Nitrocarburized Cycle, 975F .....	76
7.3-2	M50 207 Inner Ring Size Change .....	77
7.3-3	M50 NiL 207 Inner Ring Size Change .....	78
7.3-4	M50 208 Inner Ring Size Change .....	79
7.3-5	M50 NiL 208 Inner Ring Size Change .....	80
7.3-6	M50 208 Outers .....	81
7.3-7	M50 NiL 208 Outers .....	82
8.3-1	SEM Photograph, 23X, Spalled Raceway, 1486 Hours, Nitrided M50 Steel Inner Ring .....	91
8.3-2	SEM Photograph, 100X, Microspalling at Nose of Figure 8.3-1 ....	91
8.3-3	SEM Photograph, 33X, Spalled Raceway, 376 Hours, Nitrided M50 Steel Inner Ring .....	92
8.3-4	SEM Photograph, 18X, Spalled Raceway, 1194 Hours, Nitrided M50 NiL Steel Inner Ring .....	93
8.3-5	SEM Photograph, 50X, Closer View of Evidence of Fatigue Crack Propagation With and Against Ball Rolling Direction .....	93
8.3-6	SEM Photograph, 17X, Spalled Ball, 115 Hours, Hybrid M50 NiL Bearing .....	94
8.3-7	SEM Photograph, 50X (Mecholsky), Spalled Ball, 87 Hours, Hybrid M50 NiL Bearing .....	95
8.3-8	SEM Photograph, 35X (Mecholsky), Spalled Ball, 172 Hours, Hybrid M50 NiL Bearing .....	95
9.3-1	Optical Photograph of Nitrided M50 Raceway After 15 Minute Contamination, 100X .....	104
9.3-2	Optical Photograph of Nitrided M50 NiL Raceway After 15 Minute Contamination, 100X .....	105
9.3-3	Optical Photograph of Nitrided M50 Raceway After 15 Minute Contamination and 24 Hours Running in Clean Oil, 100X .....	106
9.3-4	Optical Photograph of Nitrided M50 NiL Raceway after 15 Minute Contamination and 24 Hours Running in Clean Oil, 100X .....	106
9.3-5	Optical Photograph of Nitrided M50 Raceway After 15 Minute Contamination and 208 Hours Running in Clean Oil, 100X .....	107
9.3-6	Optical Photograph of Nitrided M50 NiL Raceway After 15 Minute Contamination and 212 Hours Running in Clean Oil, 100X .....	108
9.3-7	SEM Photograph Showing Raceway Spall of Nitrided M50 NiL 208 Inner Ring After Failure at 797 Hours, Ball Rolling Direction is From the Left to the Right, 45X .....	109
9.3-8	SEM Photograph Showing the Nose of the Spall, Note Arrow Showing an Original Contamination Pit and Subsequent Spall Propagation in the Ball Rolling Direction, 300X .....	109
9.3-9	SEM Photograph Showing Raceway Spall of Nitrided M50 NiL 208 Inner Ring After Failure at 1299.8 Hours, Ball Rolling Direction is From the Right to the Left, 100X .....	110
9.3-10	SEM Photograph Showing the Nose of the Spall; Note Arrow Showing the Original Contamination Pit and Subsequent Spall Propagation in the Ball Rolling Direction, 500X .....	111



# LIST OF FIGURES (con't)

Figure		Page
9.3-11	SEM Photograph Showing Raceway Spall of Nitrided M50 NiL 208 Inner Ring After Failure at 1882.1 Hours: Ball Rolling Direction is From the Left to the Right, 60X .....	112
9.3-12	SEM Photograph Showing the Nose of the Spall; Note that there is No Shallow Contamination Pit Around the Nose of This Spall, 150X .....	112
9.3-13	Residual Stress Profiles, Nitrided M50 Steel Unrun 207 and 208 Inner Rings vs Run 207 and 208 Inner Rings .....	114
9.3-14	Residual Stress Profiles, Nitrided M50 NiL Steel Unrun 207 and 208 Inner Rings vs Run 207 and 208 Inner Rings .....	115

# List of Tables

Table		Page
4.2-1	Summary of Experimental Nitriding Parameters .....	15
5.4.1-1	Weibull Statistical Summary, M50 Steel, Nitriding Cycles versus Baseline Test .....	63
5.4.2-1	Weibull Statistical Summary, M50 NiL Steel, Nitriding Cycles versus Baseline Test .....	66
6.2-1	NBD-200 Material Properties .....	69
7.4-1	Summary of Metrology Measurements, Bearing Raceways .....	84
8.2.1-1	Hybrid Nitrided M50 207 Bearing Test Results .....	88
8.2.2-1	Hybrid Nitrided M50 NiL 207 Bearing Test Results .....	89
9.1-1	Summary of Stress/Load Baseline Comparison, 208 Bearing Test ....	99
9.2.1-1	Summary of Results for 208 Bearing Tests, Hours Maximum Contact Stress 2.62 GPa (380 ksi) .....	100
9.2.1-2	Summary of Weibull Analysis for 208 Bearing Tests Maximum Contact Stress 2.62 GPa (380 ksi) .....	100
9.2.2-1	Summary of Results for 208 Bearing Tests, Hours Approximately 7500 N (1700 Pounds) Thrust Load .....	102
9.2.2-2	Summary of Weibull Analysis for 208 Bearing Tests Approximately 7500 N (1700 Pounds) Thrust Load .....	102

## FOREWORD

This final report describes the work performed by The Torrington Company, Torrington, Connecticut, under ARPA/USAF Contract F33615-92-C-5922. The report covers the period May 1992 to December 1994.

The program was aimed at developing an improved hybrid bearing by improving the steel rings that are assembled with silicon nitride rolling elements. The program was sponsored by the Advanced Research Projects Agency (ARPA) and administered by the Air Force Wright Laboratory, Materials Directorate. The support of Dr. William Coblenz of ARPA and Mr. Karl Mecklenburg of the Wright Laboratory is greatly appreciated.

The Torrington Company work was truly a team effort with many of our associates contributing to this work. Special acknowledgements are due to Messrs Henry Daverio and Ken Galitello for the full scale bearing tests, Mr. Donald Church for the RCF tests, X-ray work, and SEM work, Mr. James Richardson for the metrology, Mr. Steve Luko for the statistical analysis, Messrs William Chmura and Mark Lamoureaux for the administrative support, and Dr. Jack Woodilla, Director of Torrington's Advanced Technology Center for his continued support and encouragement of this program.

The thin lubrication full scale bearing test method and baseline data were developed previously in collaboration with GE Aircraft Engines, supported by Wright Research and Development Center contract F33615-84-C-2430 for Improved Fatigue Life Bearing Developments. We are also grateful to Dr. J. J. Mecholsky of the University of Florida who contributed SEM investigations of spalled balls for the present program.

## **1.0 SUMMARY**

### **1.1 PURPOSE**

This final report covers a 2-year effort to develop improved hybrid rolling contact bearings using steel rings and silicon nitride rolling elements. Nitriding was used to increase the hardness and surface properties of the rings to approach the properties of silicon nitride. Several nitriding procedures were evaluated by metallographic methods, the more promising were screened by rolling contact fatigue (RCF) rig testing, and the best were tested in full scale hybrid bearings. Two bearing tests were run, one with normal testing laboratory conditions to obtain basic fatigue data, the other with a higher temperature, thin lubrication film, and exposure to contamination to simulate difficult service applications. A secondary purpose of this program was to obtain rolling contact fatigue data for the silicon nitride balls.

### **1.2 SELECTION OF PROCESSES AND MATERIALS**

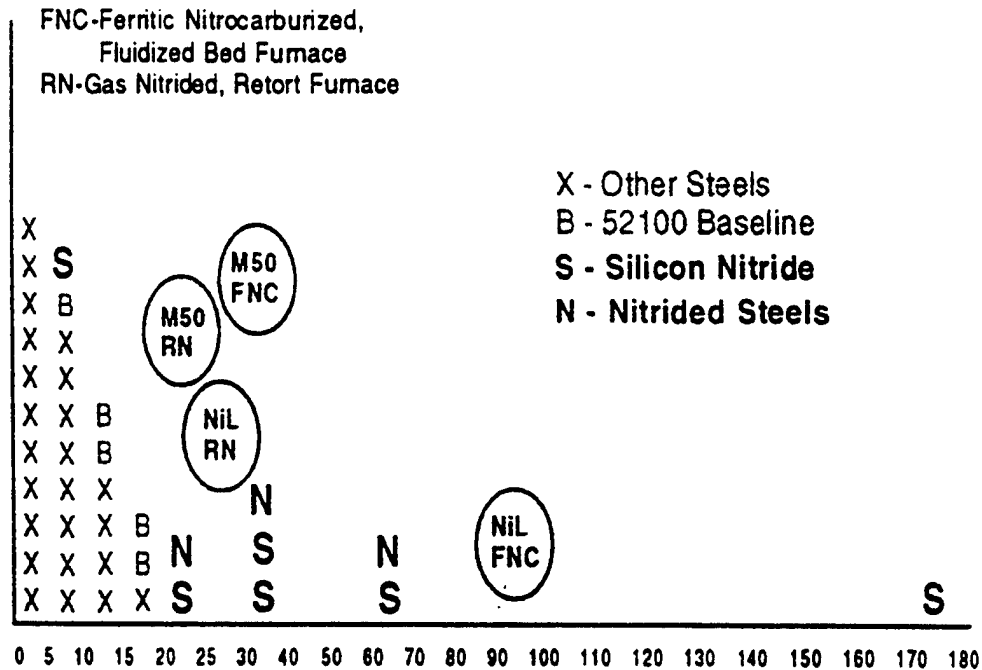
Nitriding was chosen over nitride coatings because nitriding produces a diffusion layer that is part of the microstructure, and the depth of nitrided layers is significantly greater than that of coatings. Two nitriding methods, fluidized bed ferritic nitrocarburizing and conventional gas retort nitriding, were used. M50 and M50 NiL were chosen for base steels because these are well established, high quality bearing steels used in critical applications and capable of elevated temperature bearing operation. M50 has superior wear resistance, and M50 NiL is a fracture tough steel used to prevent the fracture mode of failure when rings are subject to tensile stressing. Norton Advanced Ceramics NBD-200 silicon nitride balls were selected based upon the results of prior bearing testing.

### **1.3 EVALUATION OF NITRIDING PROCEDURES**

A total of nine time-temperature-atmosphere conditions for the fluidized bed and retort nitriding procedures were evaluated by measuring hardness, residual stress, and microstructure. In general, nitriding proved to be a desirable process, all cycles producing uniform cases with surface hardnesses near Rockwell C 70 for M50 and 68 for M50 NiL, and residual compressive stresses greater than 700 MPa (100 ksi). The microstructures had a white iron nitride layer, which is removed before rolling contact fatigue testing, and a fine nitride network which did not cause poor results in any of the subsequent fatigue tests. Longer time, deeper case cycles were chosen for fatigue test specimens because, when applied to full scale bearings, ring manufacturing could require greater amounts of stock removal after nitriding. These cycles produced hardness of Rockwell C 66 and residual compressive stress of 700 MPa (100 ksi) at approximately 0.25 mm (0.010 inch) below the nitrided surfaces.

### **1.4 ROLLING CONTACT FATIGUE RIG TESTS**

A fluidized bed and a retort nitriding cycle were tested on both M50 and M50 NiL steels using three-ball-on-rod test rigs. The results of all tests were favorable when compared to previous tests of non-nitrided steels. The fluidized bed ferritic nitrocarburized specimens exhibited longer life, therefore, this treatment was selected for full scale bearing testing. These results are summarized schematically in Figure 1.4-1. In this histogram, the B's and X's are the results of 2 years of testing 52100 and other bearing steels. The S's and N's are earlier tests of silicon nitride and nitrided steels.



L10 Life - Hours  
Figure 1.4.-1

### Histogram of FMC RCF L<sub>10</sub> Tests

#### 1.5 BEARING MANUFACTURING

Bearing rings were soft machined, carburized (M50 NiL only) hardened and tempered, rough ground, nitrided, finish ground and polished. Nitrided surfaces were ground with the same procedures (wheels, feeds, speeds) as are used for nonnitrided M50 steel. The nitrided layer caused up to 0.075 mm (0.003 inch) diametrical size change. The 35 mm bore radial bearings were made for basic fatigue life testing. In this test, the inner rings were nitrided and matched with M50 outer rings and silicon nitride balls. The thin film, contaminated lubricant test used a 40 mm bore bearing running in thrust, and for this task, both inner and outer rings were nitrided.

## **1.6 RADIAL BEARINGS FATIGUE TEST**

The hybrid bearings were loaded to run at the same maximum contact stress as has been applied to all-steel bearings in previous tests, 7050 N (1600 lbs.) on hybrid bearings vs. 10,900 N (2450 lbs.) on all-steel bearings for 3.65 GPa (530 ksi) maximum contact stress. Bearings ran at 3000 rpm with full elastohydrodynamic lubrication film conditions. Both the nitrided M50 and M50 NiL bearings exhibited good life with life factors close to 11X. Failures included silicon nitride balls as well as nitrided inner rings.

## **1.7 THIN LUBRICATION TEST**

The 40 mm bore bearings were jet engine quality, run in thrust at 10,000 RPM and at 150°C (300°F) in oil corresponding to MIL-L-7808J, to simulate application conditions. The hybrid bearings had 7500 N (1700 lb) thrust load creating 2.62 GPa (380 ksi) maximum contact stress. Bearings were initially run for 15 minutes in 150°C MIL-L-7808 oil contaminated with 2.5 ppm of 20 micron aluminum oxide to create surface damage. They were then washed and run to failure or 2000 hour suspension in clean lubricant. Ten bearings of each steel were tested. None of the M50 bearings failed within 2000 hours. Three of the M50 NiL bearings failed indicating an  $L_{10}$  life of about 1000 hours. Data from previous testing of all-steel bearings were available to compare to the hybrid performance at both equivalent stress and nearly equivalent load conditions. The hybrid bearings exhibited much longer life than all-steel bearings at both equivalent stressing and also at equivalent loading. At a test load of 1700N, the hybrid bearings had 4 to 7 times the life of all steel bearings despite operating at a higher contact stress.

## **1.8 CONCLUSION**

The successful operation at higher temperatures, thin lubrication, and exposure to contamination indicates that the goals of this project were met. Hybrid bearings have been improved for applications in difficult service conditions, thereby opening new possibilities for their use.

## **2.0 BACKGROUND**

### **2.1 HYBRID BEARINGS**

Silicon nitride has a long history of demonstrating good properties for rolling contact fatigue stressing. In theory, all-ceramic bearings would be desirable, but problems in ring manufacturing, as well as the application problems arising from the mismatch of thermal expansion properties, have limited the use of ceramic bearings. The most common use for silicon nitride is for the rolling elements in hybrid bearings using steel rings. Hybrid bearings have performed better than all-steel bearings in many applications, but the full potential for hybrids has not been realized because of the properties of the much softer conventional bearing steel rings. An opportunity exists to develop improved hybrid bearings by improving the properties of the rings.

### **2.2 BACKGROUND RIG TEST RESULTS**

The foundation for the proposal and the work in this project was the results of earlier tests of silicon nitride and nitrided M50 and M50 NiL steels. Three-ball-on-rod rolling contact fatigue rigs were used. Both the silicon nitride and the nitrided steels demonstrated capability for much longer life than any steel composition, heat treatment, or surface modification previously tested. The results have been reported (1)(2)(3) and are the earlier tests in Figure 1.4-1. From this background, the present project was initiated to make further studies of nitriding and to test the best procedures in full scale hybrid bearings.

### **2.3 ROLLING CONTACT FATIGUE RIG TEST**

The three-ball-on-rod rolling contact fatigue rig used in this project was developed by Douglas Glover at the Federal Mogul Corporation and is sometimes known as the RCF-FMC rig. This test is described fully by Glover (4). It is used by at least 15 bearing companies and research organizations throughout the world. Like all test rigs, it runs at a very high stress to obtain data in a reasonable length of time, and the results must be interpreted carefully. A



material or process that performs poorly in this test may be satisfactory at the lower stressing of most applications. When a material performs very well, it has passed a very demanding test and is clearly worthy of further development.

## **2.4 FULL SCALE BEARING TESTS**

The 40 mm bore, thin lubricant, contamination exposure test used in this project was developed for Air Force Contract F33615-84-C-2430, "Improved Fatigue Life Bearing Development" (5). Here it was recognized that the life of standard M50 steel turbine engine bearings was so long as to preclude obtaining test data in a reasonable length of time, especially for a development to demonstrate even longer life. Furthermore, it was observed that when application failures did occur, the cause was usually some abnormal surface damage. From this, the exposure to aluminum oxide contamination was chosen to represent severe application conditions. This work provides the baseline data to which the improved hybrid bearings in the present project are compared. Aluminum oxide is but one of a great many contamination possibilities, but the process of surface damage leading to fatigue and crack initiation is common to most application failures (6)(7)(8).

The 35 mm bore radial bearing test is similar to tests run by bearing companies for many years to obtain basic life data. These tests are run under fully lubricated "ideal" test conditions. It should be noted, however, that while conventional bearing theory relates bearing life to subsurface shear stresses developed by totally elastic behavior of perfectly smooth surfaces, this is never the case. Steel quality improvements have made subsurface failures rare, and some form of roughness or surface damage initiates most of the failures in this test also.

### 3.0 NOMENCLATURE

The following definitions may help the reader with the nomenclature of the bearing and heat treating industries.

1. *A HYBRID BEARING is one with steel rings and ceramic rolling elements. The ceramic is usually silicon nitride. The bearings in this project used silicon nitride balls.*
2. *RINGS are the inner and outer rings of the bearing. In other literature these are sometimes referred to as races.*
3. *RACE or RACEWAY in this report refers to the surface contacted by the rolling elements and subject to rolling contact stressing.*
4. *NITRIDING is the diffusion of nitrogen into the steel surfaces, usually at temperatures of 480°-540°C (900°-1000°F).*
5. *FERRITIC NITROCARBURIZING is basically a nitriding, not a carburizing process. Some hydrocarbon is added to the atmosphere to diffuse carbon as well as nitrogen into the surfaces. Ferritic comes from the metallographic phase at the nitriding temperatures, as opposed to austenitic which is the phase at higher temperatures used for most carburizing. All of the steel nitrided in this project had a microstructure of tempered martensite, which qualifies as ferritic for this definition.*
6. *CARBONITRIDING was not used in this project or in this report. It is a carburizing, not a nitriding process.*

7. *HIGH DISSOCIATION NITRIDING has lower nitriding potential. Gas nitriding takes place when ammonia dissociates to nitrogen and hydrogen over the work. Processes are described by the amount of dissociation that takes place before the atmosphere reaches the work chamber. High dissociation, therefore, means that there is less ammonia to dissociate over the work.*
8. *Conversely, LOW DISSOCIATION NITRIDING has more ammonia in the work chamber, therefore a higher nitriding potential.*
9. *A FLUIDIZED BED is a heat treating furnace in which the circulating atmosphere carries with it a concentration of inert refractory particles that impinge upon the work to hasten heating and cooling.*
10. *In RETORT NITRIDING the dissociated gas and the work are alone in the nitriding chamber.*

#### 4.0 EXPERIMENTAL EVALUATION OF NITRIDING PROCESSES

Nitriding has been used extensively for applications where fatigue and/or wear resistance is necessary. The present contractual work was performed to determine whether the nitriding process can be used to produce mechanical properties of steel bearing raceways that are closer to those of silicon nitride bearing balls to produce bearings which provide a significant increased rolling contact fatigue life over all steel bearings.

The first step towards testing this process in rolling contact fatigue was to determine baseline properties including hardness, case depth, residual stress profiles, and the nitrided case microstructure. Nitriding, like carburizing, is a diffusion treatment where the chemistry of the surface of the treated components is altered to produce the desired effects. During carburizing, carbon atoms diffuse into the steel. During nitriding, nascent nitrogen atoms are needed to diffuse into the steel. Ammonia is used to supply nascent nitrogen. Ammonia when exposed to heat dissociates into nitrogen gas and hydrogen gas by the following equation.



As one molecule of ammonia dissociates, there is, for a short time, the nascent nitrogen atom which in time will find another nascent nitrogen atom and form  $\text{N}_2$ . It is during this short time period when a molecule of ammonia dissociates at the surface of the steel that the nascent nitrogen atom is accepted into the steel matrix.

Changes in the processing parameters, and thus the surface chemistry, can influence the effects of the nitrided case on component performance. The processing variables which were examined were gas composition, nitriding temperature and time at nitriding temperature. All three of these variables are important achieving the desired effects in the nitrided case. The experiments used in the study were designed to determine which, if any, were clearly the most important for producing excellent steel surface properties for rolling contact stressing using silicon nitride rolling elements.

#### 4.1 TYPES OF NITRIDING

Nitriding has been used for many years as a process to enhance mechanical properties of steel components. There are currently many types of nitriding available on a commercial and developmental level. Some of the many types are liquid nitriding, gas retort nitriding, ferritic nitrocarburizing, vacuum nitriding, and plasma (or ion) nitriding. Some of these processes have been available longer than others and are more widely used in industry today.

Liquid nitriding, as the name implies, is performed in a liquid cyanide salt which supplies nitrogen to the steel by the decomposition of cyanide to cyanate. Due to environmental and waste disposal considerations, liquid nitriding was not considered for the work in this contract.

Vacuum nitriding and plasma nitriding, which may be the future of the nitriding industry, currently are not as common and commercially available as the other nitriding processes. Vacuum nitriding, as the name implies, is performed in a vacuum chamber while ammonia is introduced into the chamber at the correct temperature. Plasma nitriding is also performed in a vacuum chamber. With plasma, nitrogen gas, not ammonia, is used to supply nascent nitrogen. This involves using an electrical potential to ionize the nitrogen gas. An advantage of this process is that ammonia is not used at all, so there are none of the problems of storing, using, and disposing of ammonia.

Gas nitriding and ferritic nitrocarburizing are both nitriding processes which are common to many captive and commercial heat treating departments. Because of the current widespread use and experience with these two processes, they were chosen to be the focus of the nitriding evaluation for this contract. The advanced processes using vacuum and plasma will be investigated in future developments.

## 4.2 DISCUSSION OF NITRIDING EXPERIMENTS

This task explored some of the basic parameters of the nitriding process. Nitriding has long been known to produce a very hard case on the surface of a treated part. This hard surface lends itself to good general fatigue life because of indentation and wear resistance and compressive residual stresses at the surface. In the case microstructure after nitriding, a nitride network develops.

The first step towards completing this contract was to determine the precise nitriding process which yielded the greatest rolling contact fatigue life. Nitriding experiments were performed to determine the nitriding parameters to be used for rolling contact fatigue rig testing. This task also attempted to develop a nitriding cycle which reduced the tendency for the nitride network to form and at the same time produced the very high hardness and the high residual compressive stress layer at the surface. These three parameters were put in order of importance. Hardness was our most important criteria. If the hardness of a nitriding cycle was not close to Rockwell C 70 it wasn't considered for RCF testing on the FMC machine. Next, the residual stress profile was considered. High residual compressive stresses are known to benefit RCF life. Finally, the quality of the nitrided case microstructure was considered. The best microstructure is the one with the least nitride networking in the case microstructure.

Initially, standard nitriding cycles from two commercial heat treating companies were examined using metallography and residual stress measurements. Based on the results from standard cycles, several additional nitriding trials were performed to maximize properties and reduce or eliminate the nitride network in the nitrided case microstructure.

Two types of nitriding processes were examined: gas nitriding, performed in a retort furnace; and ferritic nitrocarburizing, performed in a fluidized bed. Both processes are similar in that they take place in the same temperature range, use ammonia to supply the nascent nitrogen for diffusion into the steel, and blend additional nitrogen gas with the gas mixture. Nitriding in a fluidized bed has one difference in that propane is also added to the gas mixture during the nitriding process.

All ferritic nitrocarburizing (fluidized bed) nitriding experiments were performed at Massachusetts Steel Treating in Worcester, Massachusetts. The dissociation rate in the fluidized bed was measured by the gas flows through the furnace. All gas nitriding experiments were performed at Lindberg Heat Treating Company also in Worcester, Massachusetts. The dissociation rate in the gas nitriding process was measured as a percent dissociation of ammonia. All trials were performed at 524°C (975°F) except for one trial of each type of nitriding performed at 537°C (1000°F).

Nitriding "potentials" are defined by the dissociation rate of the ammonia gas inside the furnace. In order for nitrogen to diffuse into steel it must be in the nascent form. The nascent form of nitrogen exists only momentarily as  $\text{NH}_3$  dissociates into nitrogen gas and hydrogen gas. The reaction must take place at the surface of the steel. Therefore, the nitriding potential is gauged by the amount of undissociated ammonia in the furnace inlet available to dissociate at the steel surface. If the dissociation rate is high (it is measured going into the furnace) then there is less ammonia available for dissociation at the steel surface, and a lower nitrogen concentration profile results. If the dissociation rate is low, then there is more ammonia available for dissociation at the steel surface, and a higher nitrogen concentration profile results.

The first group of experiments were performed in a fluidized bed at Massachusetts Steel Treating. Two nitriding times and two dissociation rates were chosen with all four combinations performed. Below, the specific parameters of the designed experiment are shown:

*Massachusetts Steel Treating, Fluidized Bed Furnace, 524°C ( 975°F)*

<u>Exp.</u>	<u>Nitriding Time</u> (hours)	<u>Nitriding Conditions</u>		
		<u>Gas flows (cfh):</u>	$\text{NH}_3$	$\text{N}_2$ Propane
16H	16		300	300 200
32H	32		300	300 200
16L	16		600	300 200
32L	32		600	300 200

The general trend seen was that the lower the dissociation rate the higher the hardness as discussed in Section 4.2.1. The magnitude of the residual compressive stress follows the same pattern as the hardness data. The compressive stress increases with a lower dissociation rate. All

of these trials produced a nitride network in the nitride case structure. Future trials will attempt to reduce or eliminate the network. The higher dissociation rate trial (16H and 32H, 300 cfh ammonia) attempted to reduce the network. It became apparent that to reduce the networking further, lowering of the dissociation rate was necessary.

Concurrently with the designed experiment at Massachusetts Steel Treating, an initial trial was performed at Lindberg in their retort gas nitriding process. The first trial was their standard process, which runs 48 hours. The first 8 hours were at 20% dissociation and the last 40 hours were at 80% dissociation. The process resembles boost-diffuse carburizing. The data for this trial are contained in Sections 4.2.1 and 4.2.2. There was a nitride network in the case microstructure.

The next cycle was to nitride 60 hours at a constant 50% dissociation rate at Lindberg. The results from this cycle are in Sections 4.2.1 and 4.2.2. In general, the hardness was good, the residual stress was good, but the nitride network remained.

We then decided on another cycle to be tried on the fluidized bed. The cycle was divided into two halves with each half having a different nitriding gas composition. The cycle gas flow rates are shown below.

<u>Exp</u>	<u>Nitriding Time</u>	<u>Nitriding Conditions</u>			
	(hours)	Gas flows (cfh)	NH <sub>3</sub>	N <sub>2</sub>	Propane
32HH	16		300	300	200
	16		150	450	200

This cycle was similar to the original boost and diffuse cycle used at Lindberg. The result of this cycle is contained in Sections 4.2.1 and 4.2.2. The hardness was good, residual stress was good, and the network remained.

The final cycle that was performed at Lindberg consisted of a repeat of the previous cycle at Lindberg except the temperature was raised to 538°C (1000°F). The effect of nitriding temperature on the degree of nitride networking was examined. The cycle showed the same nitride network; and the higher temperature, which is above the tempering temperature of M50 NiL, made this temperature too high to consider further.



A similar higher temperature cycle was performed using the fluidized bed furnace at Massachusetts Steel Treating. The furnace conditions were the standard gas compositions used in experiment 32L, except that the temperature was raised to 538°C (1000°F). Again this cycle was used to determine if raising the nitriding temperature would help to reduce the nitride network. The results showed that the hardness and residual stress were acceptable but the higher temperature during nitriding did not seem to reduce the network to any significant degree.

Cycles for rolling contact fatigue testing were chosen based upon hardness, residual stress, and depth of case. Deep cases would be needed for future processing of bearing rings. The first cycle to be tested in rolling contact fatigue was the 32 hour cycle using the fluidized bed furnace (ferritic nitrocarburizing). This cycle produced one of the higher surface hardnesses on both steels, and high compressive stresses were present in the nitrided case.

The second cycle that would be tested using the RCF rod testing machine was 60 hours with 50% dissociated ammonia and a temperature of 524°C (975°F) at Lindberg.

Both of the chosen cycles for RCF testing had high hardness and high residual compressive stress profiles for each type of nitriding. Without further nitriding trials to experiment with various gas compositions, reduction of the nitride network could not be accomplished without sacrificing hardness and compressive residual stresses.

A summary of all the nitriding experiments is shown below in Table 4.2-1. Massachusetts Steel Treating (fluidized bed, ferritic nitrocarburizing) is denoted by MST. Lindberg Heat Treating (retort furnace, gas nitriding) is denoted by LDBG. Unless noted, all cycles were performed at 524°C (975°F).

Table 4.2-1  
Summary of Experimental Nitriding Parameters

<u>Exp.</u>	<u>Nitriding Time</u> (hours)	<u>Nitriding Conditions</u>		
		Gas flows (cfh):	NH <sub>3</sub>	N <sub>2</sub> Propane
16H (MST)	16	300	300	200
32H (MST)	32	300	300	200
16L (MST)	16	600	300	200
32L (MST)	32	600	300	200
32HH (MST)	16	300	300	200
	16	150	450	200
*32L, 1000°F (MST)	32	600	300	200
48STD (LDBG)	8	20% dissociation rate		
	40	80% dissociation rate		
*60CON (LDBG)	60	50% dissociation rate		
60CON, 1000°F (LDBG)	60	50% dissociation rate		

\* Chosen for RCF rig testing of M50 and M50NiL steels

#### 4.2.1 HARDNESS

The hardness of the nitrided case was the most important factor in choosing the best nitriding cycle. The case hardness at the ground surface must be near Rockwell C 70 in order to be considered further in our analysis. The goal of producing an improved surface for silicon nitride balls to roll against dictates that the steel be significantly harder than what can now be achieved using conventional steels.

Our experiments showed that the highest hardness resulted from the most amount of available nitrogen. Whenever the nitriding "potential" was decreased to try to reduce the nitride network, the hardness dropped by one or two Rockwell C points, and the nitride network remained. Therefore, the conclusion was that whatever nitriding "potential" was necessary to reduce the nitride network would not come close to producing the high hardness desired to complement the silicon nitride balls.

Figures 4.2.1-1 and 4.2.1-2 show the hardness profiles of all of the experimental nitriding cycles for M50 and M50 NiL steels, respectively. The graphs are quite crowded with data and

are not intended to show every detail about the various hardness profiles. They should be examined with the idea of seeing the range of hardness profiles produced by all of the nitriding experiments. Figures 4.2.1-3 through 4.2.1-21 show the individual hardness profiles for each of the nitriding cycles. The hardness profiles for nitrided M50 steel are Figures 4.2.1-3 through 4.2.1-11 and the hardness profiles for the nitrided M50 NiL steel are Figures 4.2.1-12 through 4.2.1-20.

#### **4.2.2 RESIDUAL STRESS**

Residual stress was the second most important parameter behind hardness for deciding which nitriding cycle would be tested in rolling contact fatigue on the RCF rig. The same trends seen in the hardness data were observed in the residual stress data. The cycles which produced the highest hardness also produced the highest residual compressive stress profiles. No trade off decisions involving hardness and residual stress were necessary. When the nitriding "potential" was reduced to try to reduce the nitride network in the nitrided case, the beneficial residual compressive stresses become smaller in magnitude and shallower in depth. Figures 4.2.2-1 through 4.2.2-9 show the residual stress profiles for all the experimental cycles for M50 steel. Figures 4.2.2-10 through 4.2.2-18 show the residual stress profiles for all the experimental cycles for M50 NiL steel.

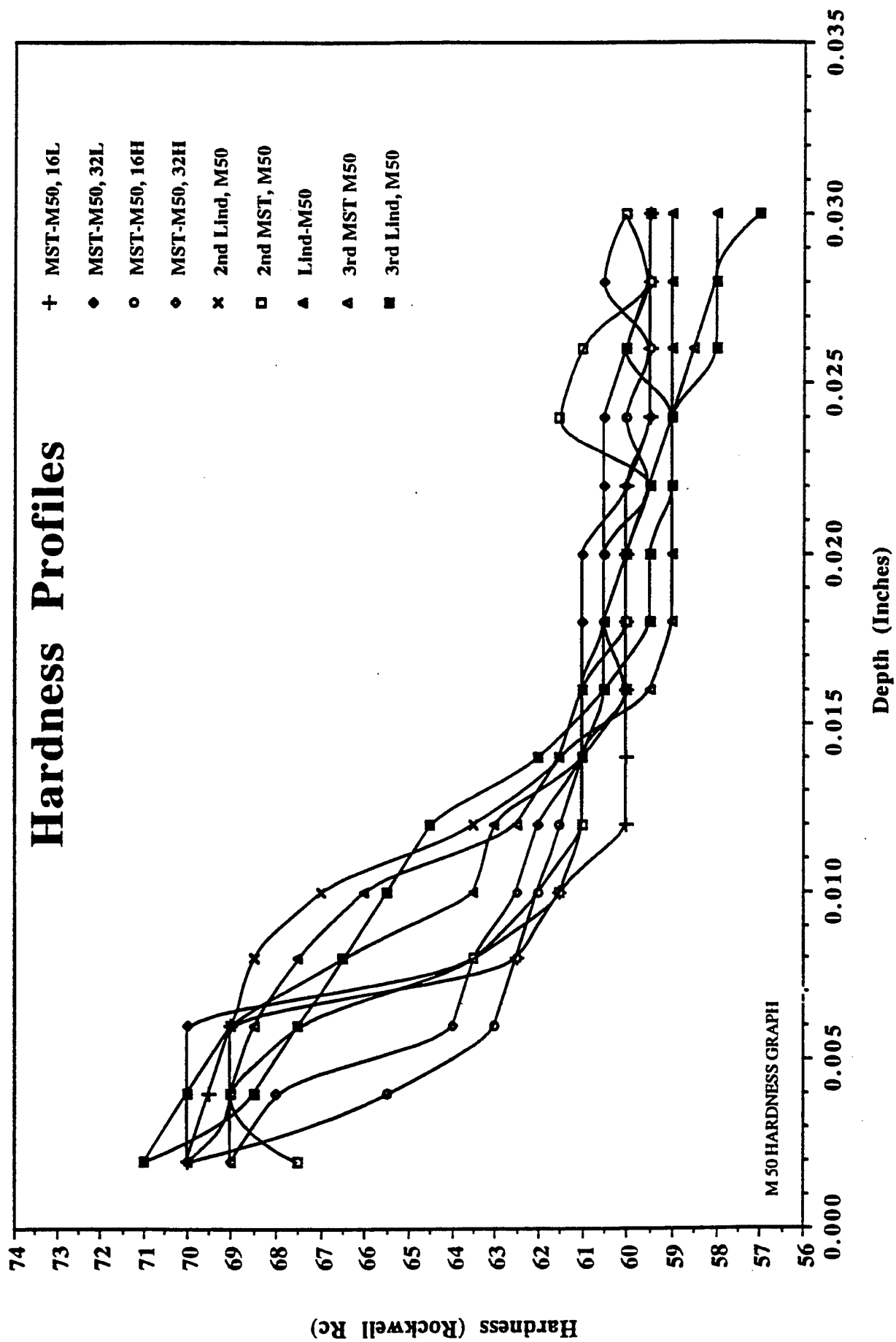


Figure 4.2.1-1 Experimental Nitriding Cycles, M50 Samples

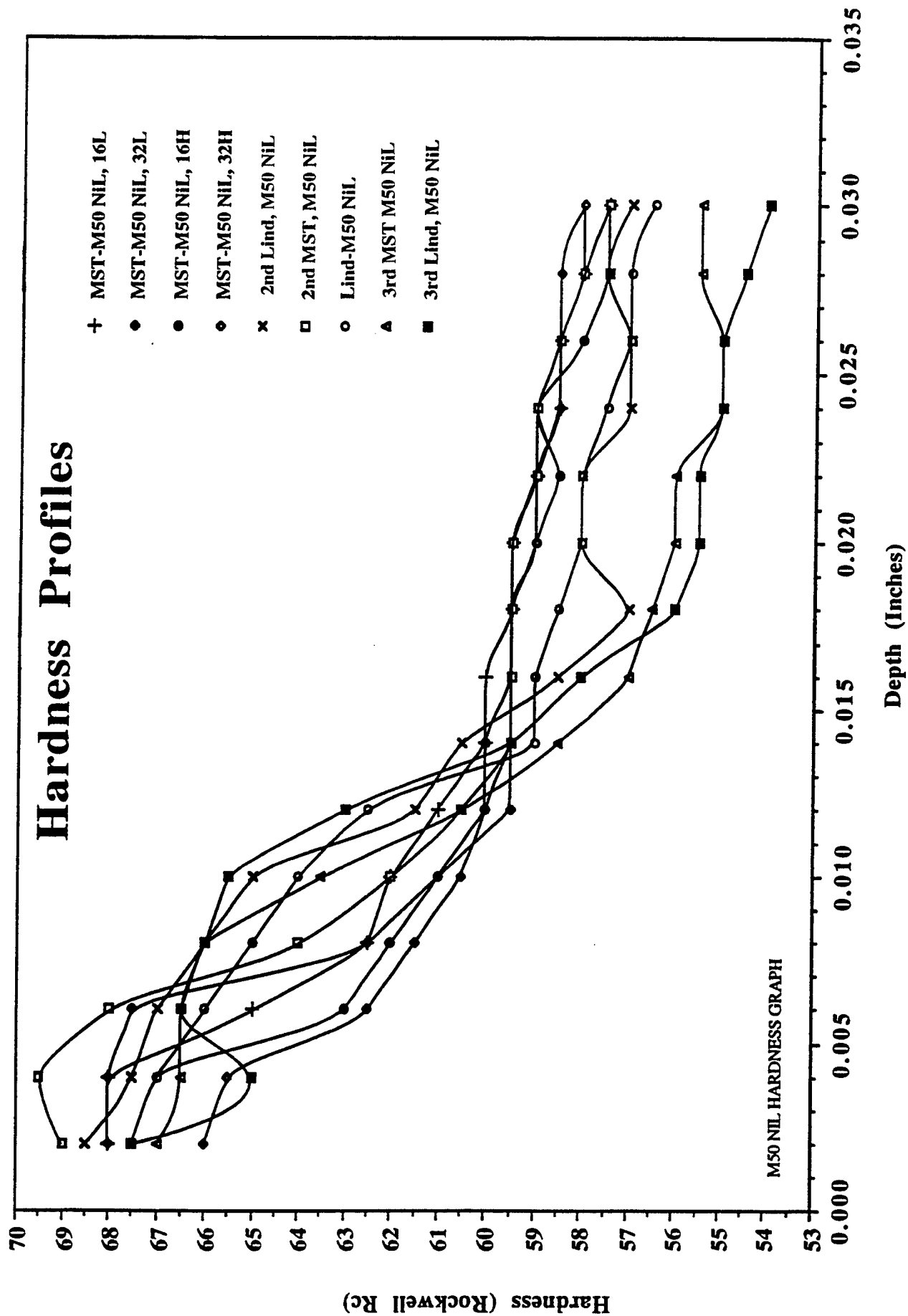


Figure 4.2.1-2 Experimental Nitriding Cycles, M50 Nil Samples

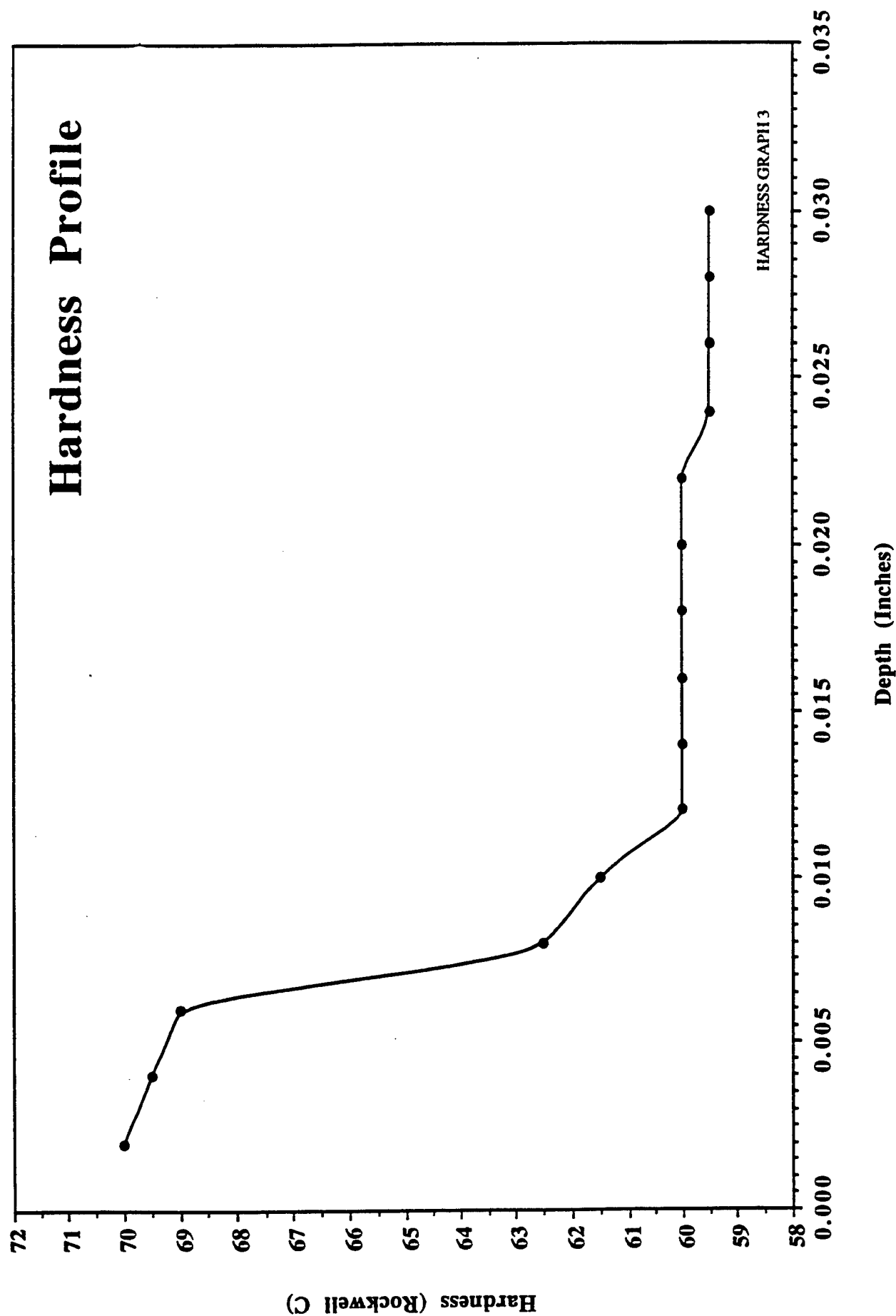


Figure 4.2.1-3 M50 Nitrided 16 hours, Low Dissociation Rate,  
975F in a Fluidized Bed Furnace

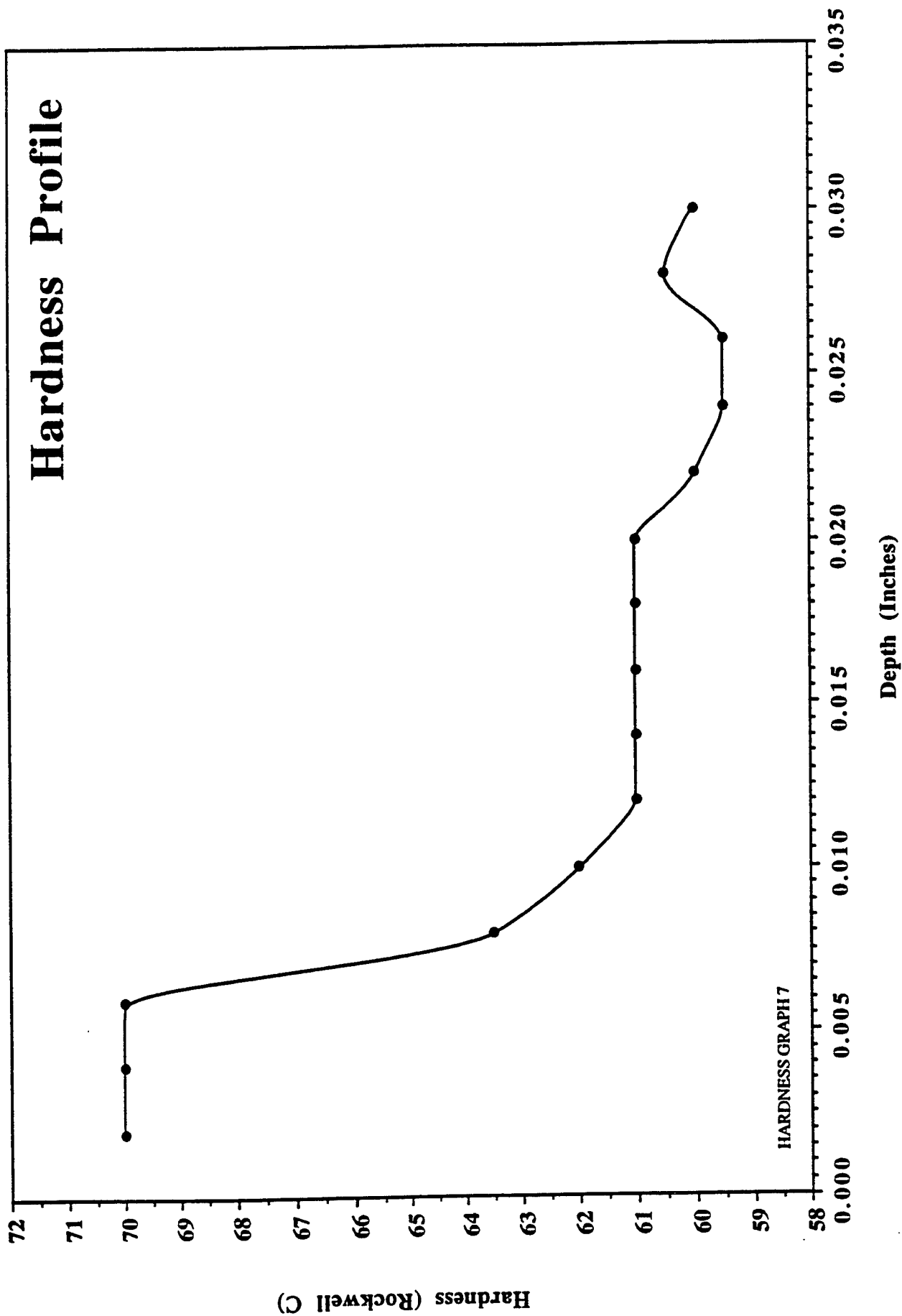


Figure 4.2.1-4 M50 Nitrided 32 hours, Low Dissociation Rate,  
975F in a Fluidized Bed Furnace

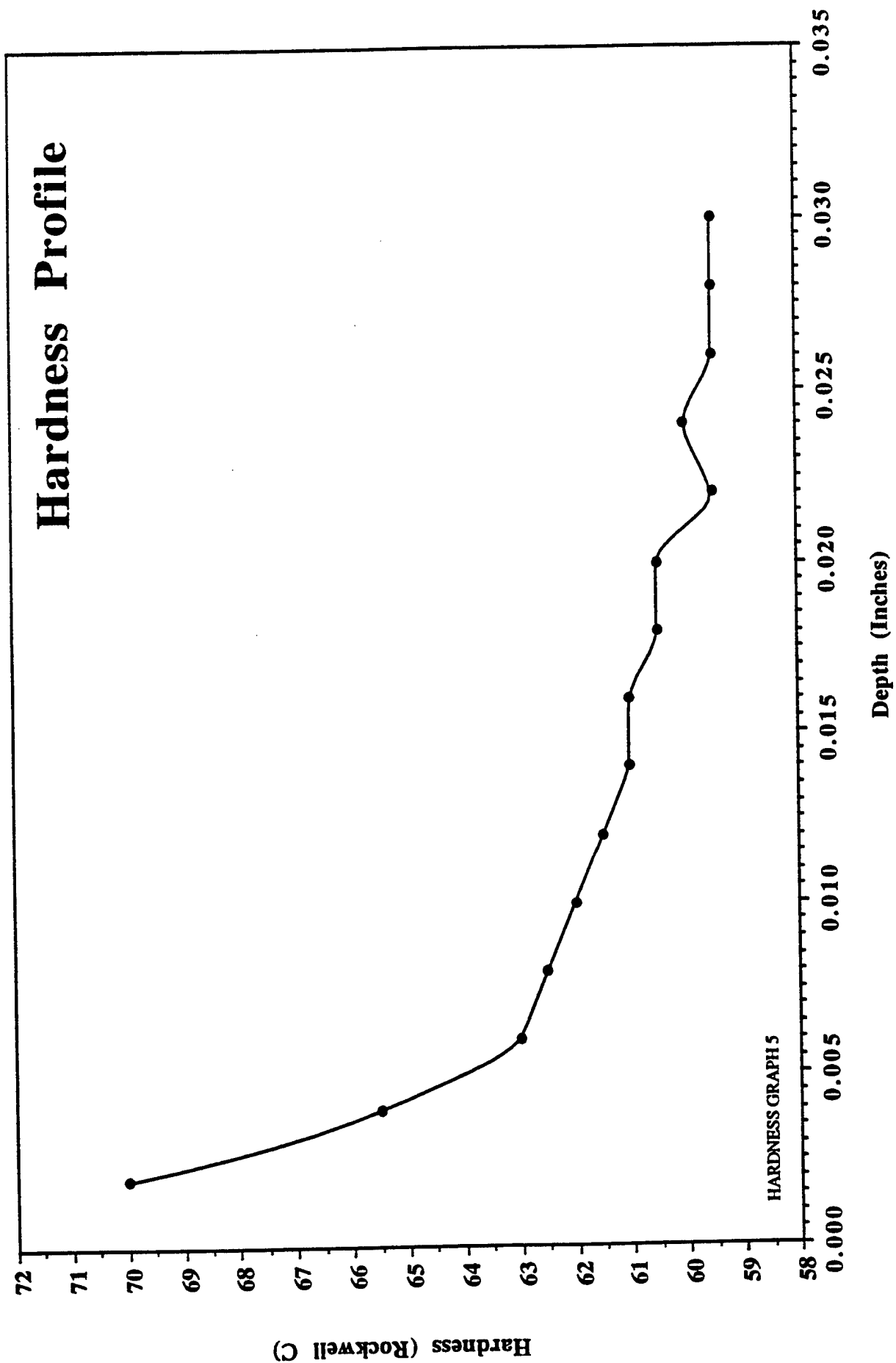


Figure 4.2.1-5 M50 Nitrided 16 hours, High Dissociation Rate,  
975F in a Fluidized Bed Furnace



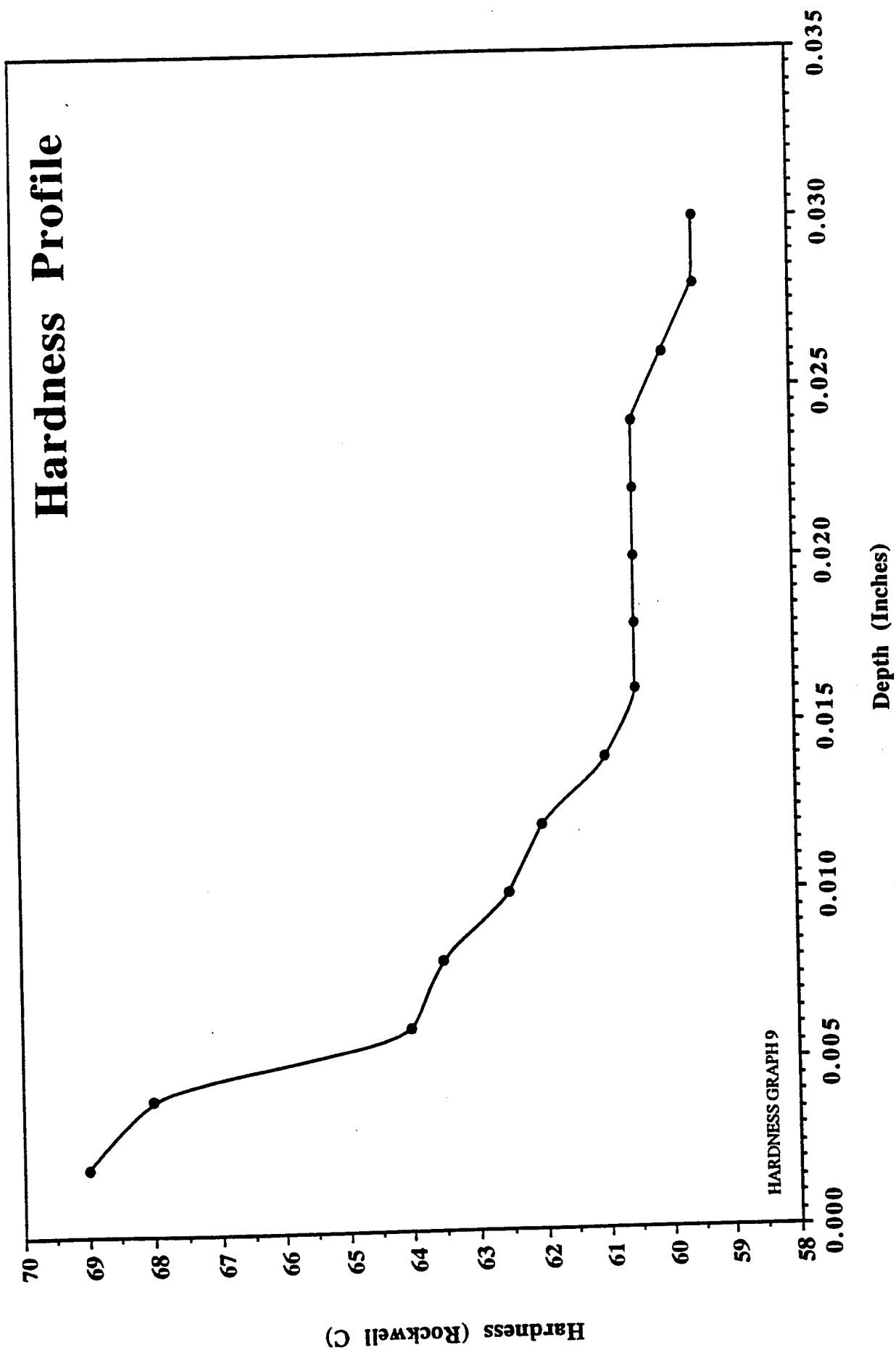


Figure 4.2.1-6 M50 Nitrided 32 hours, High Dissociation Rate,  
975F in a Fluidized Bed Furnace

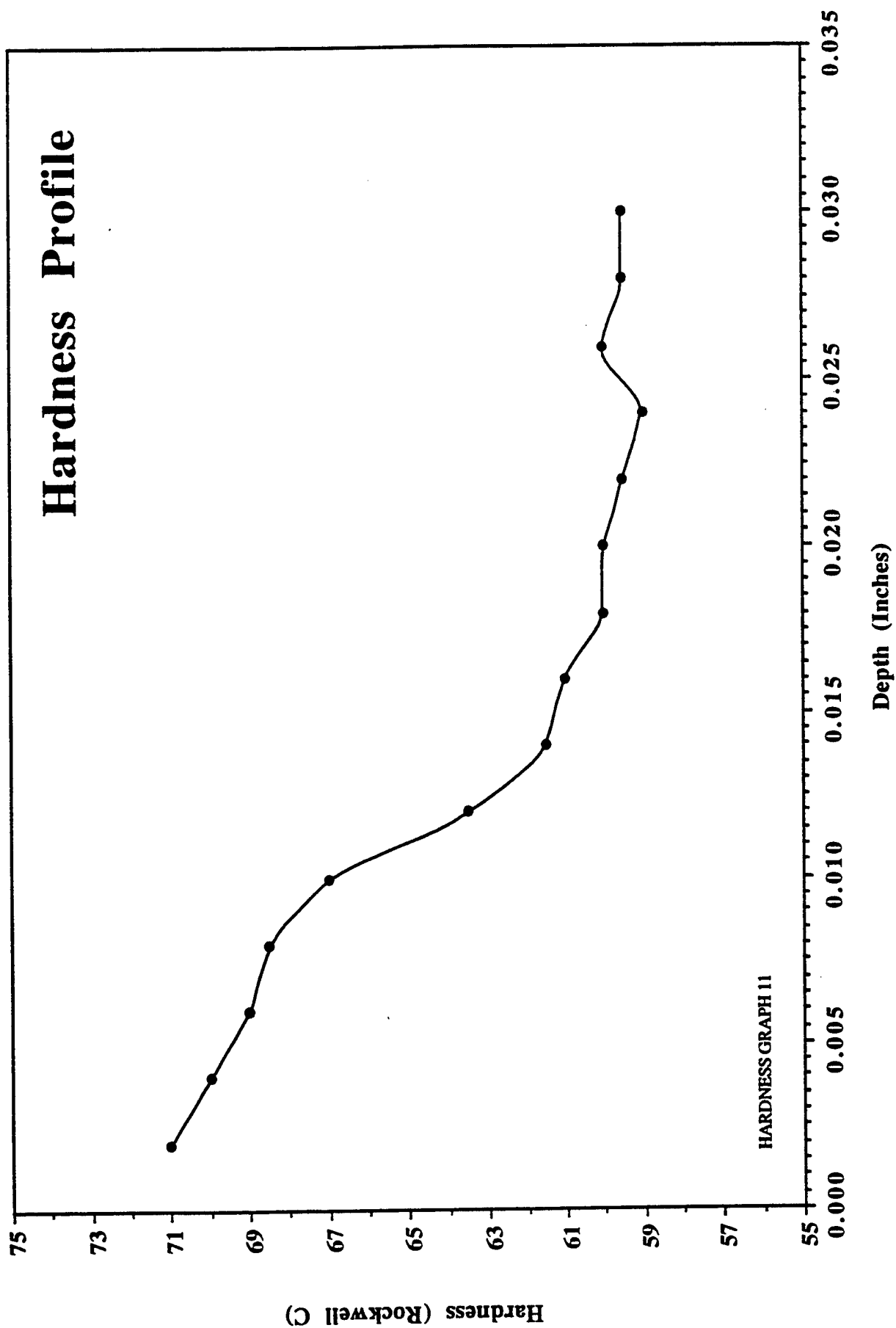


Figure 4.2.1-7 M50 Nitrided 60 hours, 50% Dissociation Rate, in a Gas Retort Furnace

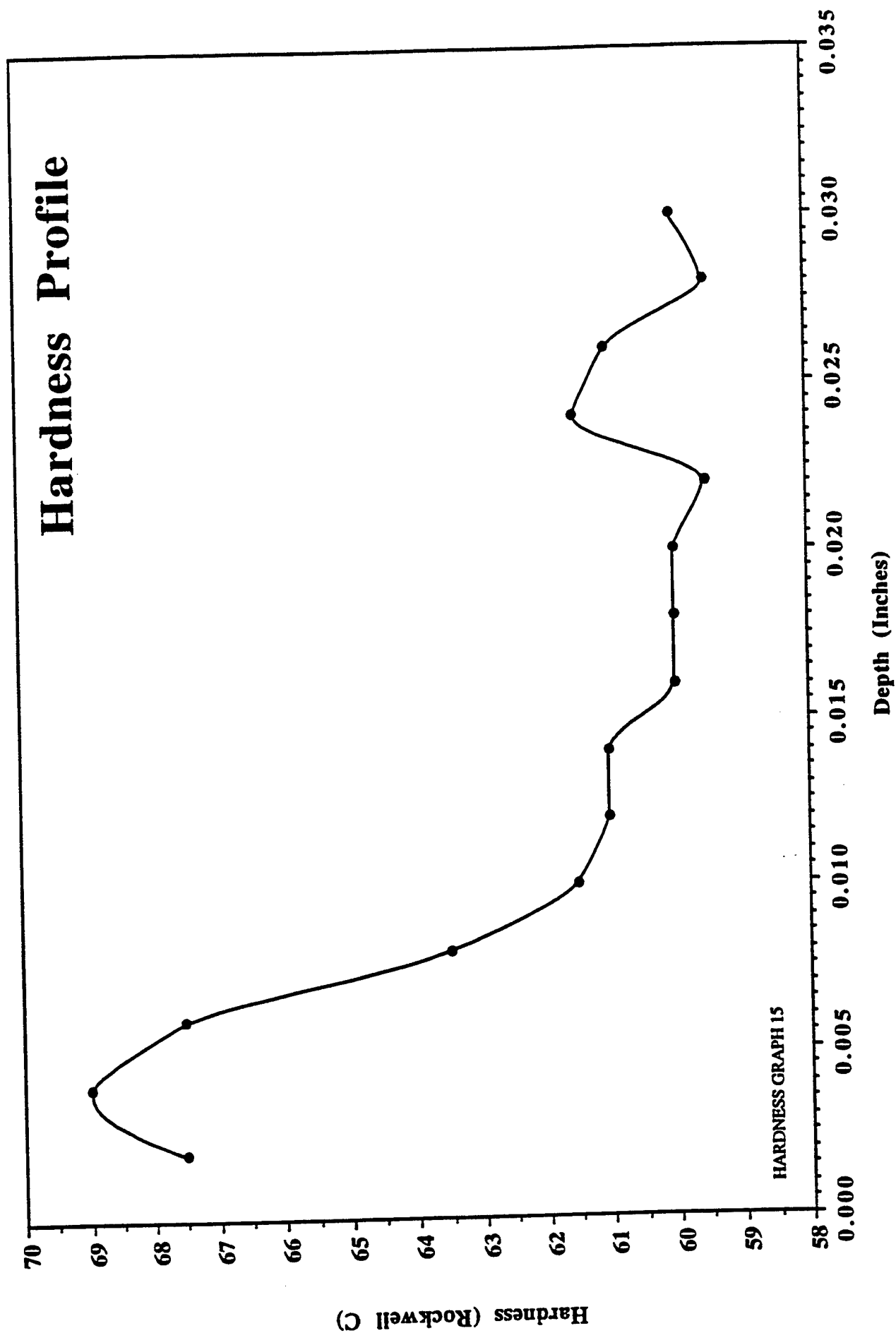


Figure 4.2.1-8 M50 Nitrided 16 hours, High Dissociation Rate  
then 16 hours at a higher Dissociation Rate,  
975F in a Fluidized Bed Furnace

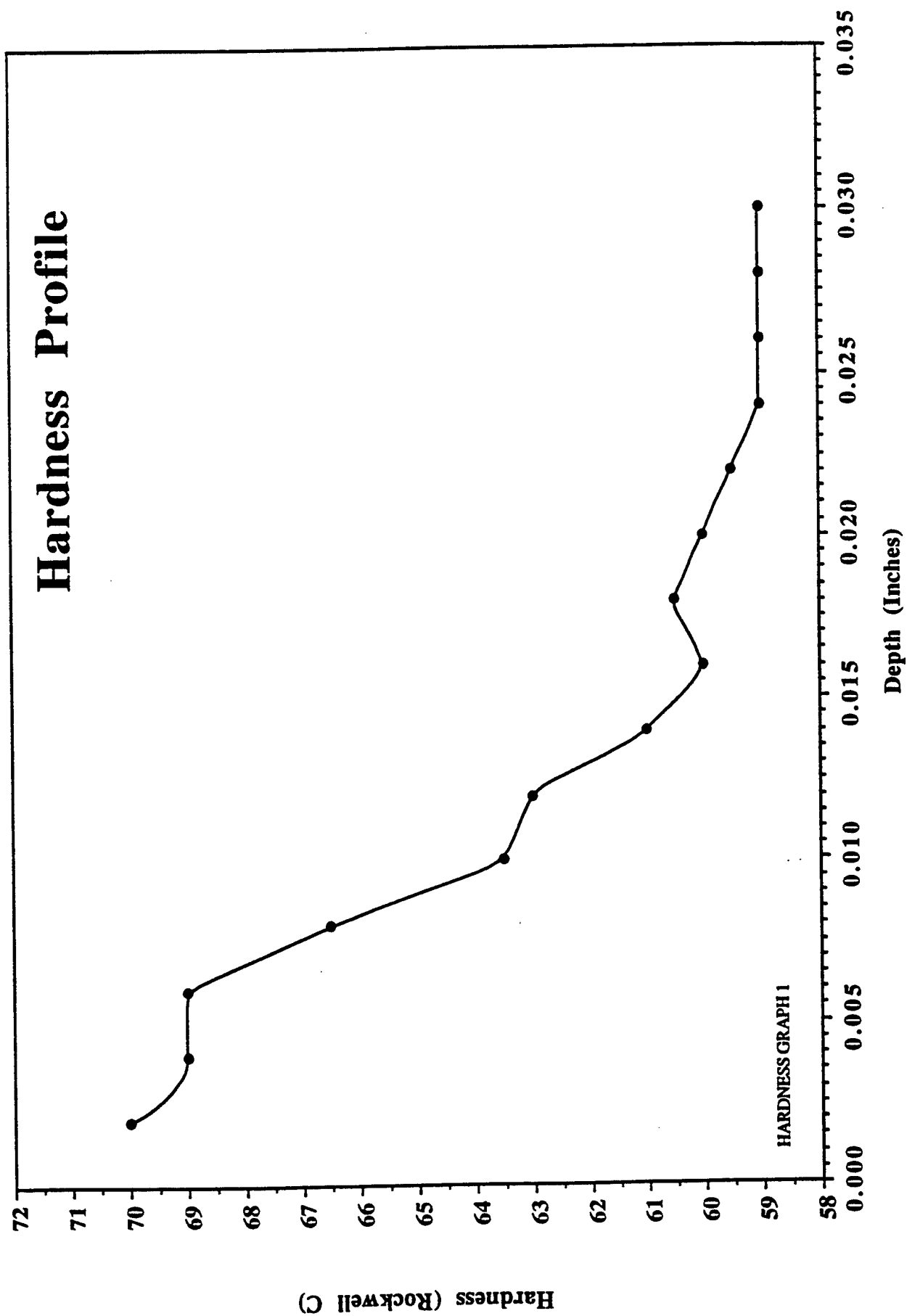


Figure 4.2.1-9 M50 Nitrided per the Lindure Process,  
975F in a Gas Retort Furnace

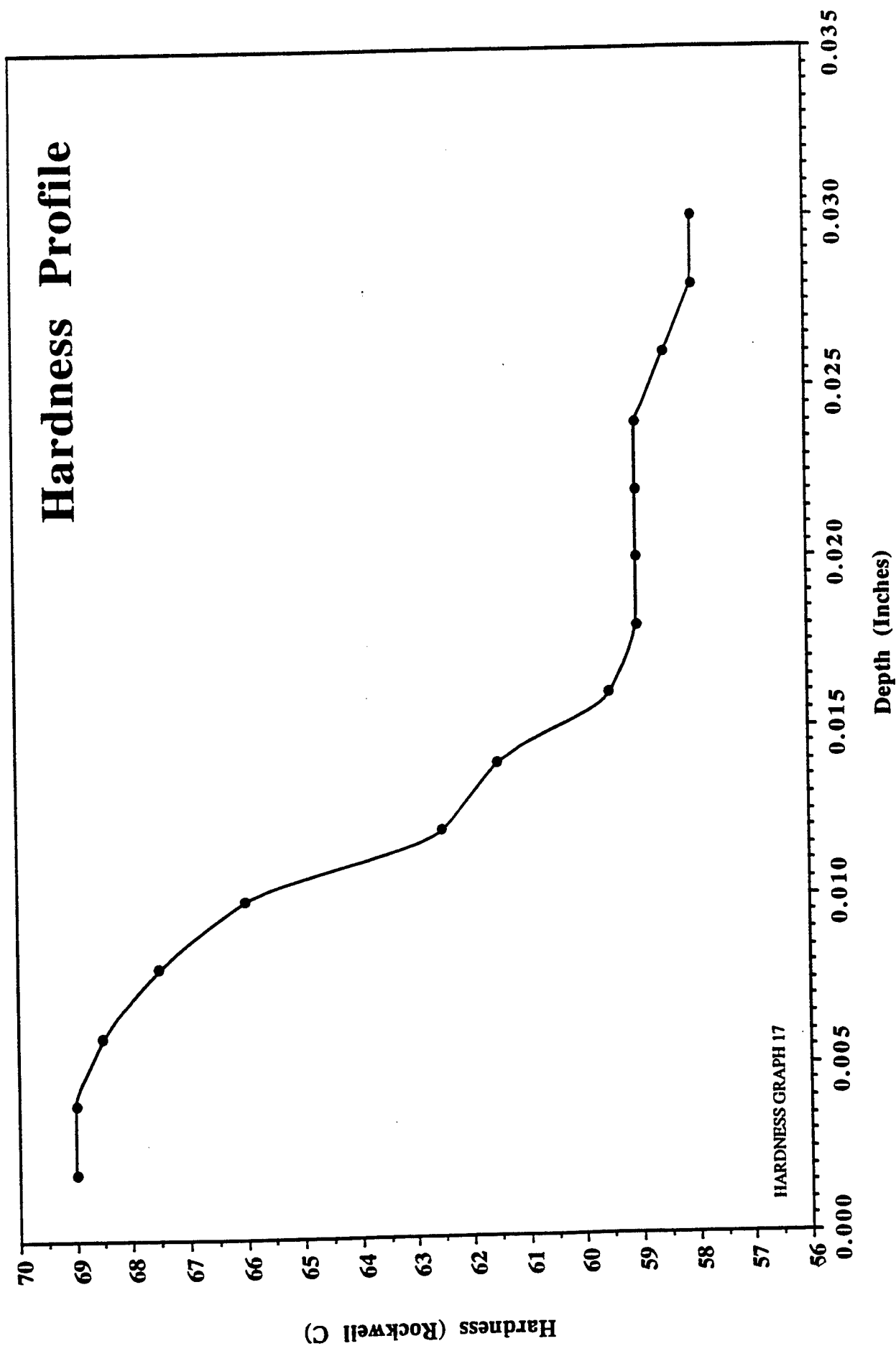


Figure 4.2.1-10 M50 Nitrided 32 Hours, Low Dissociation Rate,  
1000F in a Fluidized Bed Furnace

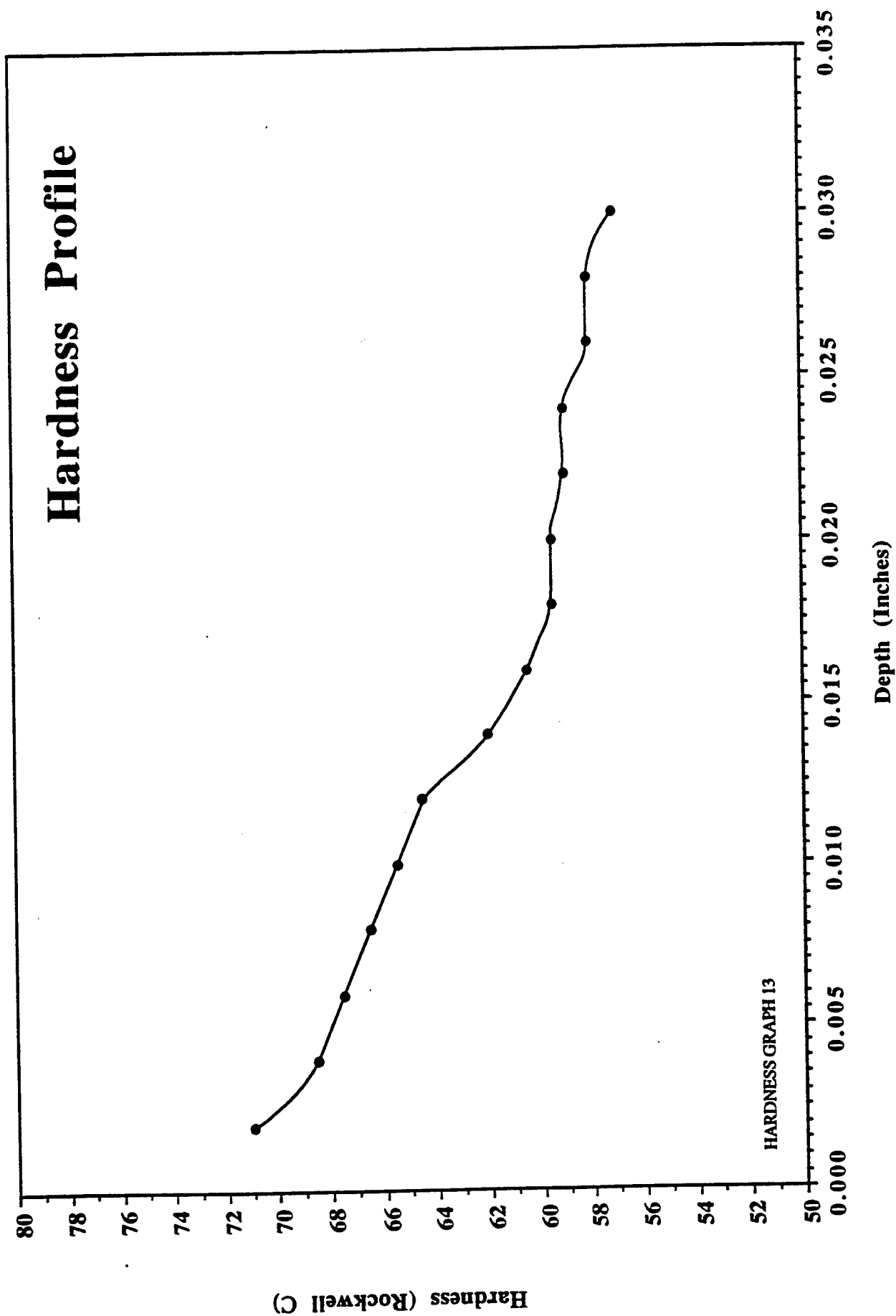


Figure 4.2.1-11 M50 Nitrided 60 Hours, 50% Dissociation Rate, 1000F in a Gas Retort Furnace

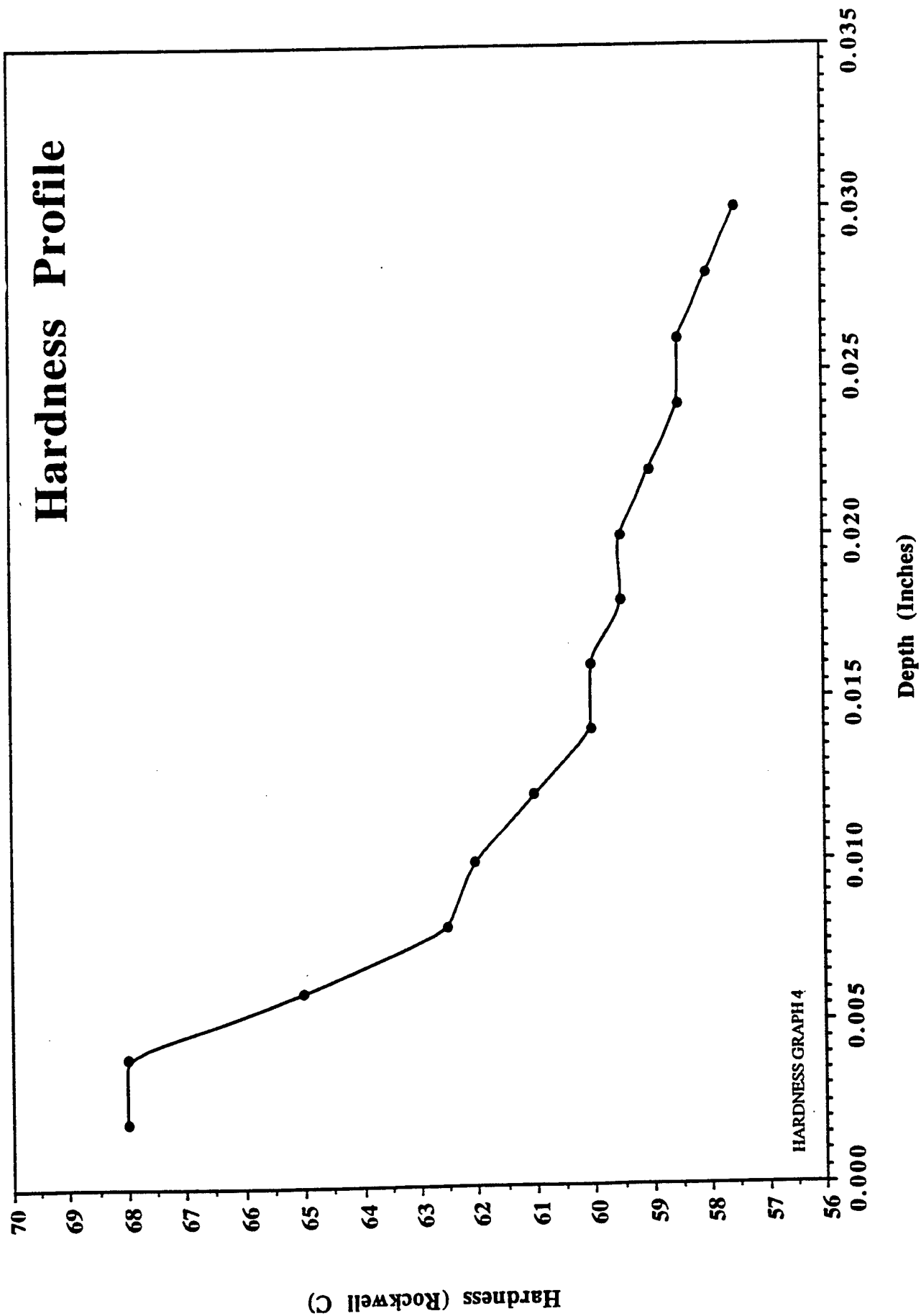


Figure 4.2.1-12 M50 NiL Nitrided 16 Hours, Low Dissociation Rate,  
975F in a Fluidized Bed Furnace

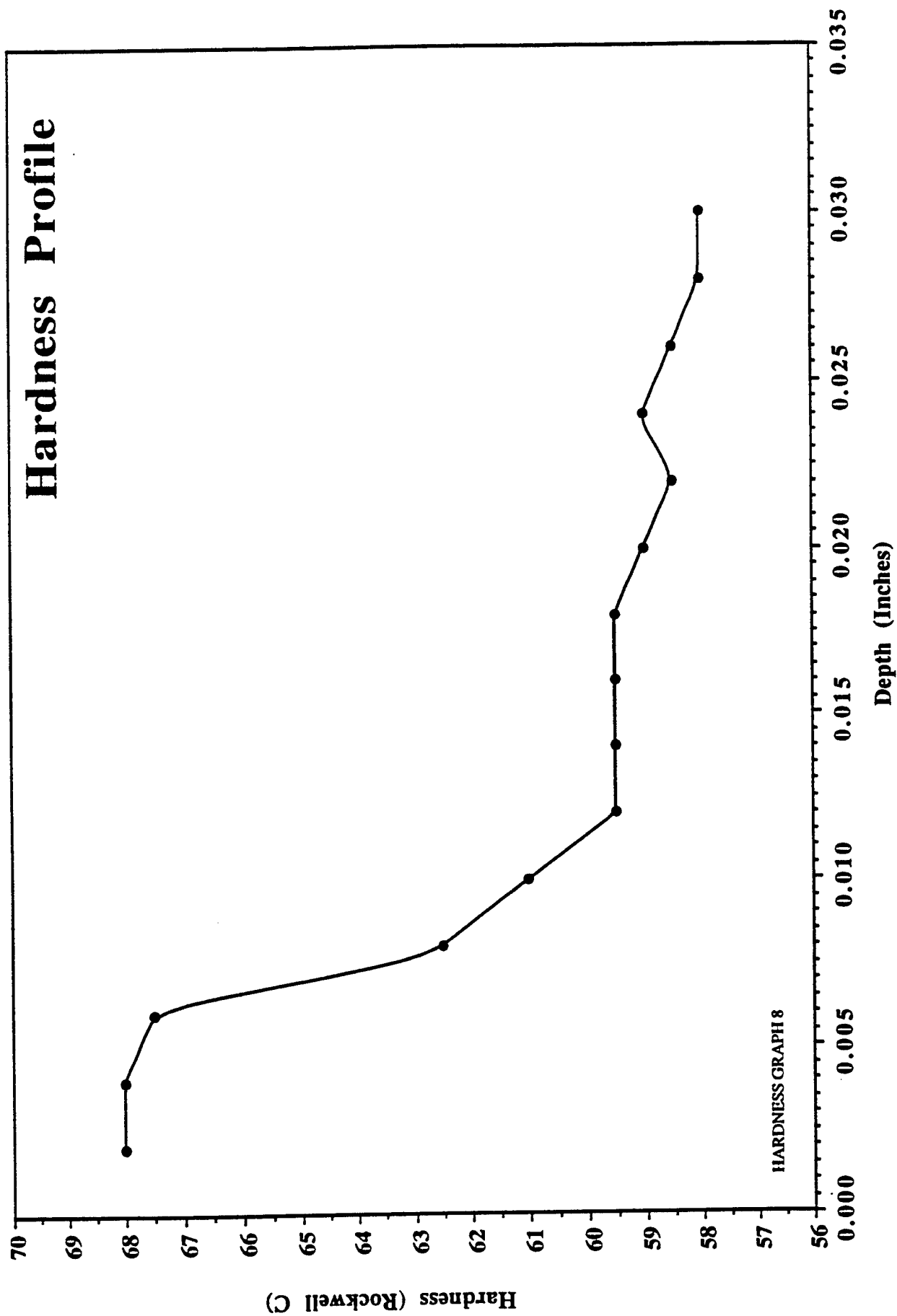


Figure 4.2.1-13 M50 NiL Nitrided 32 Hours, Low Dissociation Rate,  
975F in a Fluidized Bed Furnace



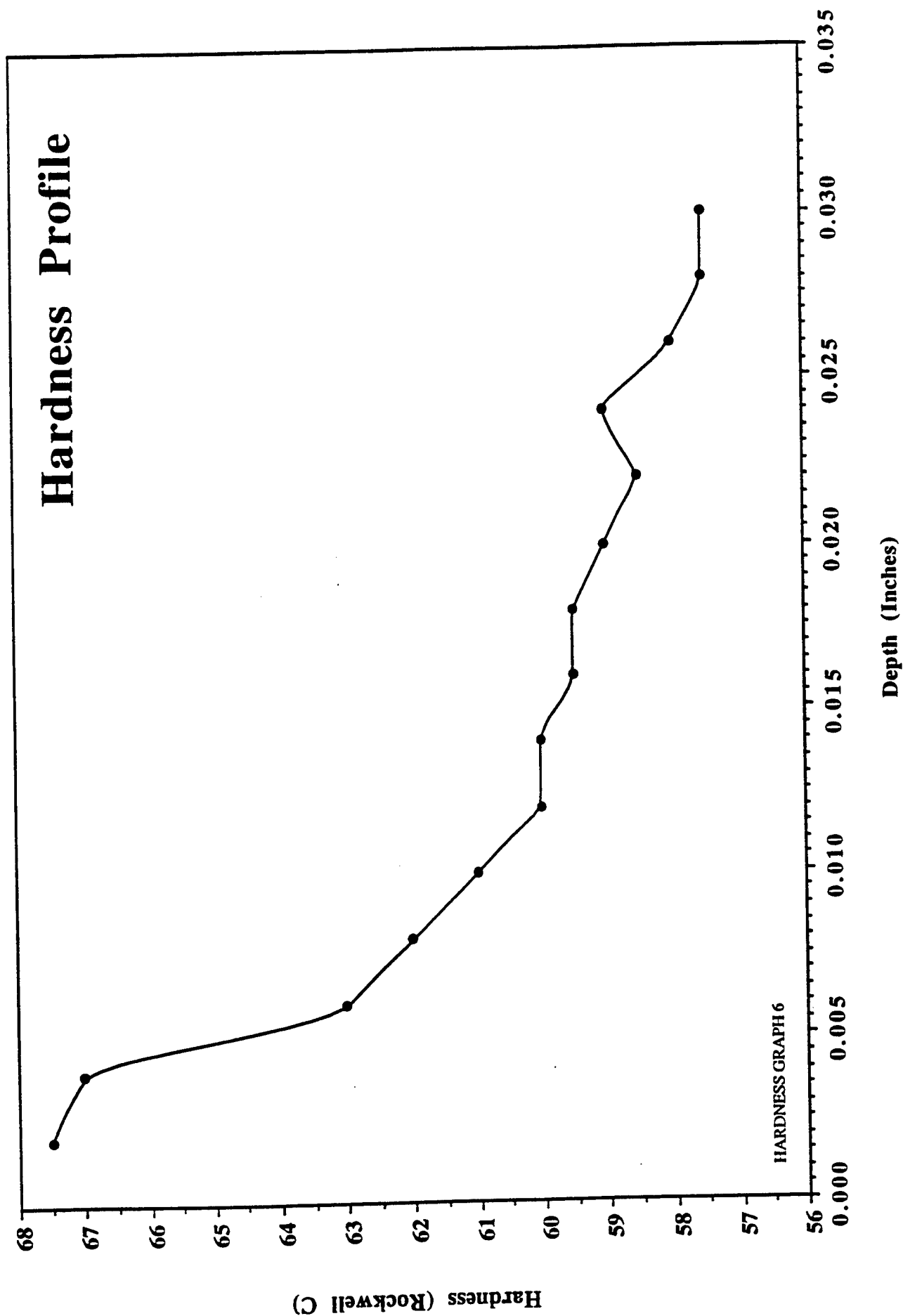


Figure 4.2.1-14 M50 NiL Nitrided 16 Hours, High Dissociation Rate,  
975F in a Fluidized Bed Furnace

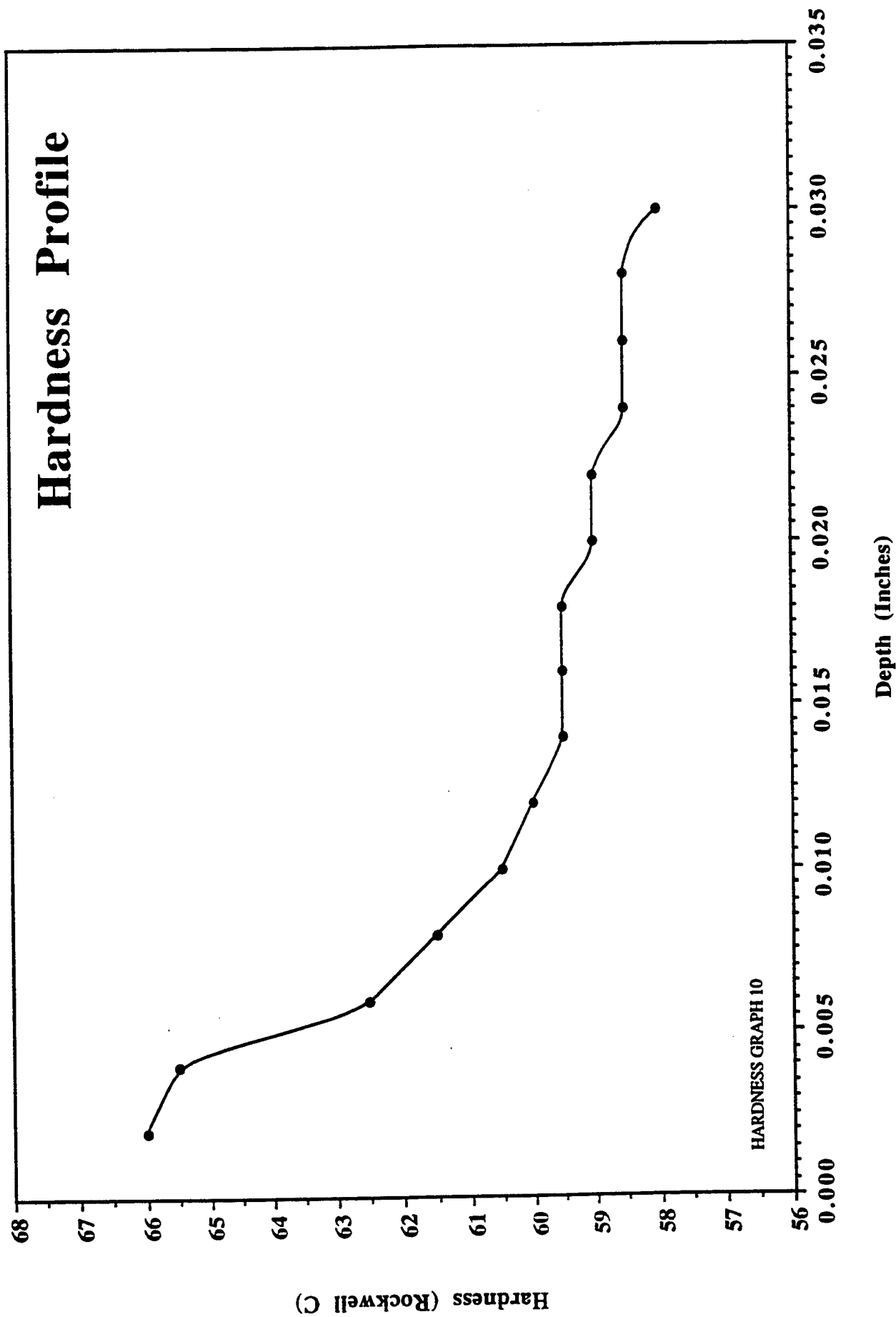


Figure 4.2.1-15 M50 NiL Nitrided 32 Hours, High Dissociation Rate, 975F in a Fluidized Bed Furnace

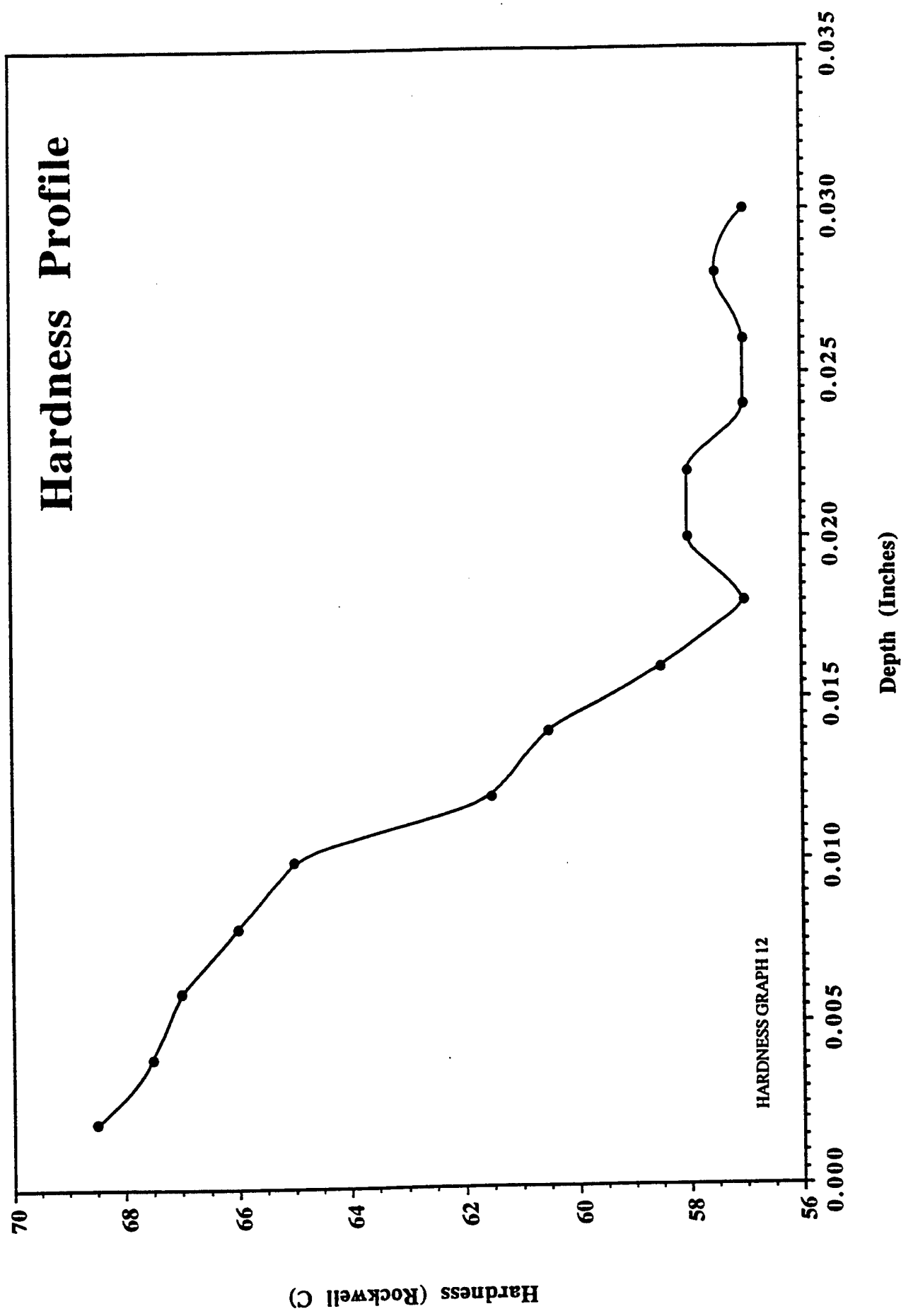
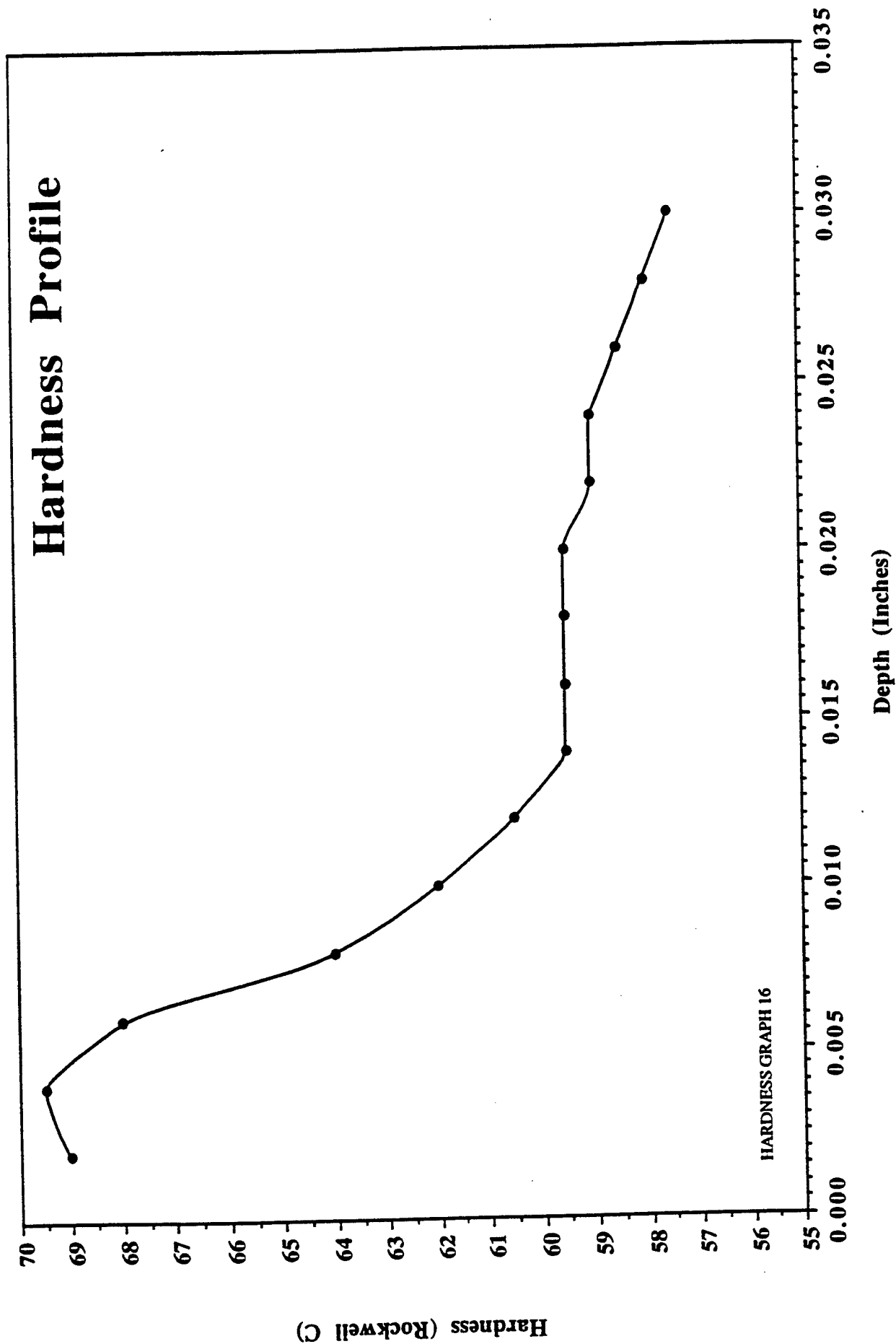


Figure 4.2.1-16 M50 NiL Nitrided 60 Hours, 50% Dissociation Rate, in a Gas Retort Furnace



**Figure 4.2.1-17 M50 NiL Nitrided 16 Hours, High Dissociation Rate then 16 Hours at a Higher Dissociation Rate, 975F in a Fluidized Bed Furnace**

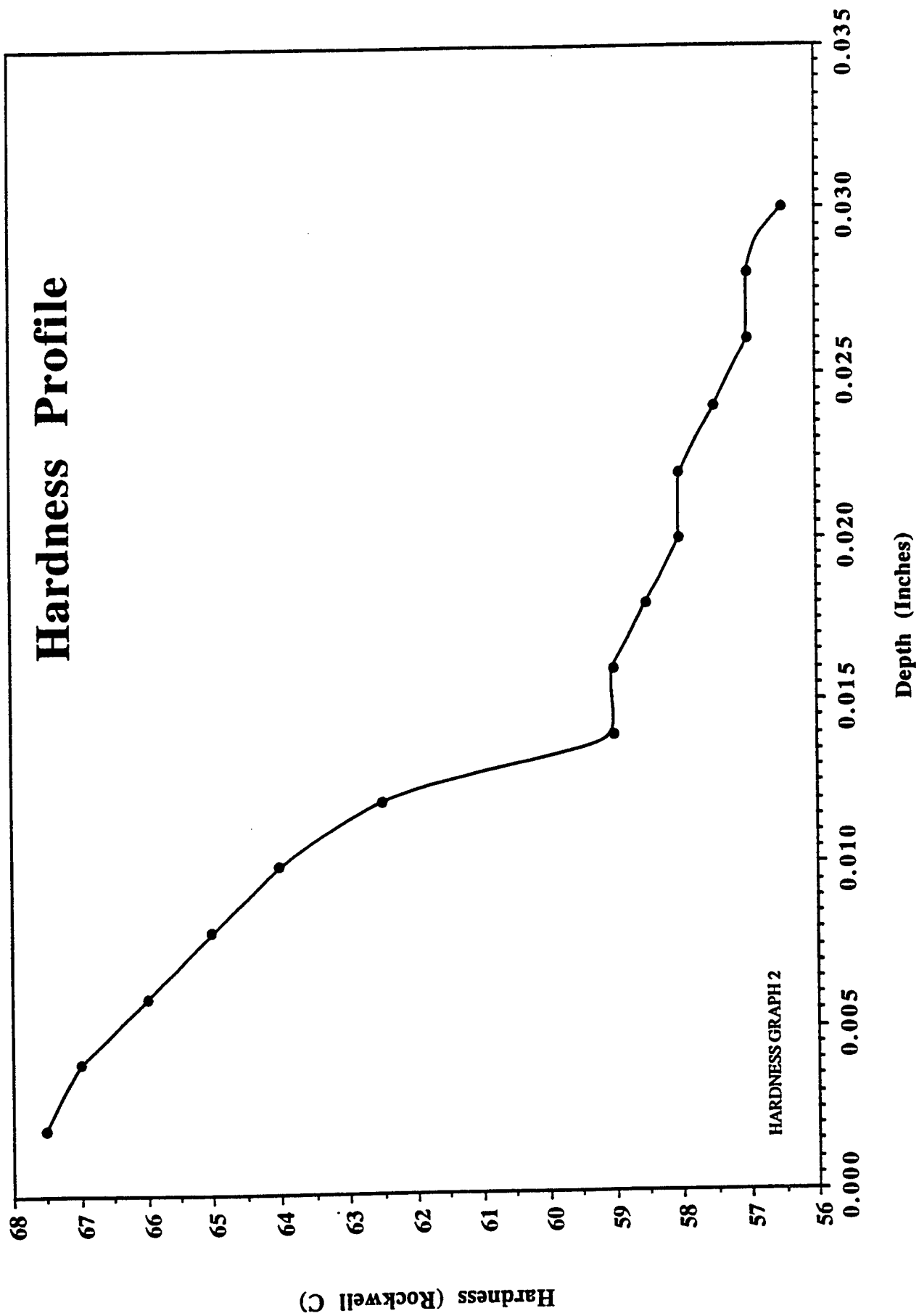


Figure 4.2.1-18 M50 NiL Nitrided per the Lindure Process,  
975F in a Gas Retort Furnace

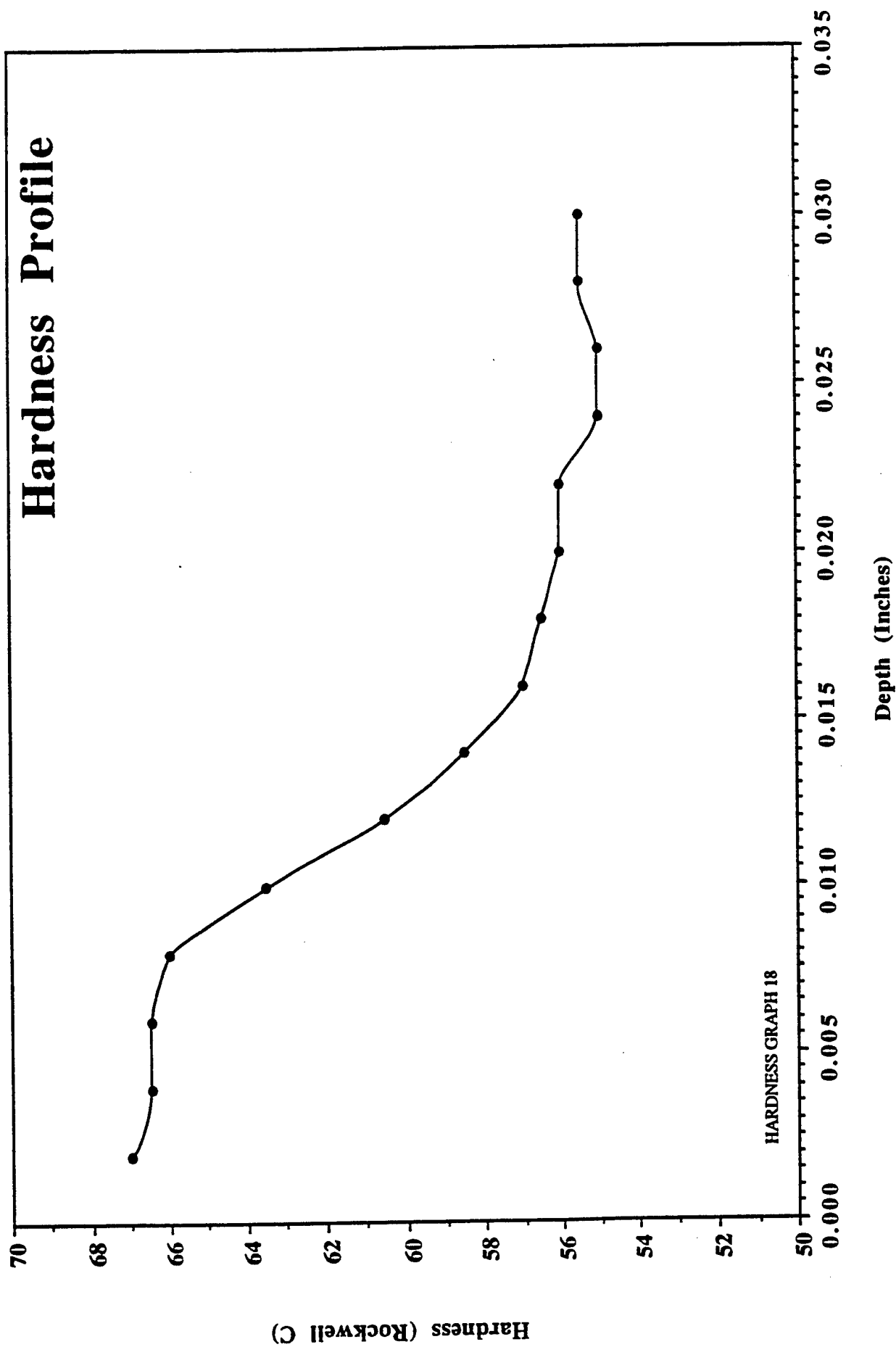
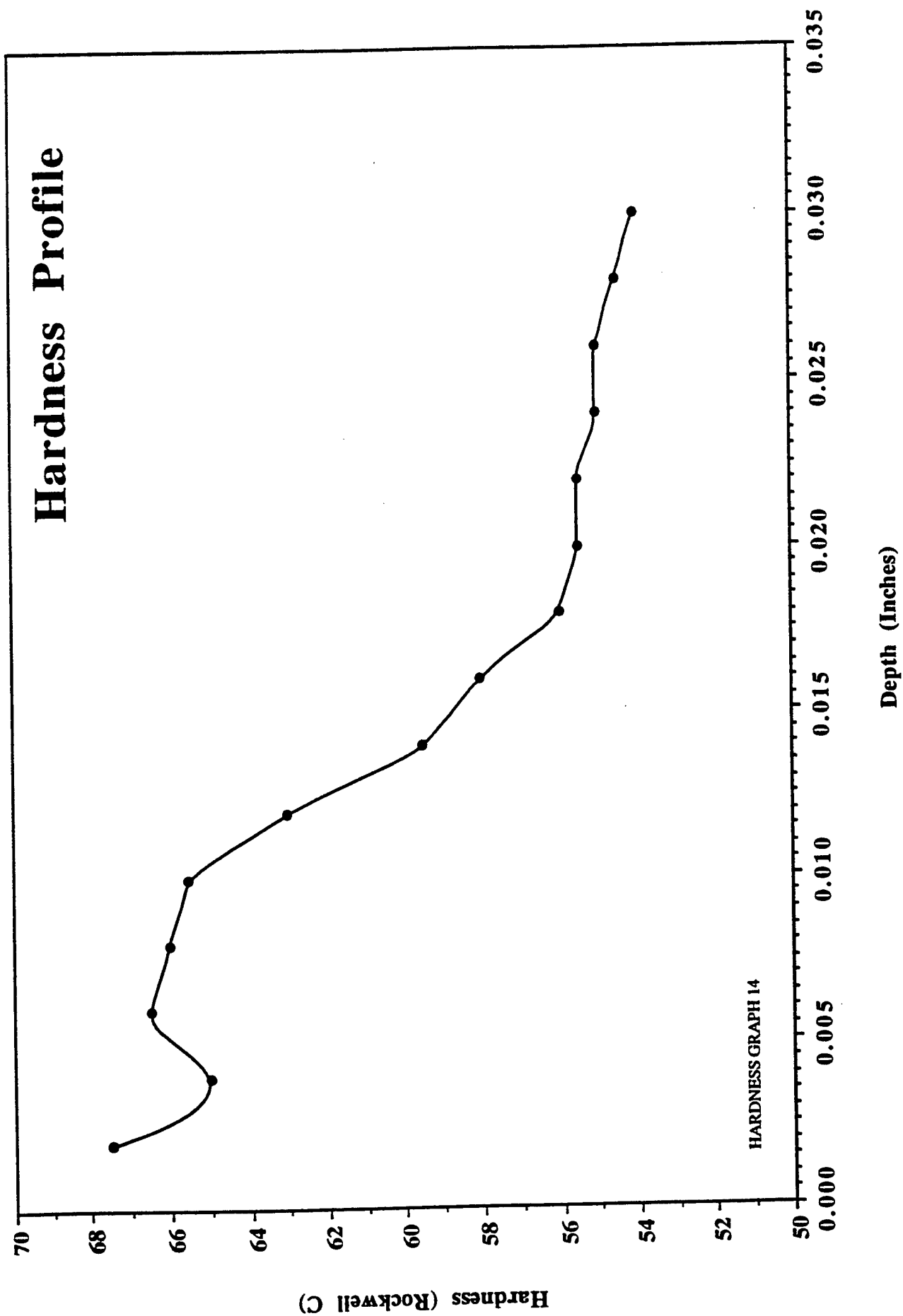


Figure 4.2.1-19 M50 NiL Nitrided 32 Hours, Low Dissociation Rate,  
1000F in a Fluidized Bed Furnace



**Figure 4.2.1-20 M50 NiL Nitrided 60 Hours, 50 % Dissociation Rate, 1000F in a Gas Retort Furnace**

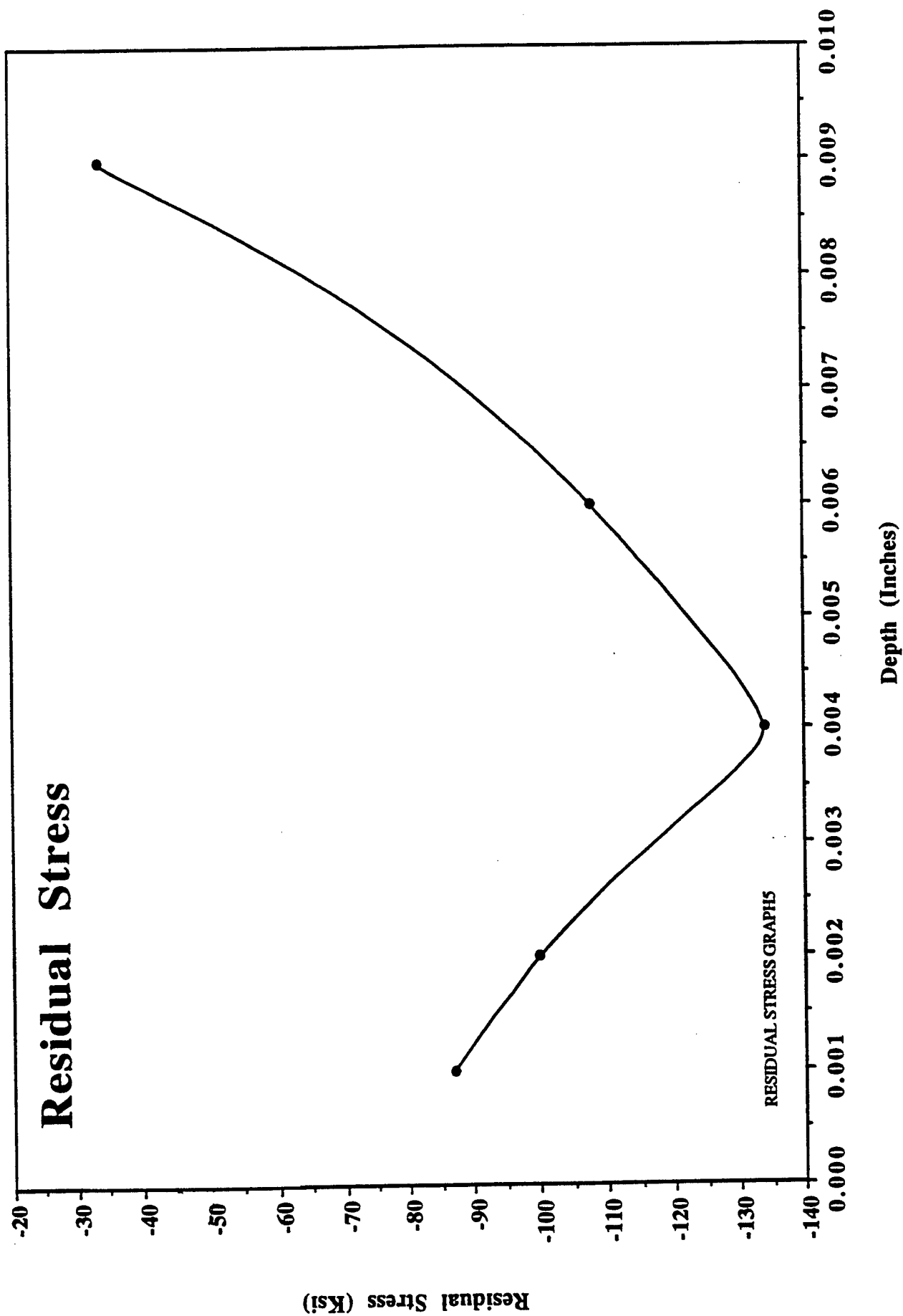


Figure 4.2.2-1 M50 Nitrided 16 Hours, Low Dissociation Rate,  
975F in a Fluidized Bed Furnace



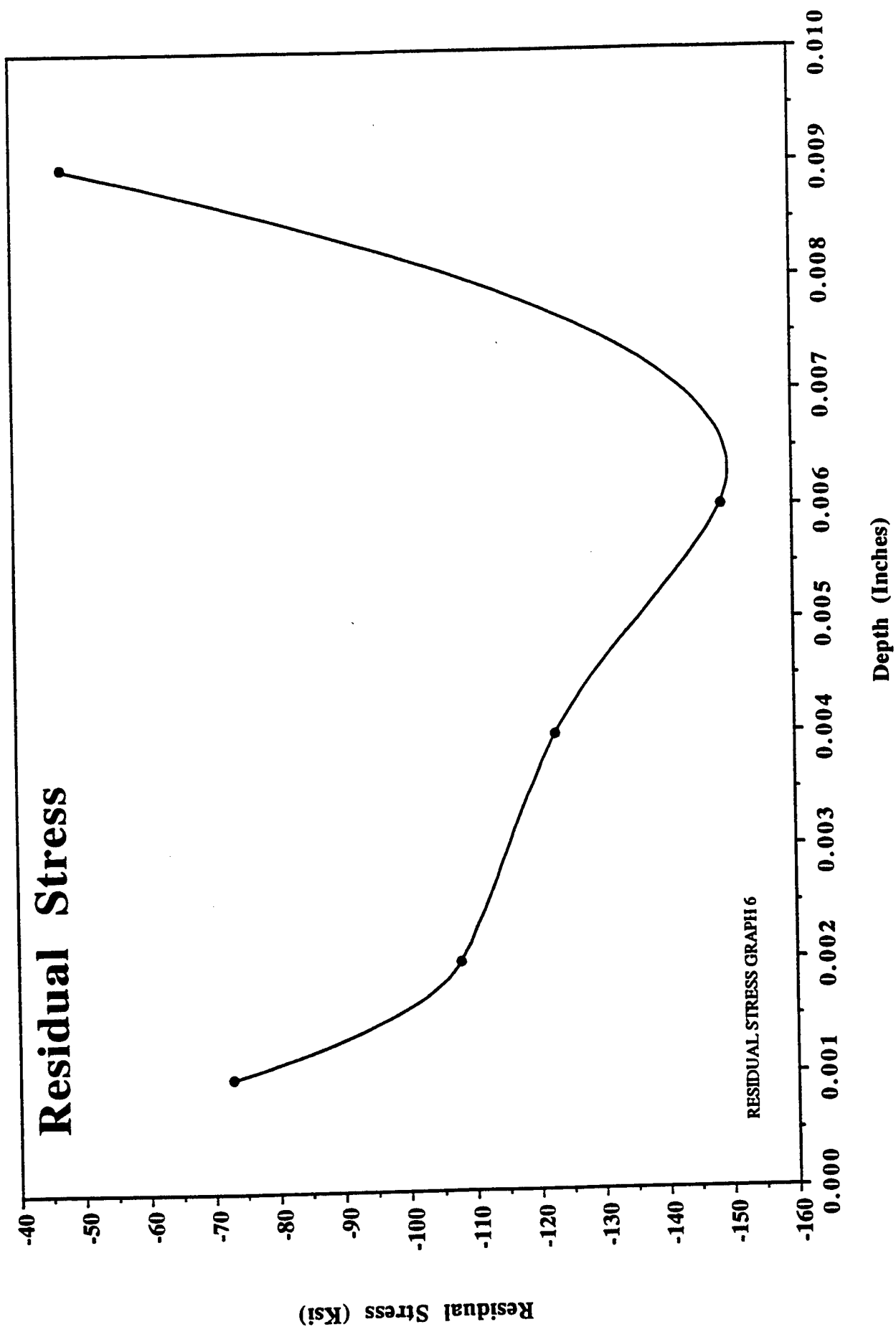
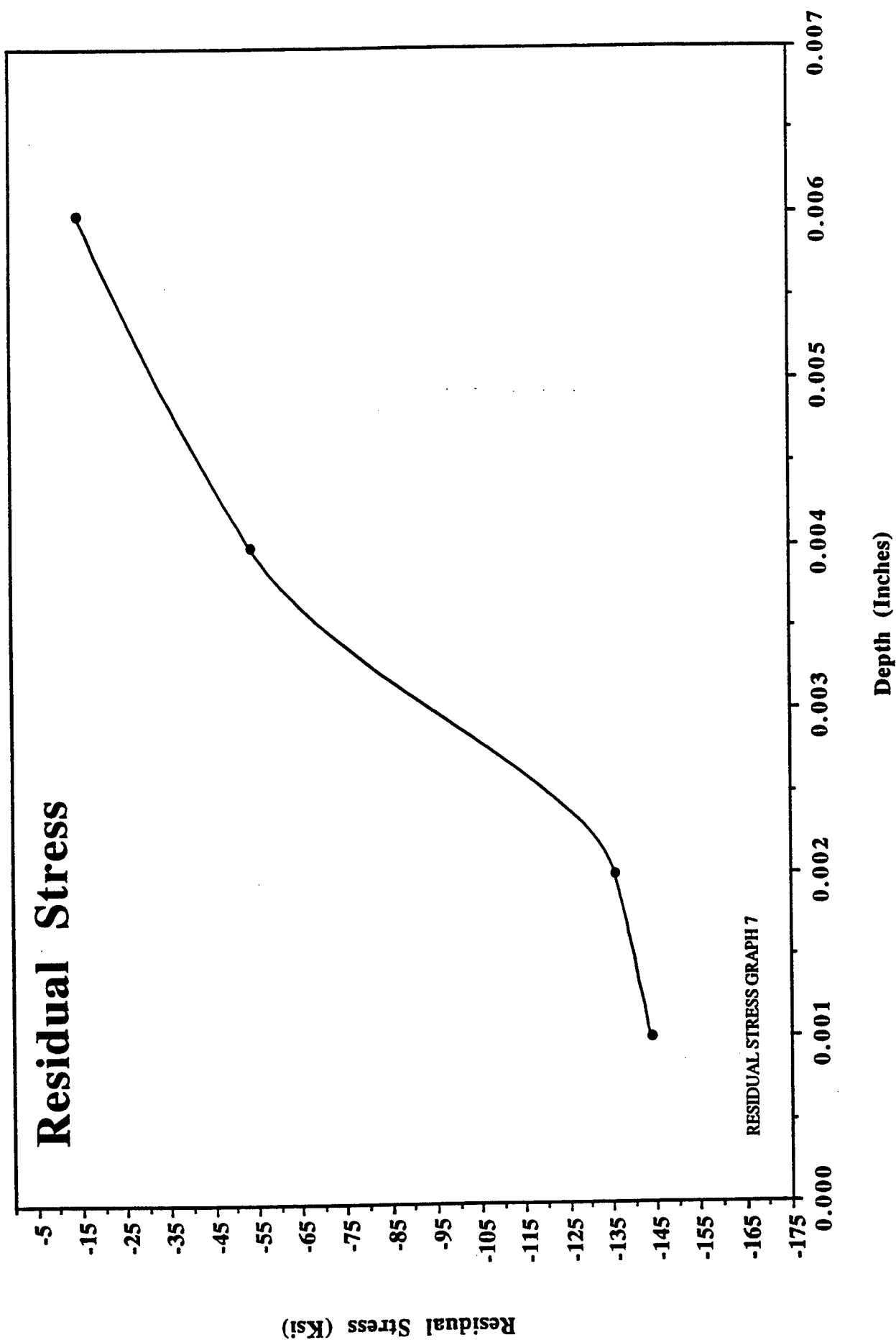


Figure 4.2.2-2 M50 Nitrided 32 Hours, Low Dissociation Rate, 975F in a Fluidized Bed Furnace



**Figure 4.2.2-3 M50 Nitrided 16 Hours, High Dissociation Rate, 975F in a Fluidized Bed Furnace**

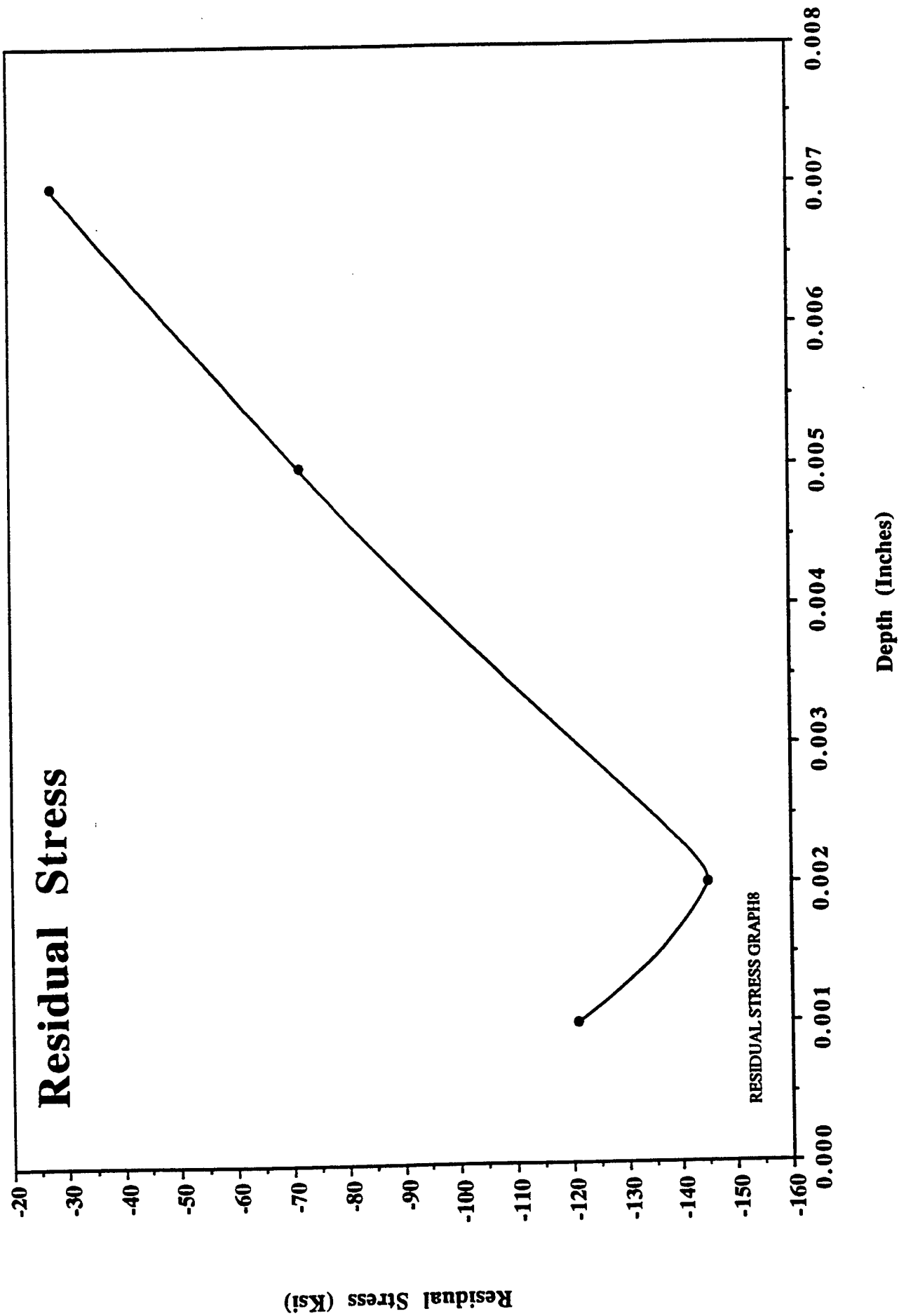


Figure 4.2.2-4 M50 Nitrided 32 Hours, High Dissociation Rate, 975F in a Fluidized Bed Furnace

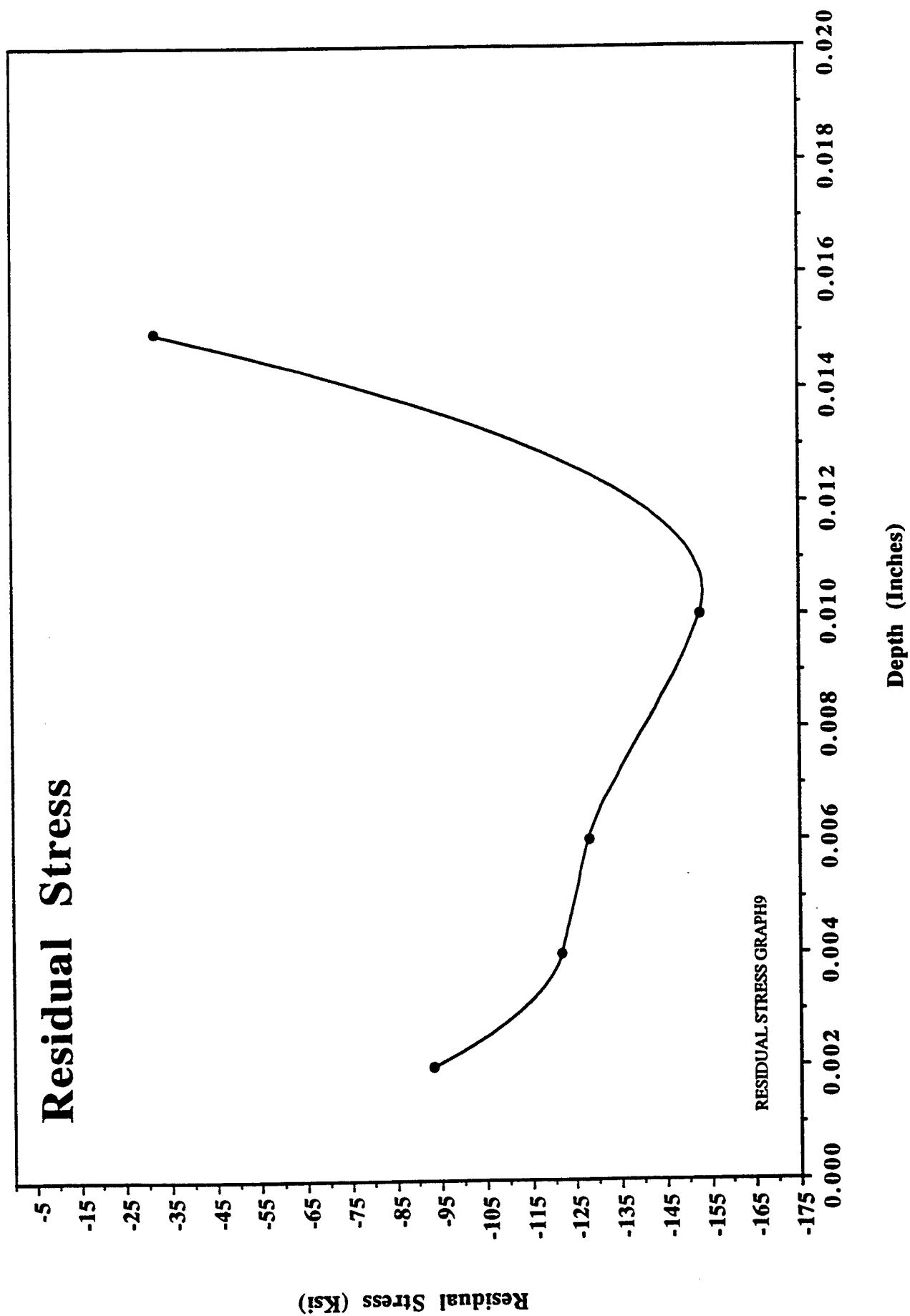


Figure 4.2.2-5 M50 Nitrided 60 Hours, 50 % Dissociation Rate  
in a Gas Retort Furnace

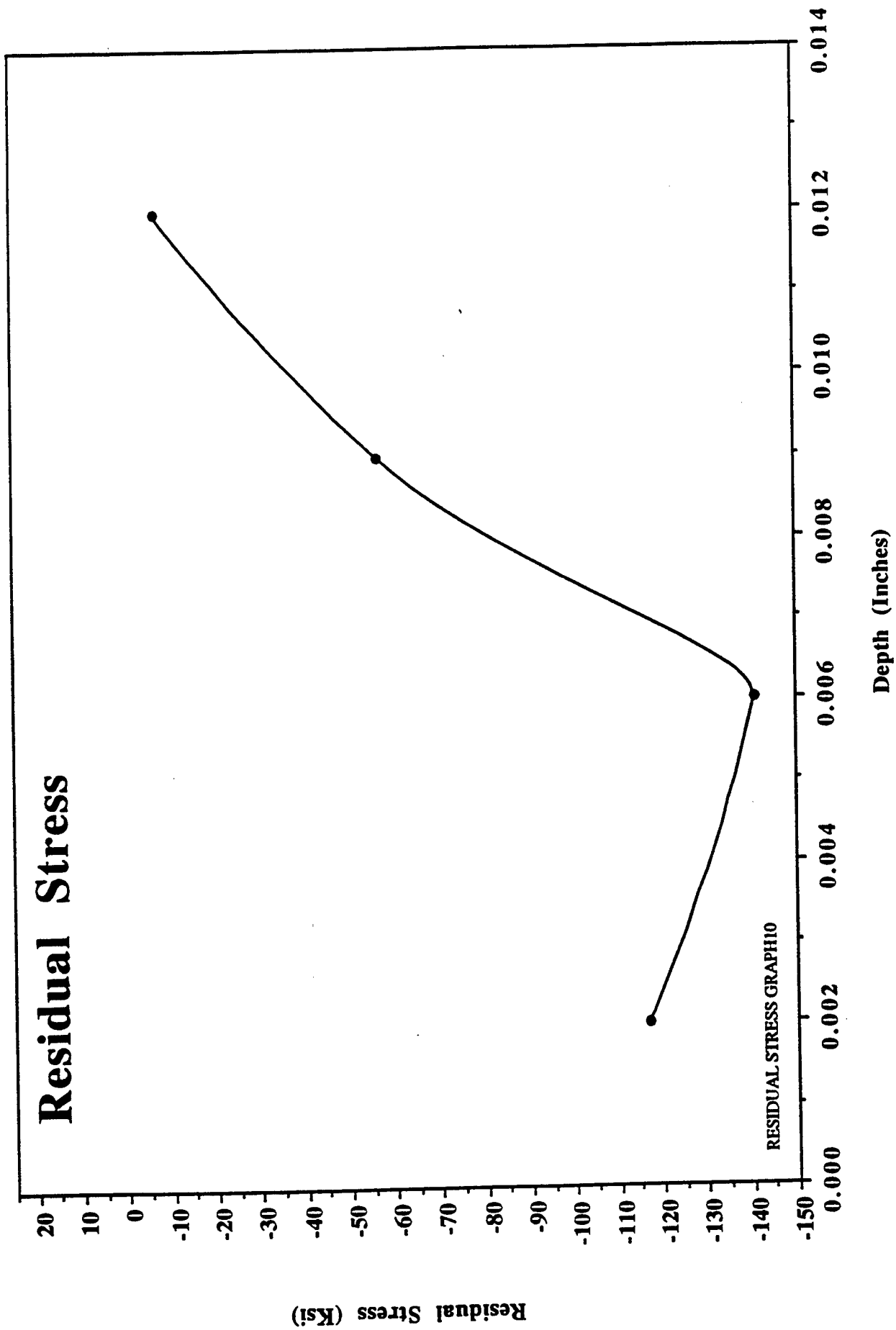


Figure 4.2.2-6 M50 Nitrided 16 Hours, High Dissociation Rate  
Then Another 16 Hours at Higher Dissociation  
Rate, 975F in a Fluidized Bed Furnace

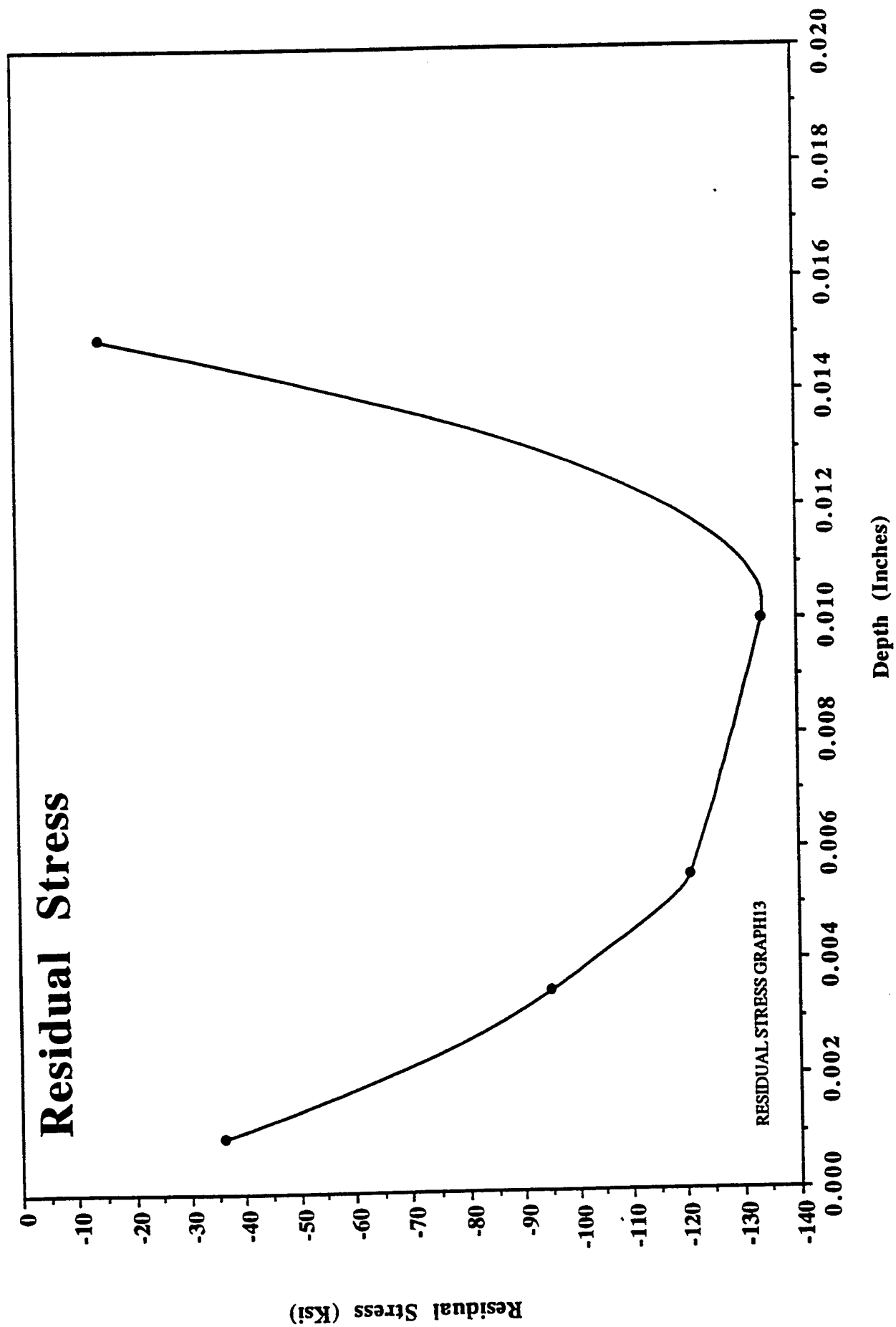


Figure 4.2.2-7 M50 Nitrided per the Lindure Process,  
975F in a Gas Retort Furnace

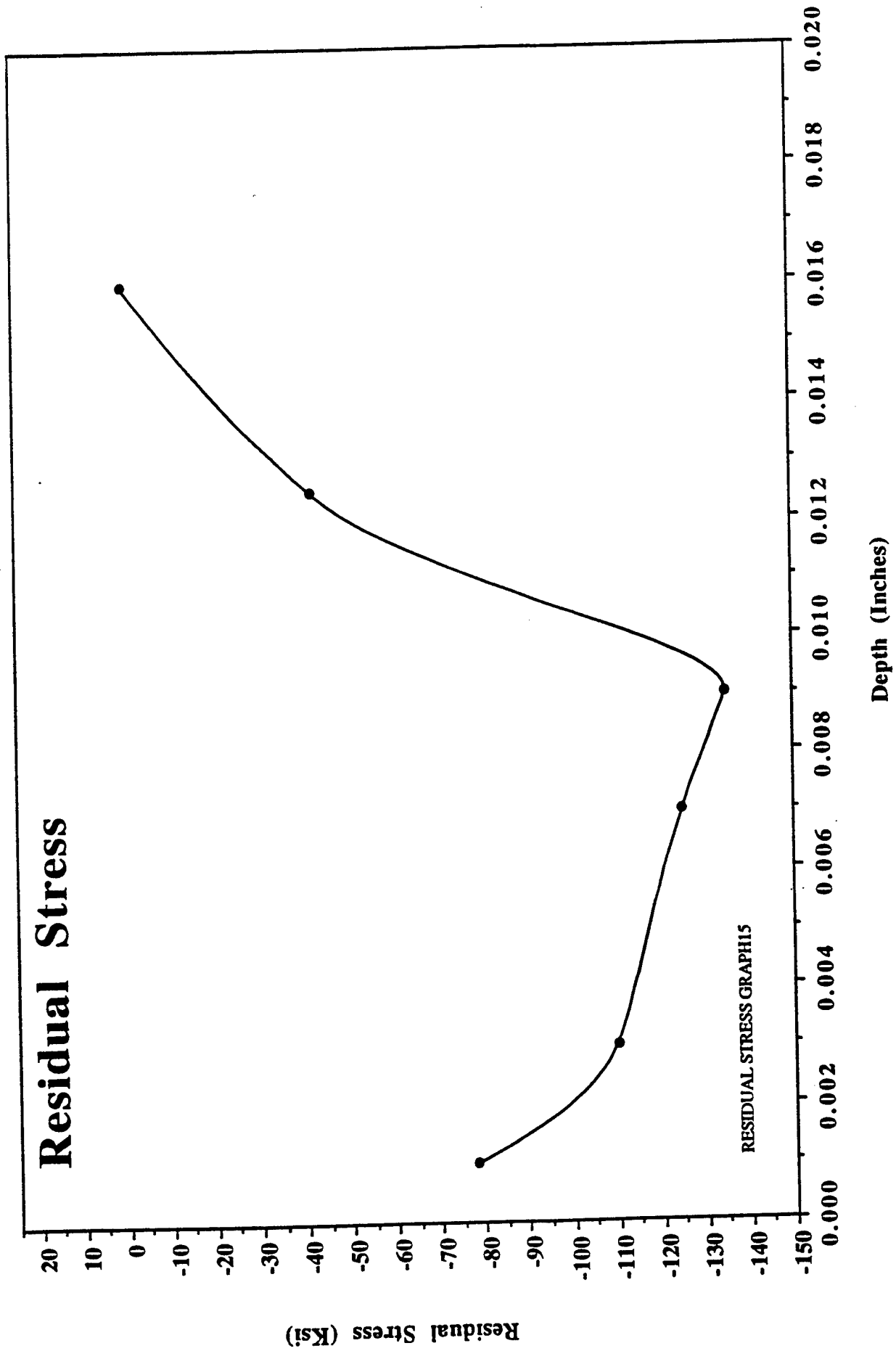


Figure 4.2.2-8 M50 Nitrided 32 Hours, Low Dissociation Rate  
1000F in a Fluidized Bed Furnace

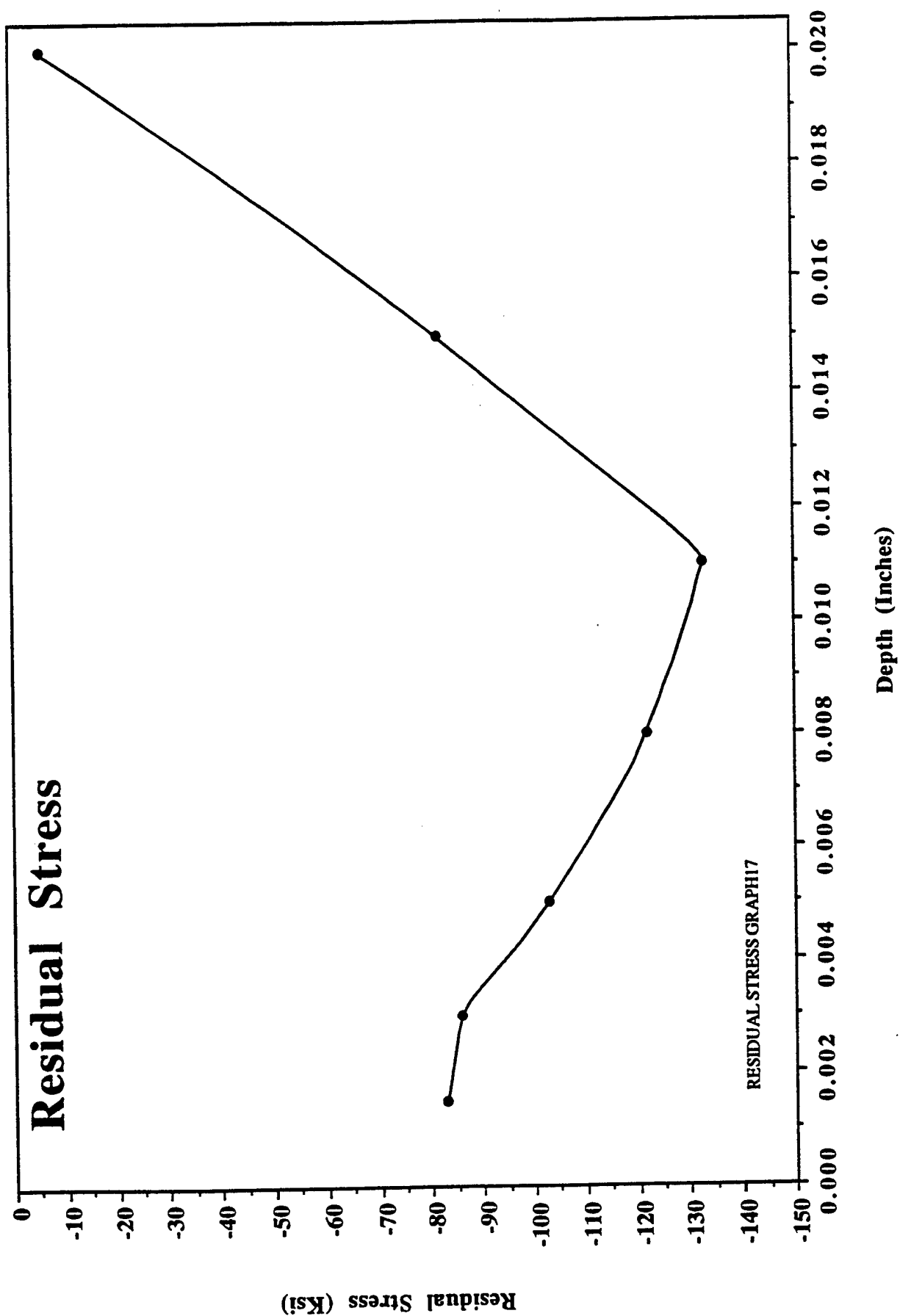


Figure 4.2.2-9 M50 Nitrided 60 Hours, 50% Dissociation Rate,  
1000F in a Gas Retort Furnace



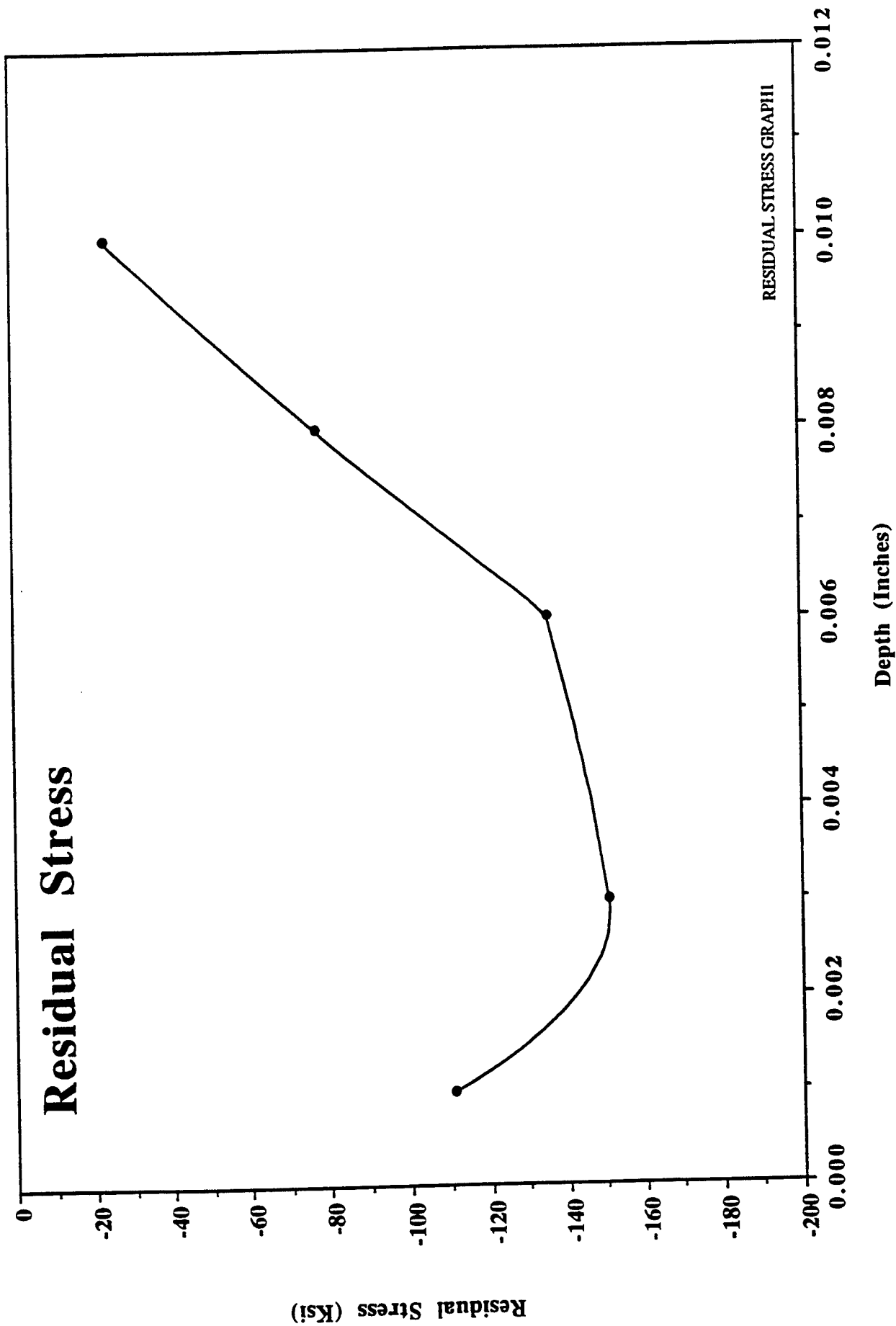


Figure 4.2.2-10 M50 NiL Nitrided 16 Hours, Low Dissociation Rate,  
975F in a Fluidized Bed Furnace

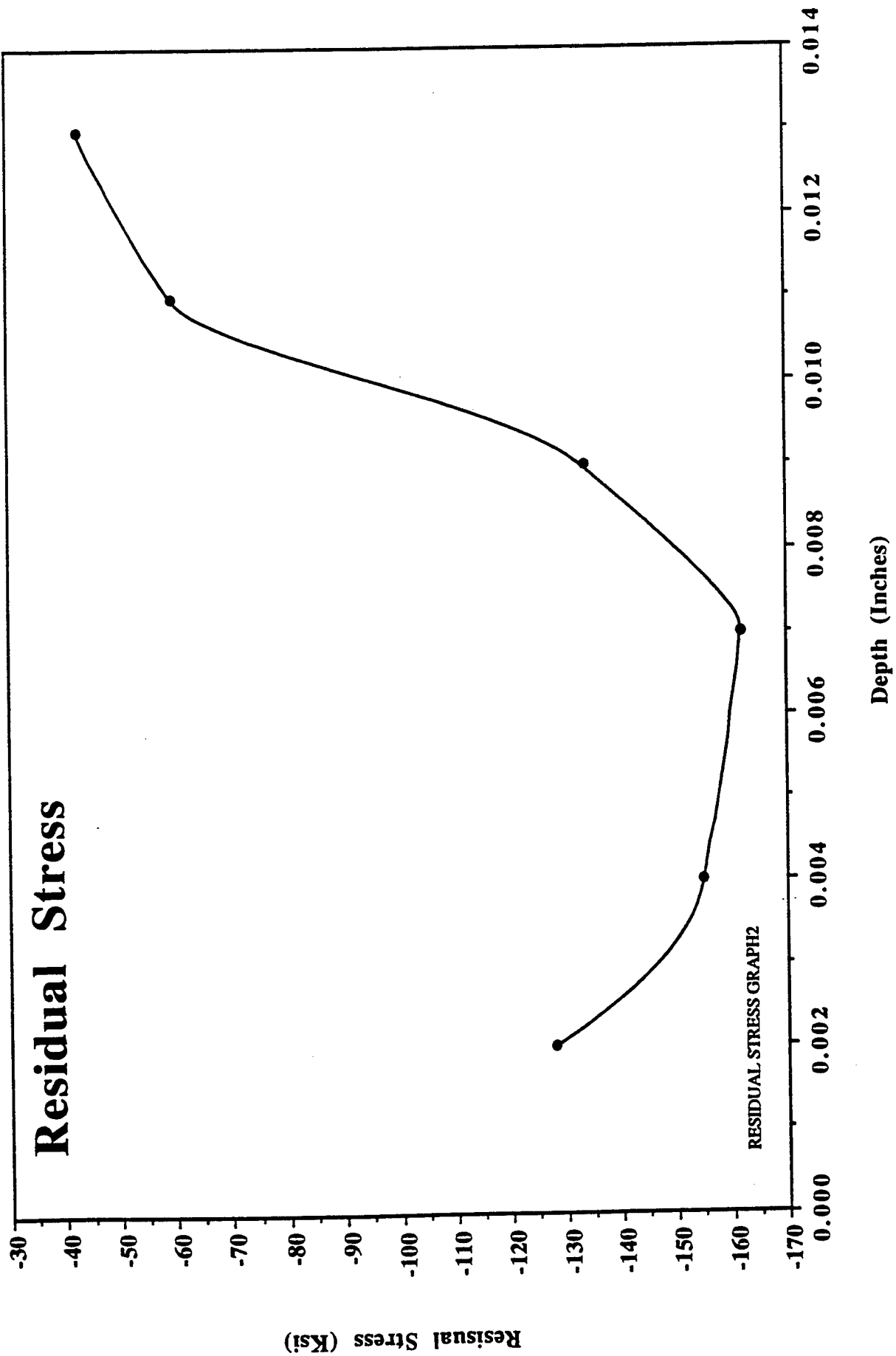
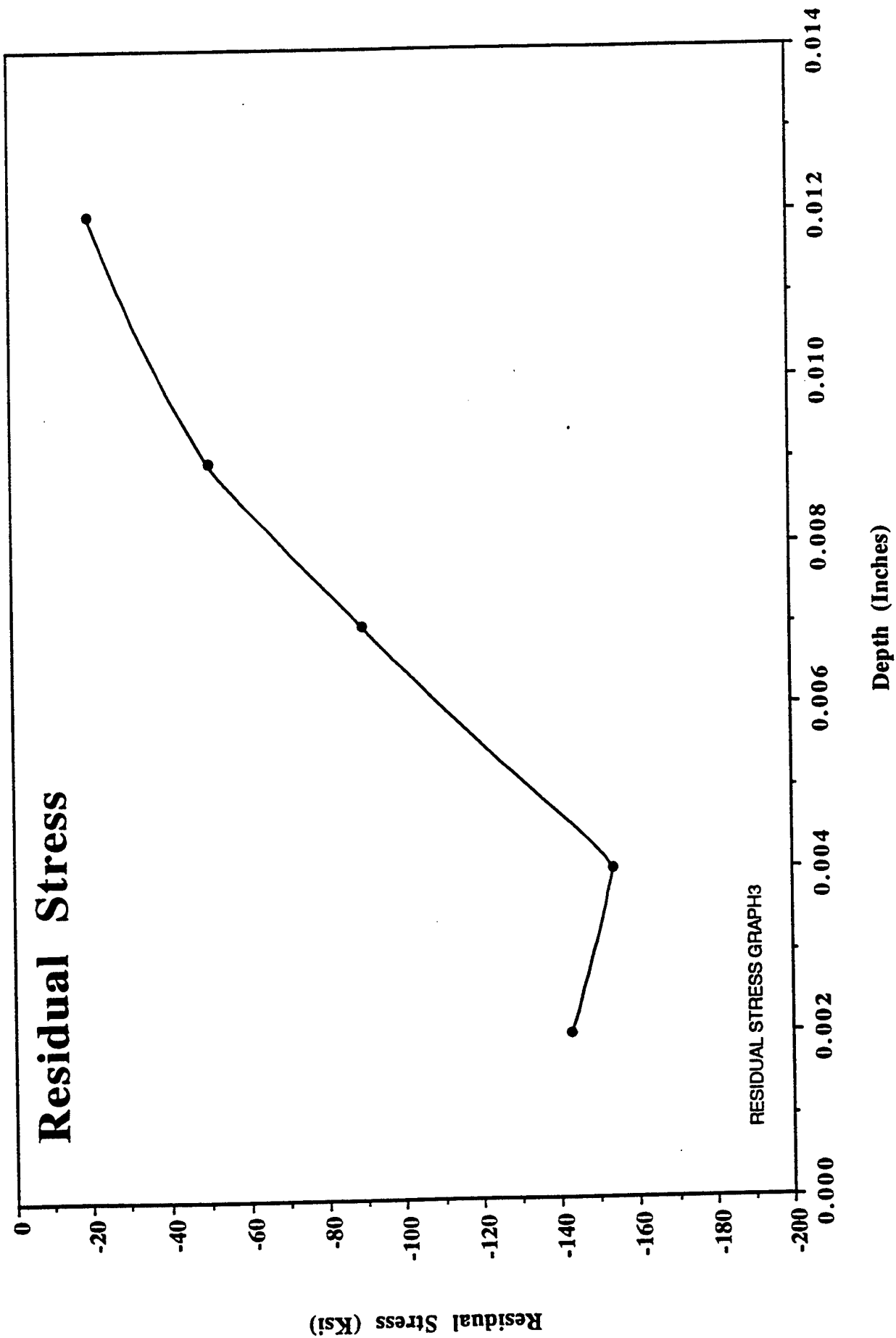


Figure 4.2.2-11 M50 NiL Nitrided 32 Hours, Low Dissociation Rate,  
975F in a Fluidized Bed Furnace



**Figure 4.2.2-12 M50 NiL Nitrided 16 Hours, High Dissociation Rate, 975F in a Fluidized Bed Furnace**

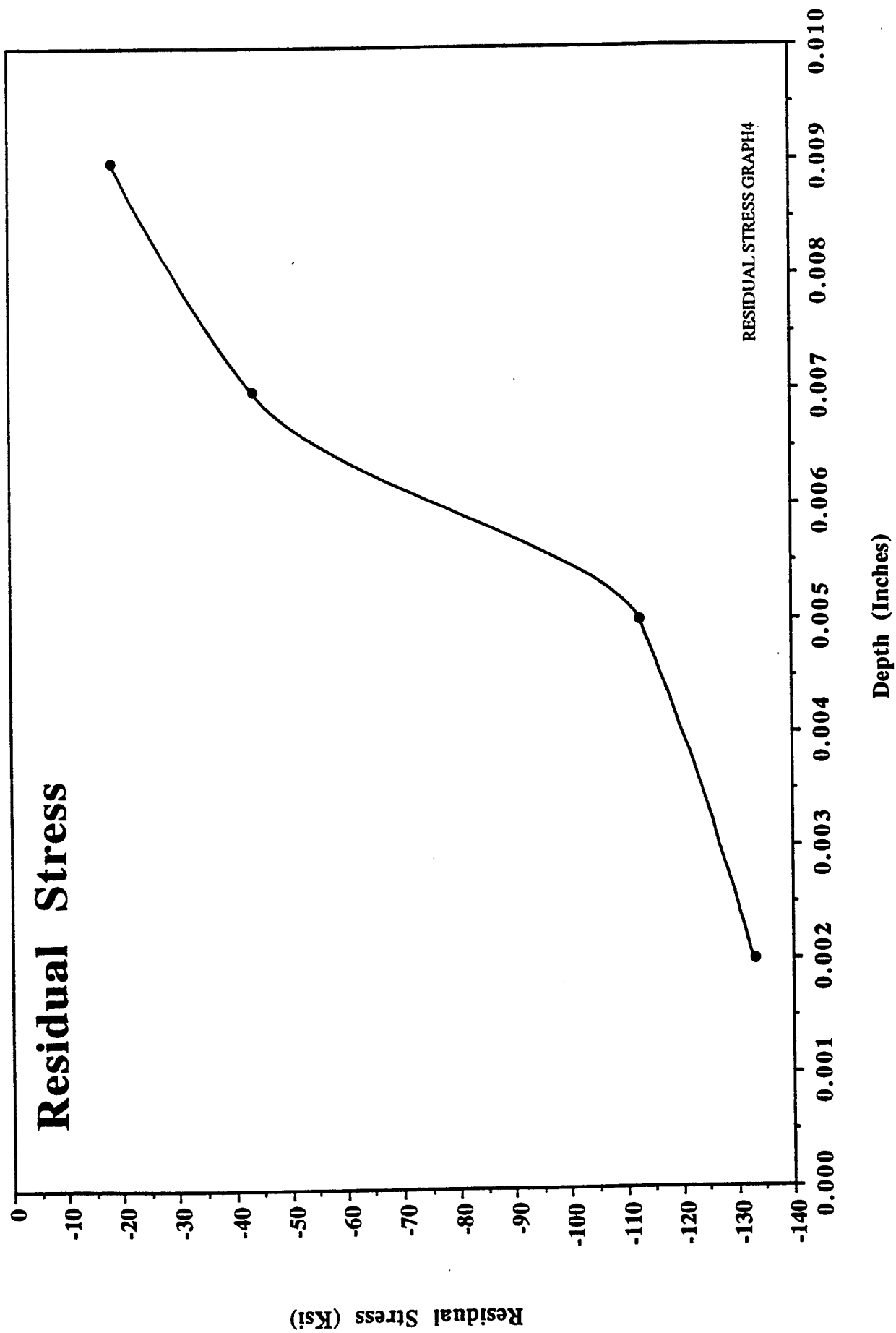


Figure 4.2.2-13 M50 NiL Nitrided 32 Hours, High Dissociation Rate,  
975F in a Fluidized Bed Furnace

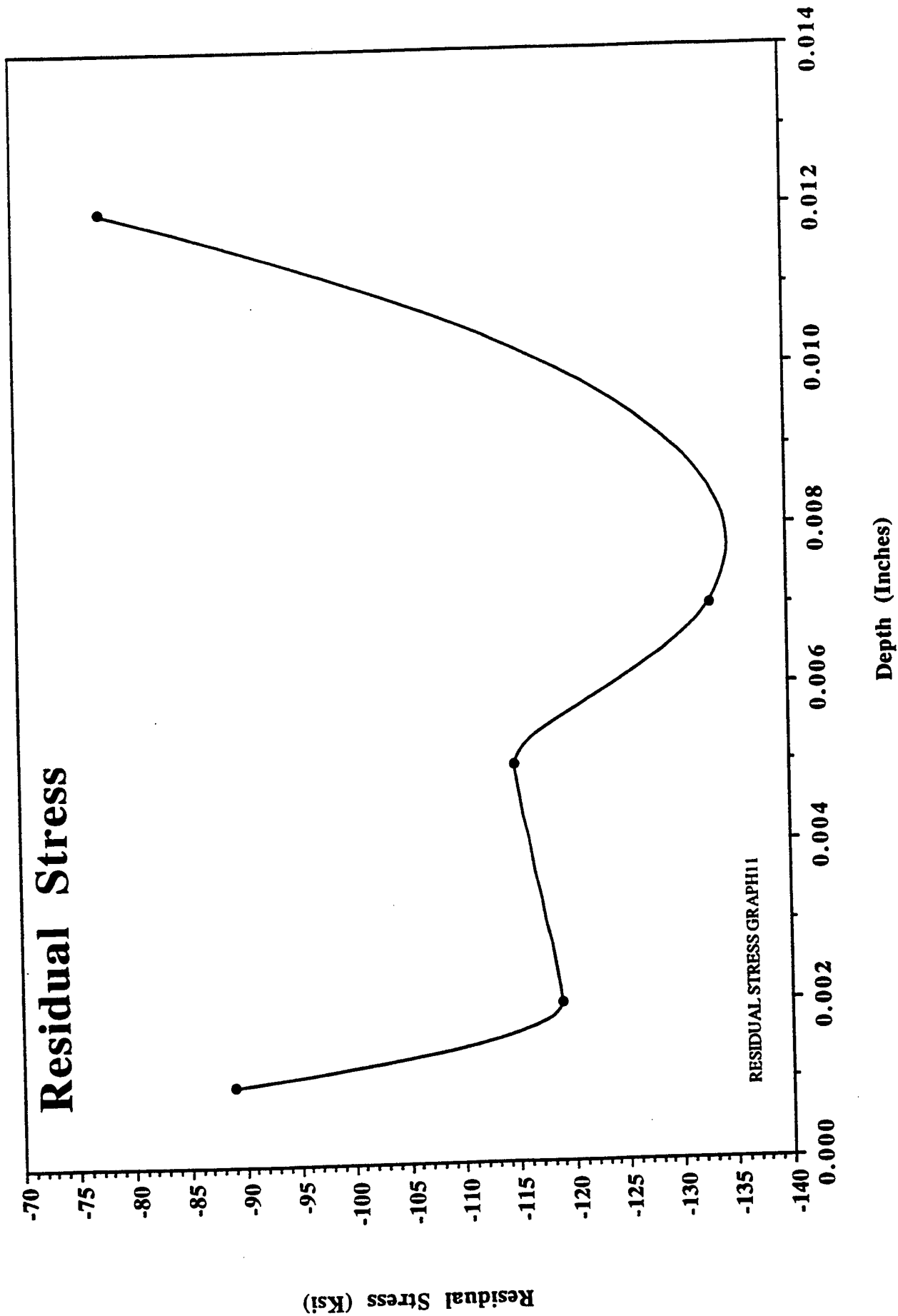
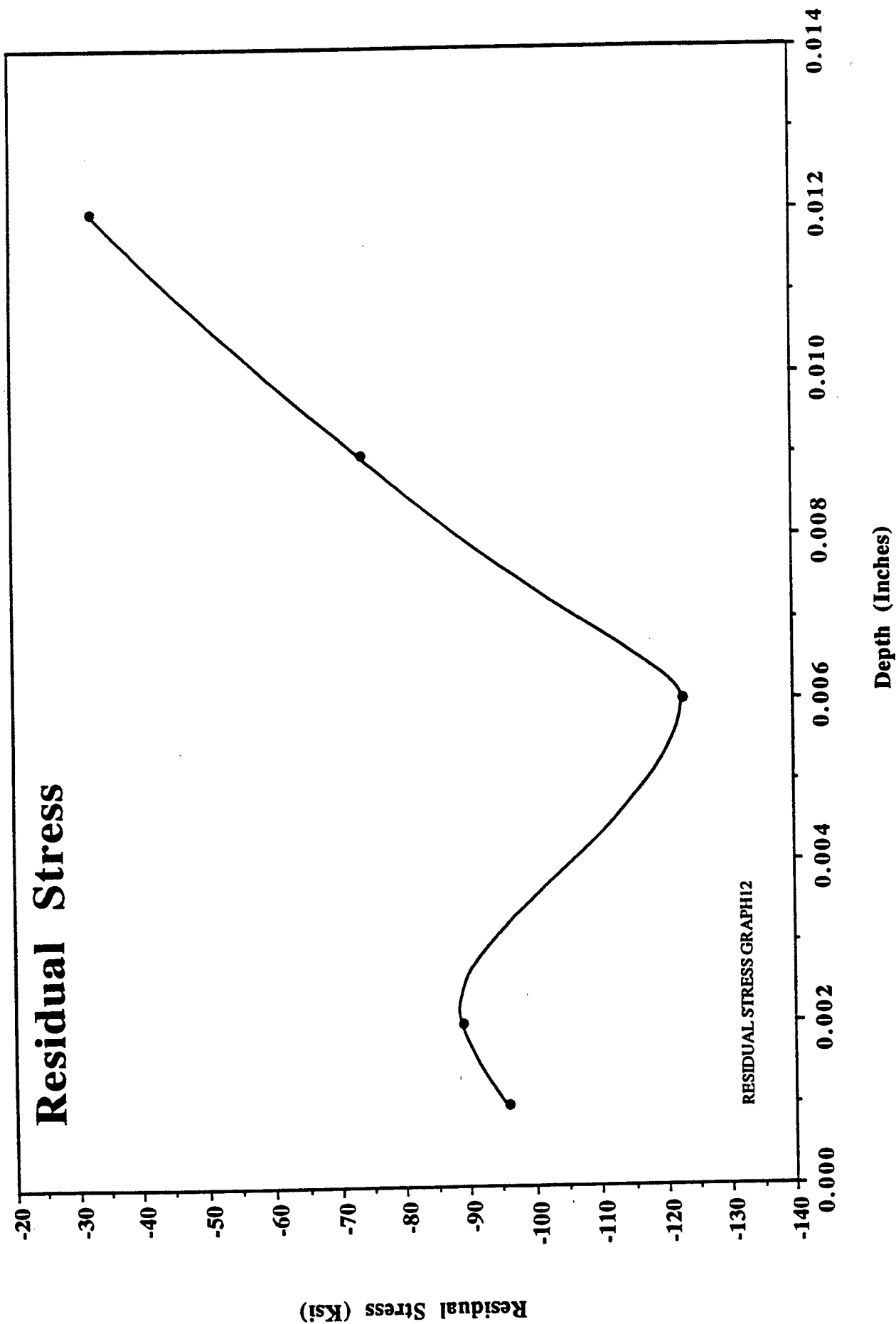
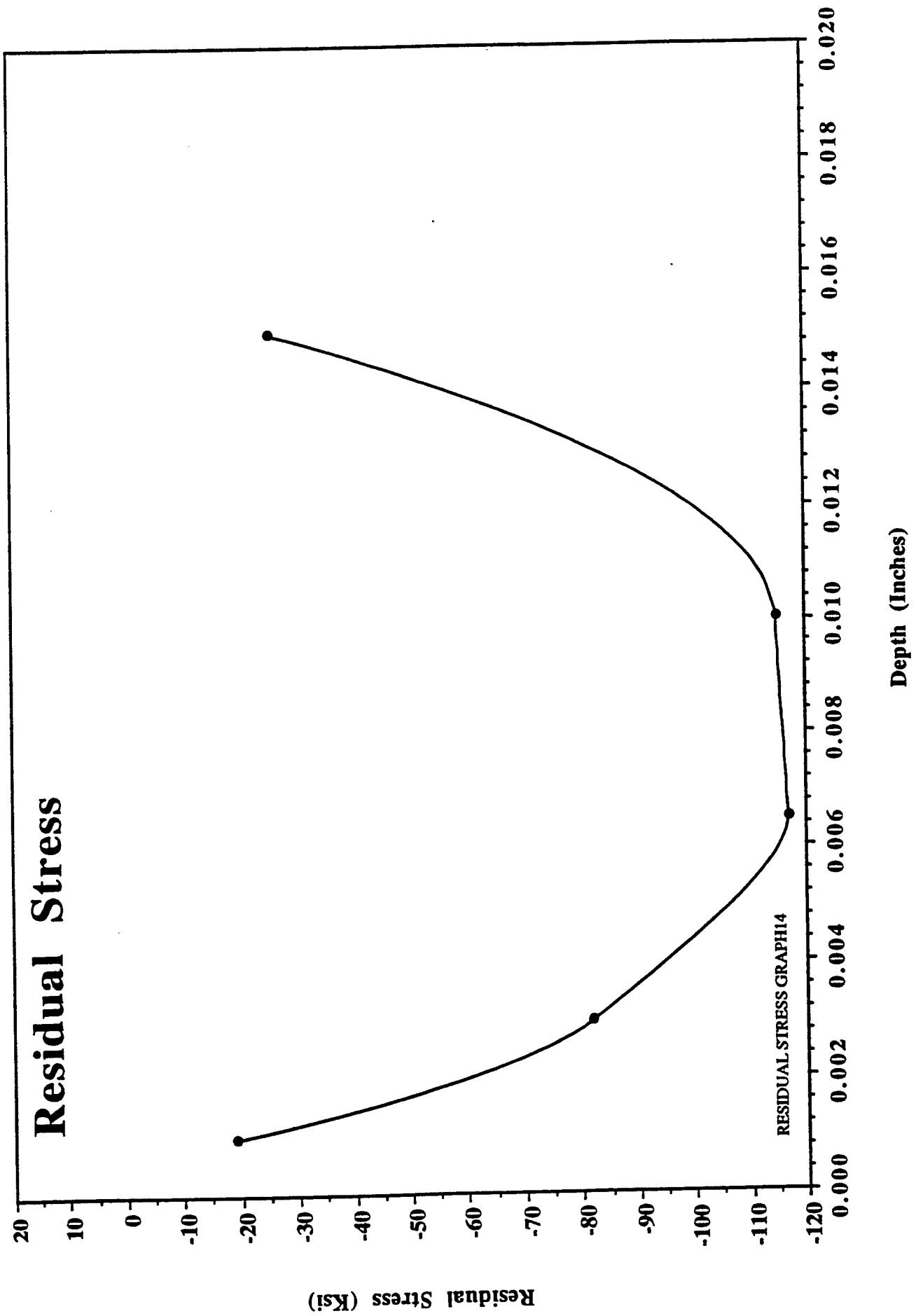


Figure 4.2.2-14 M50 NiL Nitrided 60 Hours, 50% Dissociation Rate  
in a Gas Retort Furnace



**Figure 4.2.2-15 M50 NiL Nitrided 16 Hours, High Dissociation Rate  
Then Another 16 Hours at a Higher Dissociation  
Rate, 975F in a Fluidized Bed Furnace**



**Figure 4.2.2-16 M50 NiL Nitrided per the Lindure Process,  
975F in a Gas Retort Furnace**

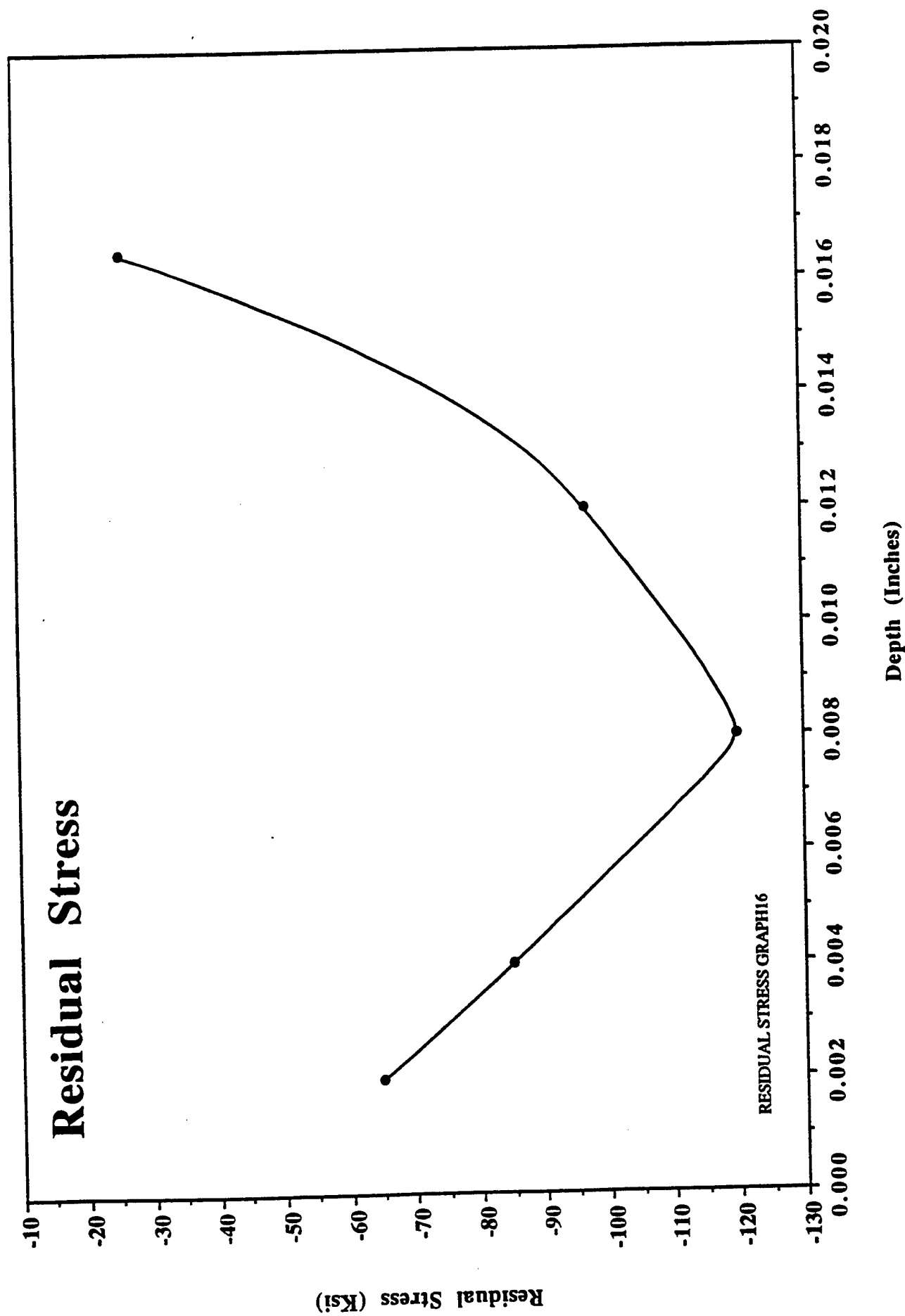


Figure 4.2.2-17 M50 NiL Nitrided 32 Hours, Low Dissociation Rate, 1000F in a Fluidized Bed Furnace



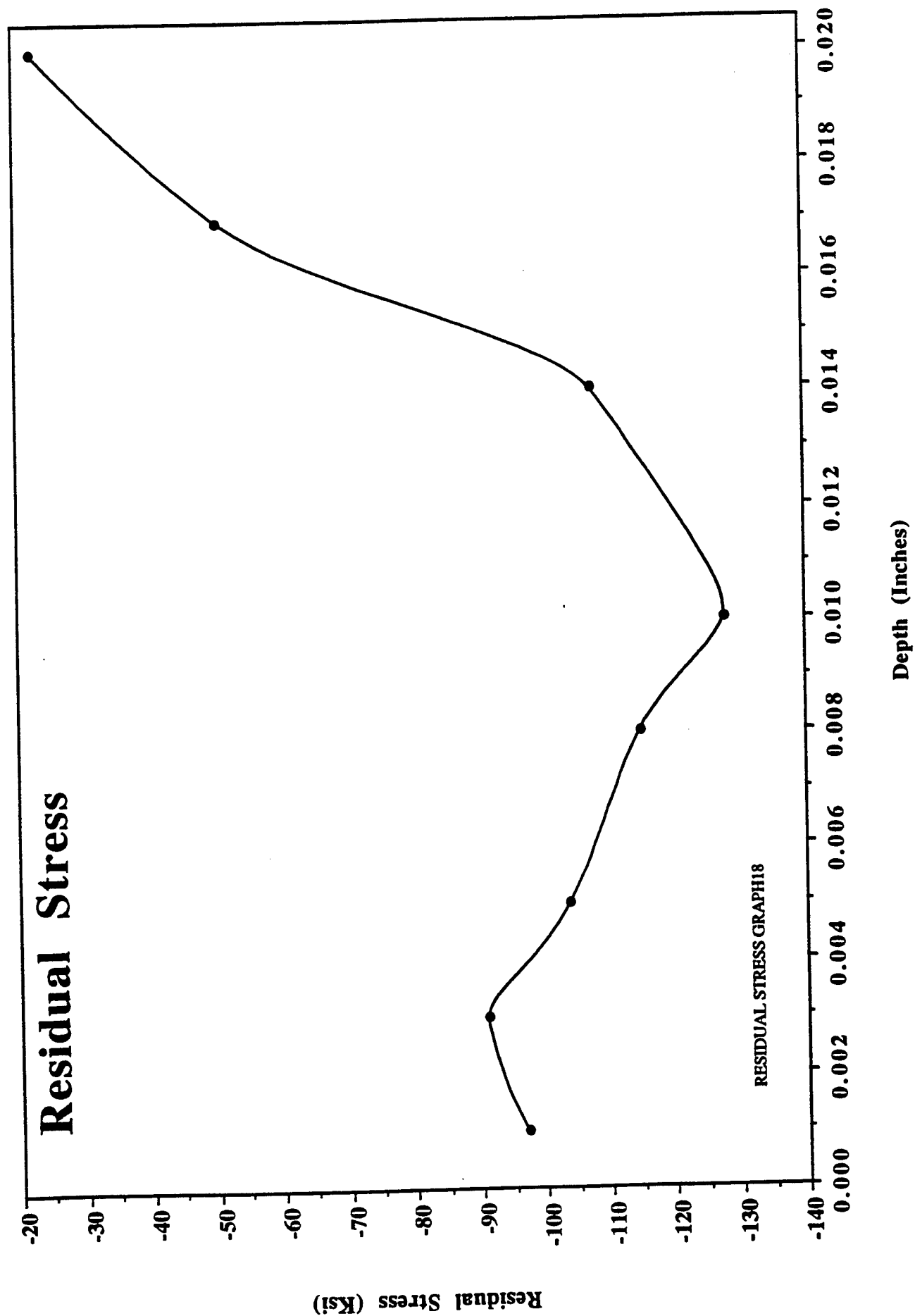


Figure 4.2.2-18 M50 NiL Nitrided 60 Hours, 50 % Dissociation Rate, 1000F in a Gas Retort Furnace

### **4.2.3 NITRIDED CASE MICROSTRUCTURE**

The nitrided case microstructure was examined for each nitriding trial. Figures 4.2.3-1 and 4.2.3-2 show a typical nitrided case microstructure for M50 steel. Note the large primary carbides present in the M50 steel. Figures 4.2.3-3 and 4.2.3-4 show a typical nitrided case microstructure for M50 NiL steel. Note the fine dispersion of carbides in the M50 NiL steel. The nitrided case microstructures did not vary much for each of the different nitriding experiments. There was also no difference in the appearance of the microstructure between the two types of nitriding processes.

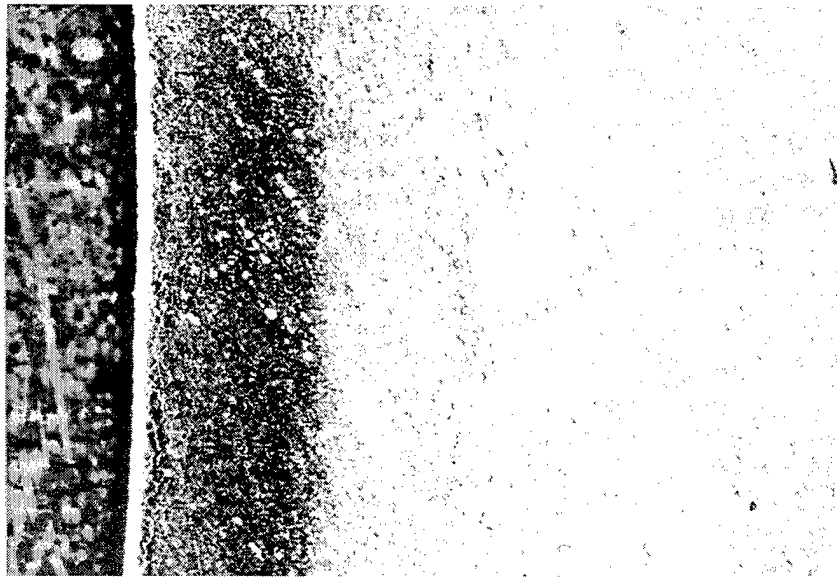


Figure 4.2.3-1  
Photomicrograph showing typical nitrided case, M50 steel  
100X, Nital Etch

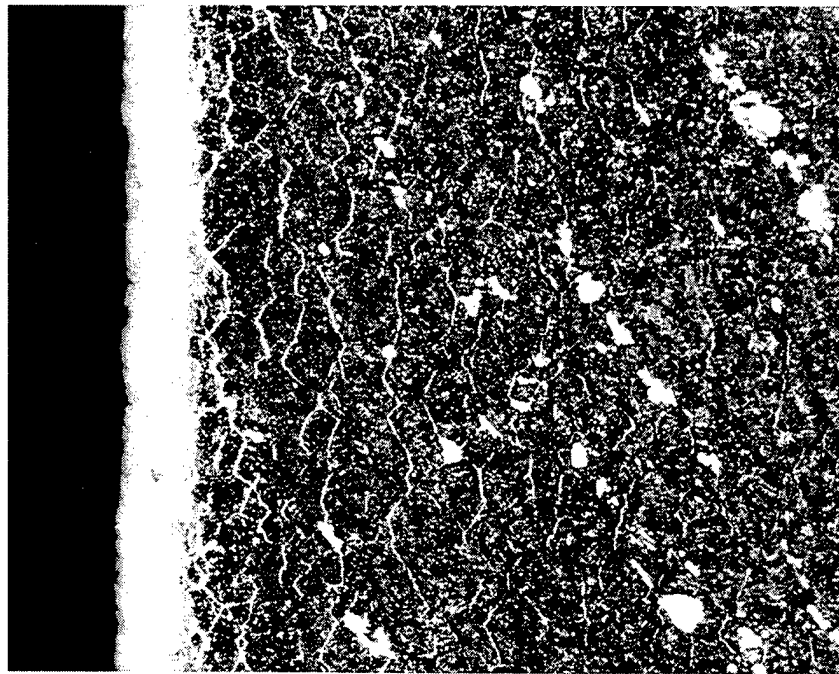


Figure 4.2.3-2  
Photomicrograph showing typical nitrided case, M50 steel  
400X, Nital Etch

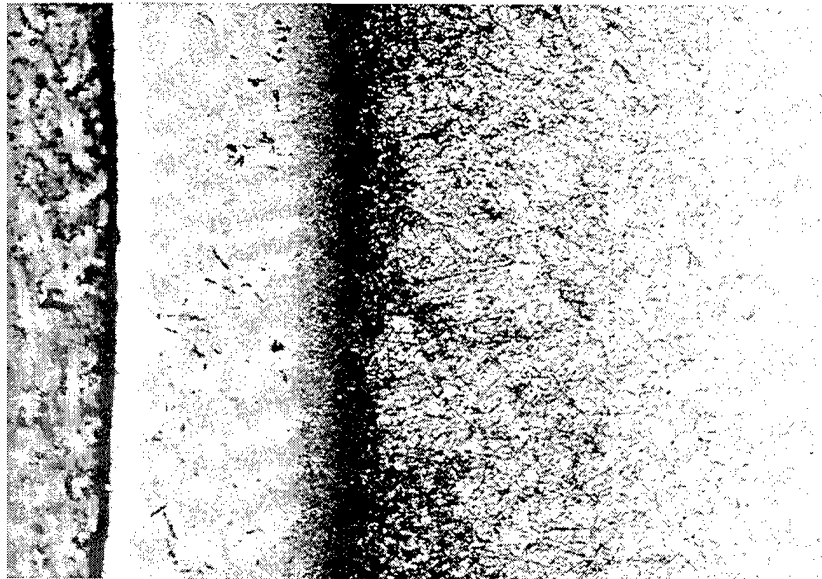


Figure 4.2.3-3  
Photomicrograph showing typical nitrided case, M50 NiL steel  
100X, Nital Etch

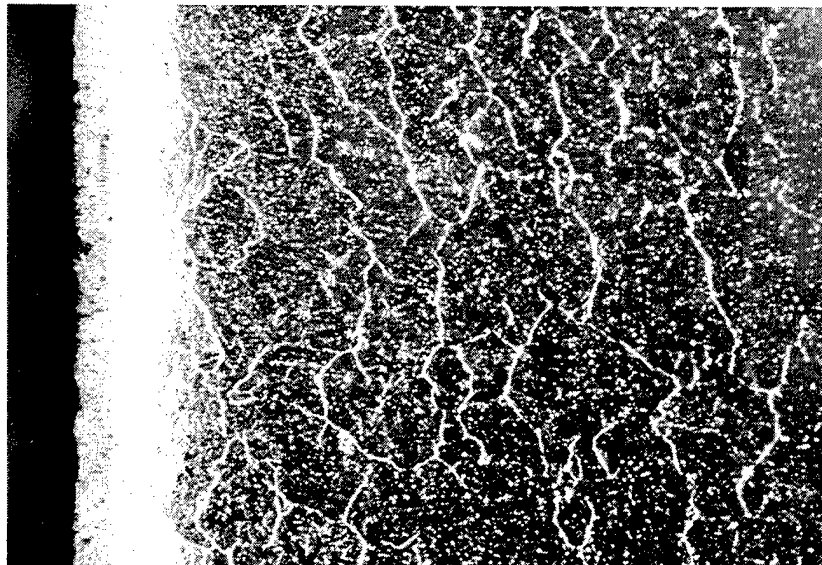


Figure 4.2.3-4  
Photomicrograph showing typical nitrided case, M50 NiL steel  
400X, Nital Etch

### 4.3 EXPERIMENTAL NITRIDING CONCLUSIONS

All of the experimental cycles produced substantial increases in hardness and residual compressive stress to some degree; therefore, we conclude that nitriding of M50 and M50 NiL steels will be a reliable process tolerant of minor production variations.

Below the white compound surface layer, which is always removed for rolling contact service, the variations in microstructure for the different nitriding cycles were small.

High nitriding potential (LOW dissociation rate) of the atmosphere is the most important factor in producing deep cases, more so than time in the furnace.

The optimum cycles selected for rolling contact fatigue rig testing, based upon hardness, residual stress and case depth, were:

*Ferritic Nitrocarburizing, fluidized bed furnace, 32 hours, 524°C  
(975°F), Standard Low Dissociation rate at Massachusetts Steel  
Treating, Worcester, Massachusetts.*

*Gas Nitriding, retort furnace, 60 hours, 524°C (975°F), 50%  
dissociation rate at Lindberg Heat Treating Company, Worcester,  
Massachusetts.*

## 5.0 ROLLING CONTACT FATIGUE RIG EVALUATION

Initial rolling contact fatigue was studied using a standard RCF rolling contact fatigue test machine. The expense of manufacturing full scale bearings for rolling contact fatigue testing is not feasible for studying many different variables affecting the fatigue life. The rod machine samples are relatively simple to manufacture and the test gives fatigue results in a timely manner.

The RCF test was used to compare nitriding cycles and determine the nitriding cycle which yielded the greatest fatigue life for each material, and the nitriding cycle which shows the longest life for each material to be used for the full scale bearing testing.

### 5.1 TEST CONDITIONS

The RCF three-ball-on-rod testing machine is shown schematically in Figure 5.1-1. The test specimen consists of a 9.525 mm (0.375 inch) diameter cylindrical specimen which was finished to the print in Figure 5.3-5. The specimen is inserted into a locking collar which is connected to the drive shaft of an electric motor. There is an assembly which positions three roughened 52100 steel balls at 120° from each other around the shaft. The balls are roughened to 0.089  $\mu\text{m}$   $R_a$  (3.5  $\mu\text{in}$   $R_a$ ). Springs in the assembly are tightened down, pushing the balls against the shaft with enough force to result in a maximum contact stress of 5.42 GPa (786 ksi). The shaft rotates at 3600 rpm. The lubrication for the test is supplied by dripping oil onto the shaft/retainer at a rate of one drip every 8 to 12 seconds. The lubricant is a light Turbo oil (2380) produced by Exxon.

The springs are calibrated frequently to ensure that the correct force and therefore that the correct maximum rolling contact stress is being applied to the test specimens.

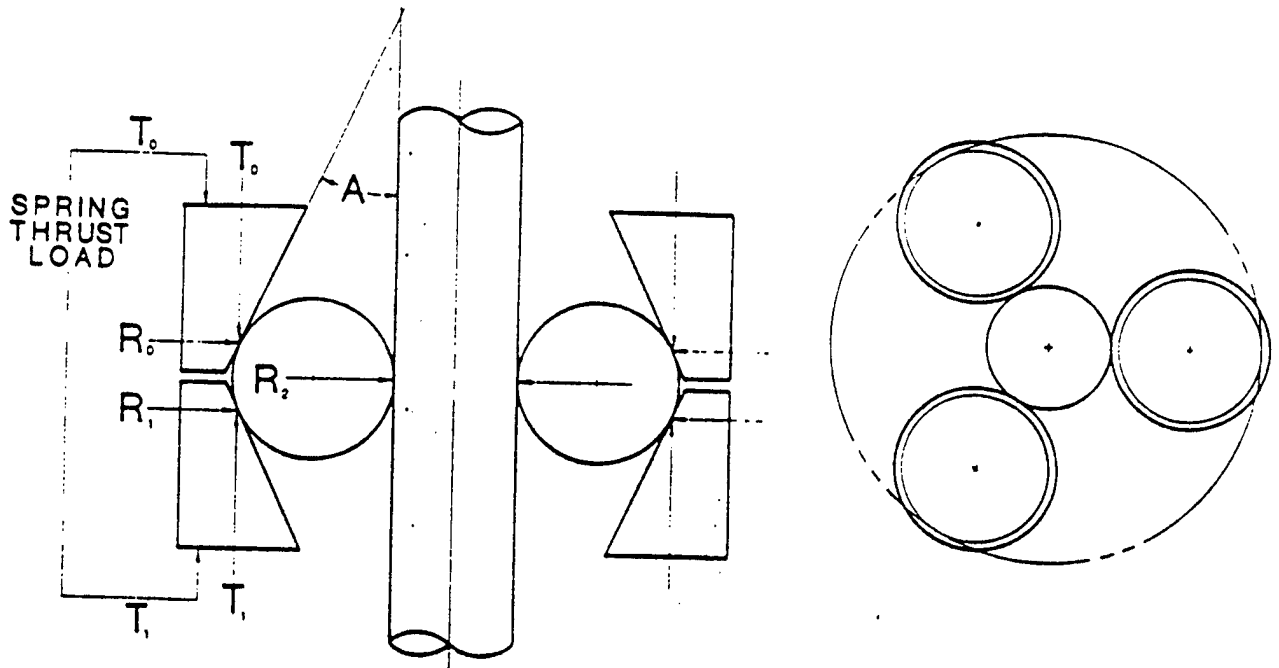


Figure 5.1-1  
Diagram showing the RCF Test Rig, Glover (4)

## 5.2 BASELINE DATA

The results of the tests of the nitrided M50 and M50 NiL steels under this contract were compared to previous tests of non-nitrided M50 and M50 NiL steels. Weibull analyses were used to evaluate and compare the data from all tests.

### 5.3 MANUFACTURING PROCESS, RCF SPECIMENS

The manufacturing process is diagrammed in Figure 5.3-1, below.

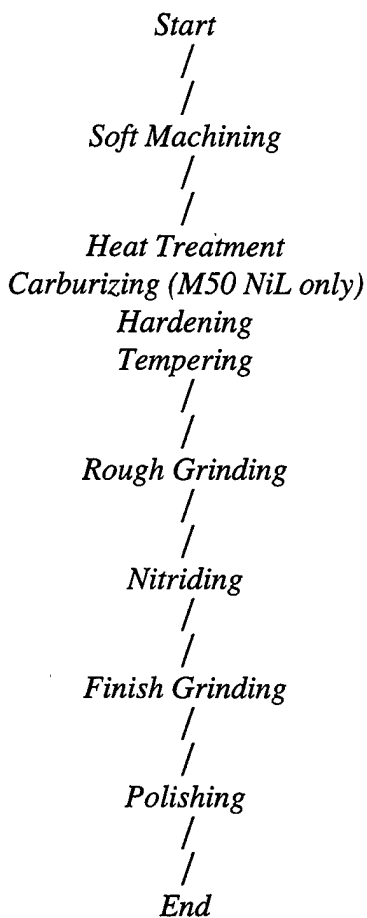


Figure 5.3-1  
Manufacturing process for nitrided steel bearing components

When these materials are used in manufacturing without nitriding, rough and finish grinding is performed after heat treatment. Nitriding changes the process slightly. Nitriding has a relatively shallow effect on the treated parts and must be performed with a minimum of grinding



stock on the part; otherwise the nitrided case will be ground off. Surfaces must be rough ground, nitrided, and then finish ground. Rough grinding removes the surface effects and corrects any distortion from the heat treating operations. The size change during nitriding is very small because there are no phase changes or quenching in this process; therefore, finish grinding needs only remove any compound layer and create a smooth surface for testing.

The first step in manufacturing the RCF specimens was the soft machining of the samples. The steel was ordered in the form of half inch diameter bearing quality bar stock. Next, for each steel, M50 and M50 NiL, the bar was soft machined to the diameter shown in Figures 5.3-2 and 3, respectively. The diameters of the soft machined RCF rods were different for each type of steel because the basic heat treatment given to the RCF rods differs for each steel. As seen in the figures, the M50 steel RCF rods were machined to a diameter of 10.033/10.160 mm (0.395/0.400 inches). The M50 NiL steel RCF rods were machined to 10.287/10.414 mm (0.405/0.410 inches) diameter. The M50 RCF rods only were through hardened, while the M50 NiL RCF rods were both carburized and hardened. The carburizing can produce more distortion and surface effects in the rods and, therefore, more grinding stock is left on these rods. After soft machining, the RCF specimens were ready for heat treatment.

Both materials were put through the standard heat treating cycles for these materials. Samples were taken at the end of the heat treatment process for both materials and destructively tested for hardness and microstructure. After assurance that the heat treated rods were of acceptable metallurgical quality, they were ready for prenitriding (or rough) grinding.

At this point, both materials were ground to the same dimensions because there is very little dimensional change during the nitriding process. Also, both the fluidized bed and gas retort nitriding cycles were ground to the same prenitriding size. For both steels and nitriding processes, less than 0.0762 mm (0.003 inches) were removed from the diameter of the RCF specimen after nitriding. The pre-nitriding print for the RCF rods is shown in Figure 5.3-4.

With all RCF rods ground to 9.5885/9.6012 mm (0.3775/0.3780 inches) diameter, half of the rods made from each material were nitrided per the two cycles chosen for the RCF testing as detailed earlier in this report. Finally, after the rods were nitrided, they were ready for finish

grinding. The finish grinding print is shown in Figure 5.3-5. The specifications on the surface finish for the RCF specimens are maximum Least Squares Cylinder of 0.635  $\mu\text{m}$  (25  $\mu\text{inch}$ ) radial deviation and maximum  $R_a$  of 0.102  $\mu\text{m}$  (4  $\mu\text{inch}$ ). All RCF rods for this contract were within these specifications. The RCF rods were finished after nitriding at Zerocheck, Litchfield, CT.

## 5.4 SUMMARY OF RCF TESTING

This section discusses the results of the two RCF tests for each material. Each test is compared to the existing baseline of each material.

### 5.4.1 SUMMARY OF RCF TESTING, M50 STEEL

The RCF test using nitrided M50 steel showed improvement over the baseline test of M50 steel. Table 5.4.1-1 shows the Weibull analysis results including the  $L_{10}$ ,  $L_{50}$ , slope, and the correlation coefficient for both of the nitriding cycles for this contract as well as a baseline test for M50 not performed under this contract.

Table 5.4.1-1  
Weibull Statistical Summary, M50 steel  
Nitriding cycles versus baseline test

<i>Sample</i>	<i><math>L_{10}</math> (hrs)</i>	<i><math>L_{50}</math> (hrs)</i>	<i>Slope</i>	<i><u>Corr. Coef.</u></i>
<i>M50, baseline</i>	<i>4.9</i>	<i>13.1</i>	<i>1.91</i>	<i>0.992</i>
<i>M50, 32 hr cycle, FNC</i>	<i>31.5</i>	<i>63.8</i>	<i>2.67</i>	<i>0.962</i>
<i>M50, 60 hr cycle, Gas</i>	<i>22.3</i>	<i>88.7</i>	<i>1.37</i>	<i>0.907</i>

# M50 RCF Rod

Soft machining print

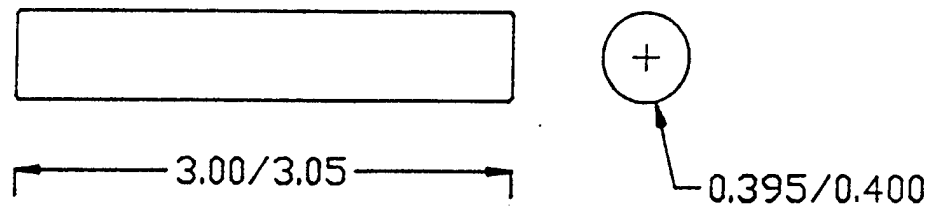


Figure 5.3-2

Soft Machining Dimensions  
RCF Test Specimen  
M50 Steel

# M50 NiL RCF Rod

Soft machining print

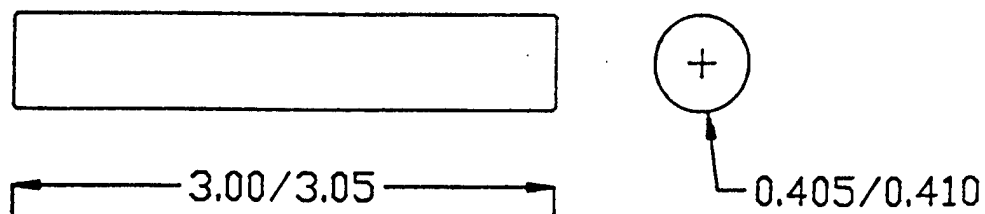


Figure 5.3-3

Soft Machining Dimensions  
RCF Test Specimen  
M50 NiL Steel

## M50 and M50 NIL RCF Rod

Pre-nitriding grinding print

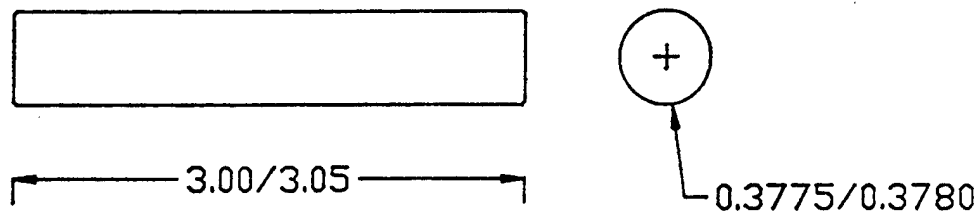
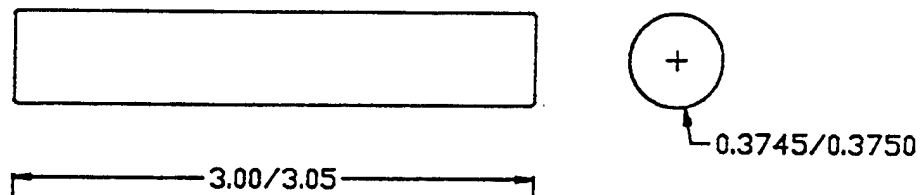


Figure 5.3-4

Pre-Nitriding Dimensions  
RCF Test Specimen  
M50 and M50 NiL Steels

## M50 and M50 NIL RCF Rod

Finish grinding print



Metrology Specs:

Max. LSC 25 micro inches radial deviation

Max. Ra 4 micro inches

Figure 5.3-5

Finish Grinding Dimensions  
RCF Test Specimen  
M50 and M50 NiL Steels

#### 5.4.2 SUMMARY OF RCF TESTING, M50 NiL STEEL

The FMC RCF test using nitrided M50 NiL steel showed improvement over the baseline test of M50 steel. Table 5.4.2-1 shows the Weibull analysis results including the  $L_{10}$ ,  $L_{50}$ , slope, and the correlation coefficient for both of the nitriding cycles for this contract as well as a baseline test for M50 NiL not performed under this contract.

Table 5.4.2-1  
Weibull Statistical Summary, M50 NiL Steel  
Nitriding cycles versus baseline test

<u>Sample</u>	<u><math>L_{10}</math> (hrs)</u>	<u><math>L_{50}</math> (hrs)</u>	<u>Slope</u>	<u>Corr. Coef.</u>
M50 NiL, baseline	8.8	19.0	2.43	0.951
M50 NiL, 32 hr cycle, FNC	91.9	462.4	1.16	0.974
M50 NiL, 60 hr cycle, Gas	26.8	126.6	1.21	0.978

#### 5.5 RCF TEST CONCLUSIONS

The results of the four rolling contact fatigue tests show very clearly that both M50 and M50 NiL steels benefit from the nitriding process. Both the  $L_{10}$  and  $L_{50}$  lives of both materials improved significantly with the nitrided case in the rolling contact zone. The slope of the Weibull plots indicate both tests are valid, as the slopes are greater than 1.0. If the Weibull slope is less than one, it indicates an infant mortality situation in the data. These results relative to other tests are shown schematically in Figure 1.4-1.

The combination of the increased hardness and the high residual compressive stress generated in the nitrided case were responsible for the increased fatigue life of the steel rods.

The nitride network which forms in the nitrided case microstructure was not detrimental to the fatigue life of the steel.

The results of the nitrided M50 steel tests show no statistical difference between the two nitriding cycles.

There was an increase in the fatigue life of the carburized and nitrided M50 NiL steel produced by the ferritic nitrocarburizing (fluidized bed furnace) over the gas nitrided cycle. The ferritic nitrocarburizing cycle was, therefore, chosen for all the nitrided steel components for the full scale bearing tests.

## 6.0 PROCUREMENT OF SILICON NITRIDE BALLS

The following two sections detail the process for choosing Norton Advanced Ceramics' NBD-200 silicon nitride material. Two materials were considered and the decision was made based on full scale bearing testing. The Torrington Company's Bearing Test Lab had tested material from Norton Advanced Ceramics (formerly CERBEC) and Hoover (Toshiba).

## 6.1 DISCUSSION OF PAST TEST EXPERIENCE WITH CERAMIC BALLS

The Torrington Company has had experience testing full scale hybrid bearings in the past. Three sets of bearings had been tested, with each set having a different type of silicon nitride ball for the rolling elements. The three types of silicon nitride material evaluated were Norton Advanced Ceramics's NBD-100, Norton Advanced Ceramics's NBD-200, and Hoover's (Toshiba) TSN-03H. All of these ball materials were evaluated in a 207 bearing test, which is a radially loaded bearing. The specific test conditions were:

*7050 N (1600 lbs.) radial load*  
*Inner max. contact stress, 3.65 GPa (530 ksi)*  
*3000 rpm*  
*Lubricated with DTE Ex Heavy oil*

Normally, 24 bearings are tested to evaluate a set of test bearings. Only the test of the bearings with NBD-100 silicon nitride balls included 24 bearings. Eight bearings were tested with NBD-200 silicon nitride and five bearings were tested with the Hoover TSN-03H silicon nitride. Therefore, statistical certainty is not possible in determining the best silicon nitride material, but that was not within the scope of this contract. The bearings in this contract were to be manufactured using commercially available silicon nitride bearing balls.

The performance of each group was compared to the calculated life for the bearing and test conditions. The results showed that Norton Advanced Ceramics's NBD-200 had the best fatigue life. The ratio of the test  $L_{10}$  life to the calculated  $L_{10}$  life was 18.5, with one ball failure at 1077 hours. For the NBD-100 test, the fatigue life ratio was 4.7, with ball failures at 5.3 and 44.5

hours. Finally, the Hoover TSN-03H silicon nitride ball tests showed a fatigue life ratio of 7.4, with one ball failure at 228 hours.

On the basis of these tests, NBD-200 was chosen for all the 207 and 208 bearings in this contract.

## 6.2 NORTON ADVANCED CERAMICS NBD-200

NBD-200 is the next generation of hot isostatically pressed silicon nitride for use as anti-friction bearing components. Norton Advanced Ceramics reports NBD-200 has improved mechanical and fatigue properties over other silicon nitride materials due to material processing developments.

The mechanical and thermal properties of NBD-200 are shown in Table 6.2-1. The information has been supplied by Norton Advanced Ceramics.

Table 6.2-1  
NBD-200 Material Properties

<u>Mechanical</u>		<u>Units</u>	<u>Value</u>	
<i>Strength, 20°C</i>				
<i>Flexural, Mean, MiL Std, 1942B</i>	<i>Mpa</i>	<i>(ksi)</i>	800	(116)
<i>Weibull Modulus</i>	-	-	9.7	-
<i>Tensile, Mean, As HIPped</i>	<i>Mpa</i>	<i>(ksi)</i>	400	(58)
<i>Compressive, Bulk</i>	<i>GPa</i>	<i>(ksi)</i>	3	(435)
<i>Hertz Compressive, Ball on Flat</i>	<i>GPa</i>	<i>(ksi)</i>	28	(4060)
<i>Fracture Toughness, K<sub>IC</sub></i>	<i>MPA-m<sup>1/2</sup></i>	<i>(ksi-in<sup>1/2</sup>)</i>	4.1	(3.7)
<i>Density</i>	<i>g/cc</i>	<i>(lb/in.<sup>3</sup>)</i>	3.16	(0.117)
<i>Elastic Modulus</i>	<i>GPa</i>	<i>(psi X 10<sup>6</sup>)</i>	320	(46)
<i>Poissons ratio</i>	-	-	0.26	-
<i>Hardness, Vickers (10 kg)</i>	<i>GPa</i>	<i>(psi X 10<sup>6</sup>)</i>	16.6	(2.4)
<i>Hardness, Hrc</i>	-	-	>70	-
<u>Thermal</u>				
<i>Thermal Expansion Coef., -170°C to 20°C</i>	<i>10<sup>-6</sup>/°C</i>	<i>(10<sup>-6</sup>/°F)</i>	0.43	(0.24)
<i>20° to 1000°F</i>			2.9	(1.6)
<i>Thermal Conductivity 100°C</i>	<i>W/m-K</i>	<i>(BTU-in/hr-ft<sup>2</sup> - °F)</i>	29.3	(203)
<i>500°C</i>			21.3	(147)
<i>1000°C</i>			15.5	(107)
<i>Maximum Use Temperature</i>	<i>°C</i>	<i>(°F)</i>	1000	1800



## **7.0 MANUFACTURING PROCESSES, M50 AND M50 NiL STEEL RINGS**

The manufacturing of the 207 radial bearings through rough grinding was concurrent with the initial nitriding experiments, selection of the ceramic balls, and the manufacture and testing of the RCF specimens. The general manufacturing sequence of operations was similar to the RCF specimens, i.e., soft machining, heat treating, rough grinding, nitriding, and finally, finish grinding.

The 207 bearings were manufactured with nitrided M50 and nitrided M50 NiL inner rings and NBD-200 ceramic balls. All of the bearings with the nitrided M50 and the nitrided M50 NiL inner rings were matched with non-nitrided M50 outer rings. The outer rings were not nitrided because the design of the bearing places the highest contact stress on the inner ring. Therefore, outer ring failures during 207 bearing testing are rare. The inner ring is the test specimen in the 207 test.

The 208 bearings had the same material/nitriding processing for both the inner ring and the outer ring. The inner ring receives the higher contact stress but the conditions of thin film, contamination, temperature, and operation in thrust make it necessary for the outer ring as well as the inner to have improved properties.

The following two sections discuss the processing for M50 and M50 NiL steels, respectively.

### **7.1 HEAT TREATMENT OF M50 STEEL**

M50 steel is a high alloy, high carbon steel commonly used in high performance bearing applications. M50 is used in many applications where higher operation temperatures exist. This is possible because M50 steel can be hardened and tempered at the secondary hardening peak. The high tempering temperature allows the steel to resist prolonged exposure in the 150°C to 230°C

(300°F to 450°F) temperature range with no softening or dimensional changes to the steel bearing components.

The M50 steel rings were manufactured from VIM VAR (Vacuum Induction Melt plus Vacuum Arc Remelt) bearing quality bar stock. Soft machining dimensions in the raceway were altered slightly from standard 52100 bearing steel 207 rings to allow more grinding stock in the raceways. The additional stock in the raceways was needed because of the nitriding process, which will be explained in more detail later in this section.

After soft machining, the rings received conventional heat treating. For M50 steel this includes hardening and tempering to the correct hardness. M50 steel is hardened at 1093°C (2000°F), followed by an air quench. The rings are then tempered 2 hours at 538°C (1000°F), five separate times. Multiple tempers are used to insure very low retained austenite in the microstructure, which makes the rings dimensionally stable during thermal cycling and over time. Typical retained austenite levels for M50 steel after heat treatment are less than 2 percent.

The hardness and retained austenite were measured after the heat treatment was completed. Several samples from each type of ring, i.e., 207 inners, 207 outers, 208 inners, and 208 outers were checked for hardness. All of these rings were measured on the faces of the rings. All hardness readings were Rockwell C 62 to 63. The specification for heat treated M50 steel is Rockwell C 60 to 64. One ring was checked for retained austenite. The retained austenite was determined to be 1.3%, The specification is less than 3%. In addition the microstructure was examined and was a normal mix of tempered martensite, low levels of retained austenite, and finally primary and secondary carbides.

## 7.2 HEAT TREATMENT OF M50 NiL STEEL

M50 NiL steel is a high alloy, low carbon steel used in high performance bearing applications where tensile stressing could otherwise cause ring fracture. M50 NiL steel must be carburized to develop the high hardness case needed for rolling contact bearing components. M50 NiL was developed as a carburizing modification of M50 steel. The benefits of carburizing are twofold. First, the relatively high residual compressive stresses that are developed in the carburized case prevent radial crack propagation. Second, the low carbon core provides increased core toughness for added fracture resistance. M50 NiL, like M50 steel, is hardened and tempered at the secondary hardening peak and is therefore resistant to softening and dimensional change during application conditions.

The M50 NiL rings were manufactured from VIM VAR bar stock. Like the M50 rings, some changes to the normal soft machining dimensions were necessary because of the nitriding process. More grinding stock was left on the raceway because of the extra grinding step in the processing.

Heat treating M50 NiL differs from the heat treatment of M50 steel in that the M50 NiL must be carburized in order to attain the high case hardness needed for rolling contact fatigue resistance. The M50 NiL heat treatment began with an air oxidation process which is necessary to allow good uniform carbon diffusion throughout the whole surface of the part. One hour at 954°C (1750°F) in air is sufficient. After the air oxidation process, the parts were ready to be carburized. Carburizing consisted of a standard 36 hour carburizing cycle at 954°C (1750°F). The parts were oil quenched after carburizing, then given a stress relieve for 2 hours at 648°C (1200°F). The parts were then hardened at 1093°C (2000°F), oil quenched, tempered at 524°C (975°F) for two hours, deep frozen

at -84°C (-120°F), then tempered four more times at 524°C (975°F). Again, as with the M50 steel, multiple tempers are used to control the retained austenite in the carburized case. The retained austenite in the case microstructure is also below three percent when the heat treatment is completed. There is no problem with retained austenite in the core of M50 NiL as it is low in carbon.

Metallography from M50 NiL samples after heat treating showed surface hardness of Rockwell C 61 to 62. The specification for the heat treated M50 NiL steel is 60 to 64 Rockwell C. Retained austenite measured at a depth of about 0.127mm (0.005 inches) on the heat treated surface was 1.7%. The specification of retained austenite in the case is 6% maximum. Inspection of the case microstructure revealed a normal case microstructure consisting of tempered martensite, some retained austenite, and a uniform dispersion of fine carbides.

### **7.3 NITRIDING PROCESS, BEARING RINGS**

The RCF rolling contact fatigue tests indicated that the best fatigue life was produced by the 32-hour ferritic nitrocarburizing cycle in a fluidized bed furnace. All the rings were nitrided at the same time in one furnace lot to avoid any differences between nitriding cycles. There was no masking planned for these rings. All surfaces of each bearing ring had a nitrided case after the process was completed.

Several samples from the lot were destructively tested after the nitriding process. Figure 7.3-1 shows the hardness profiles directly after nitriding of two M50 samples and two M50 NiL samples. In all cases, the nitrided case was about Rockwell C 70. The M50 steel retained a higher hardness

after nitriding because the nitriding process was performed at the tempering temperature of M50 NiL while it was below the tempering temperature of the M50 steel. Future work on nitrided raceways should consider investigating a nitriding temperature about 25°C (50°F) below the tempering temperature of the steel being used.

The rings were also measured for dimensional change during the nitriding process. The raceways of both the inner rings and the outer rings were measured before and after nitriding. Figures 7.3-2 and 7.3-3 show the size change of the race diameter for the 207 inner rings before and after nitriding. The race diameter for both materials grew about 0.0762 mm (0.003 inches). Figures 7.3-4 and 7.3-5 show the same information for the 208 inner rings. Again, the race diameter grew by about 0.0762 mm (0.003 inches). Figures 7.3-6 and 7.3-7 show the race diameter for the 208 outer rings. This measurement was on an internal surface of the rings and note how the race diameter changed very little. These data can be partly explained by the fact that during nitriding, a white layer rich in nitrogen grows on the surface of the steel. The inner ring measurements were taken on the outer diameter of the ring and therefore the white layer added to the diameter during the nitriding process.

The outer ring size change data are not as easily explained. It would have been expected that the outer ring race diameter would have become smaller due to the growth of the white layer on the surface of the steel, but it did not change. Residual stresses, metallurgical changes and/or gauging errors could be present. Residual stresses and metallurgical changes, however, could account for only a small percentage of difference from expected size change. The residual stresses are in a thin

layer that represents only a small percentage of the ring volume. Metallurgical change to cause growth would come from transformation of retained austenite, and little or no austenite was present in the rings before nitriding. The outer rings were measured on the internal raceway surfaces only, and gauging error is suspected here.

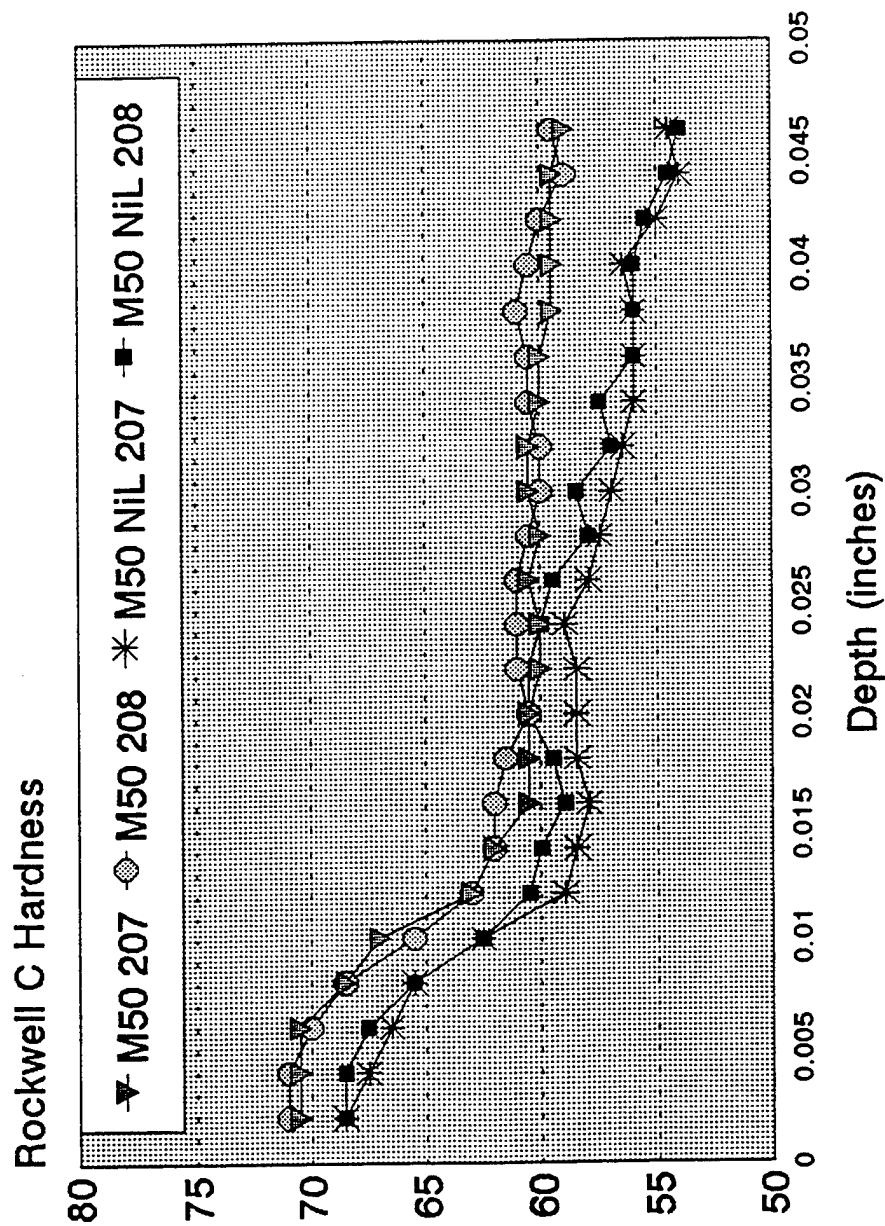


**Figure 7.3-1 Hardness Profiles, M50 and M50 NiL Steel Bearing Rings**  
 As Nitrided, 32 hour Ferritic Nitrocarburized Cycle, 975F

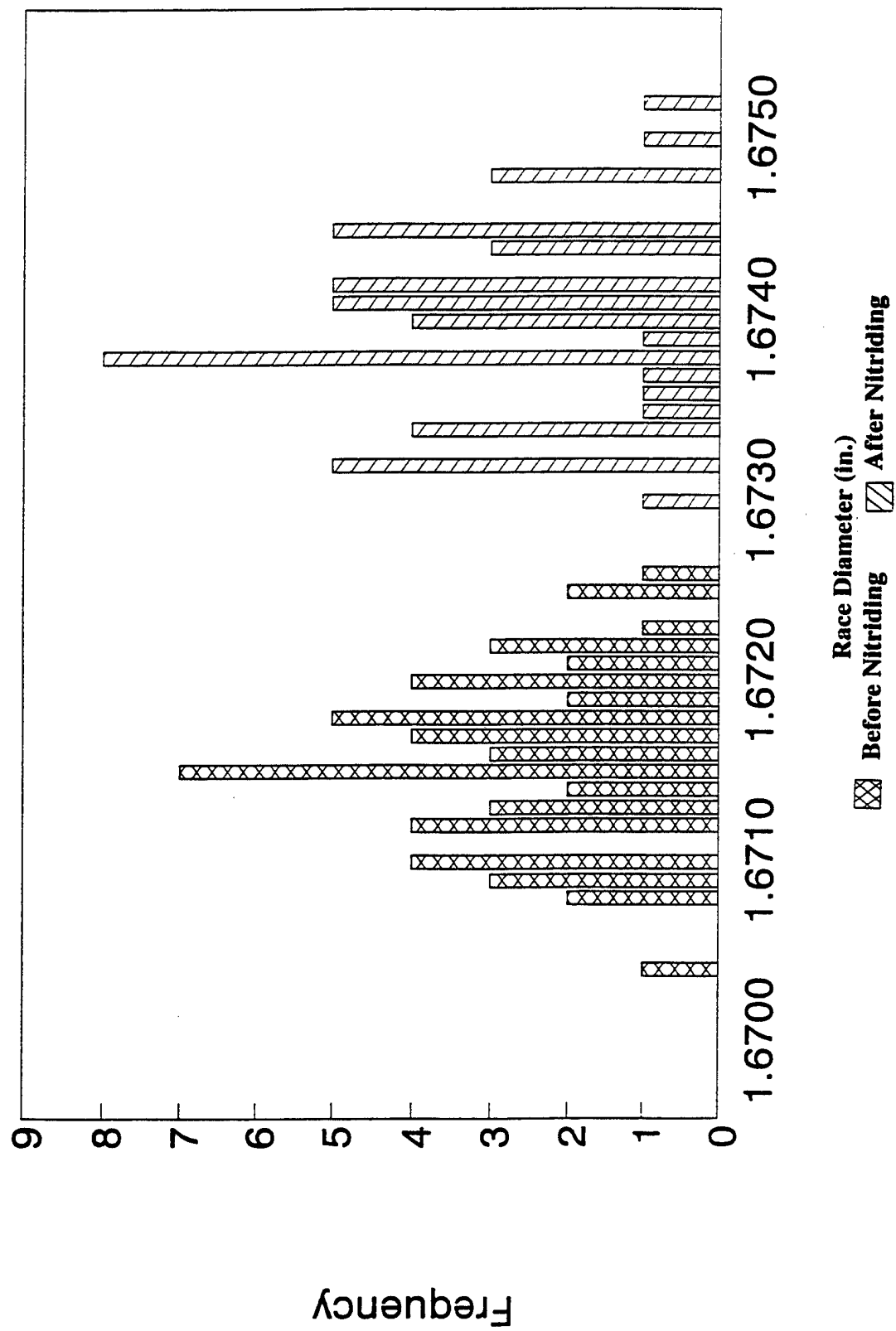


**Figure 7.3-2 M50 207 Inner Ring Size Change**



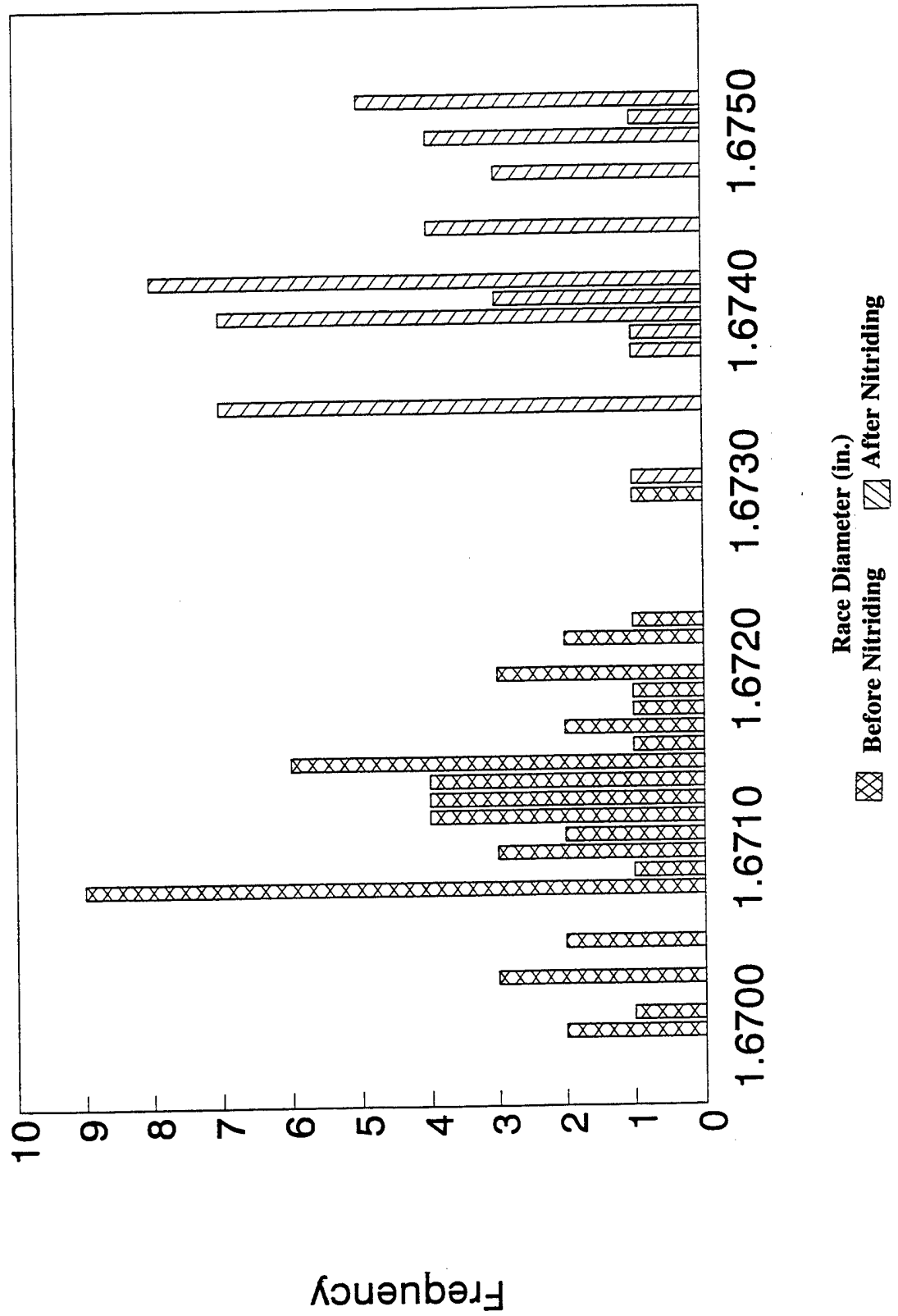


**Figure 7.3-3 M50 NiL 207 Inner Ring Size Change**

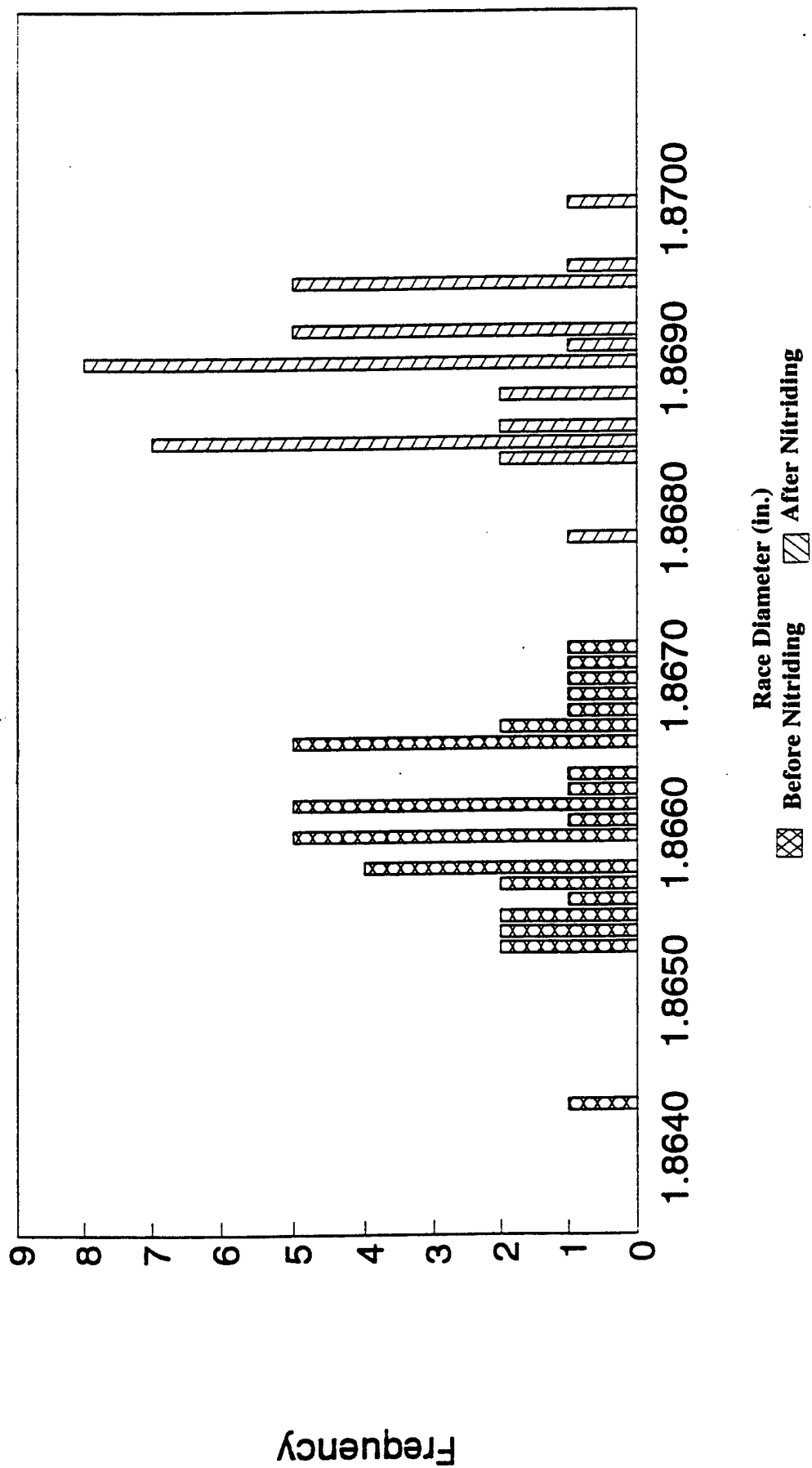


**Figure 7.3-4 M50 208 Inner Ring Size Change**

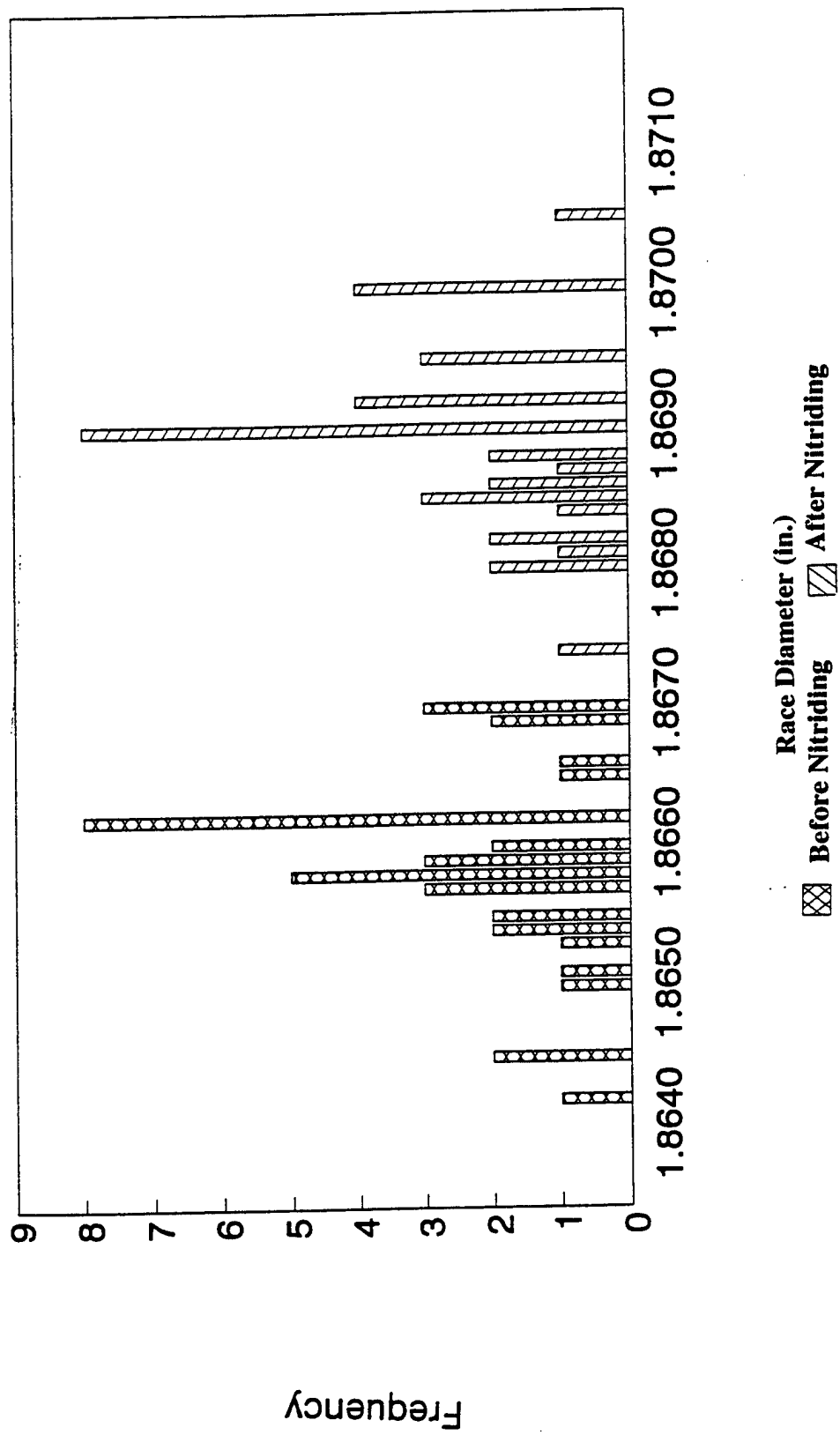


**Figure 7.3-5 M50 NiL 208 Inner Ring Size Change**

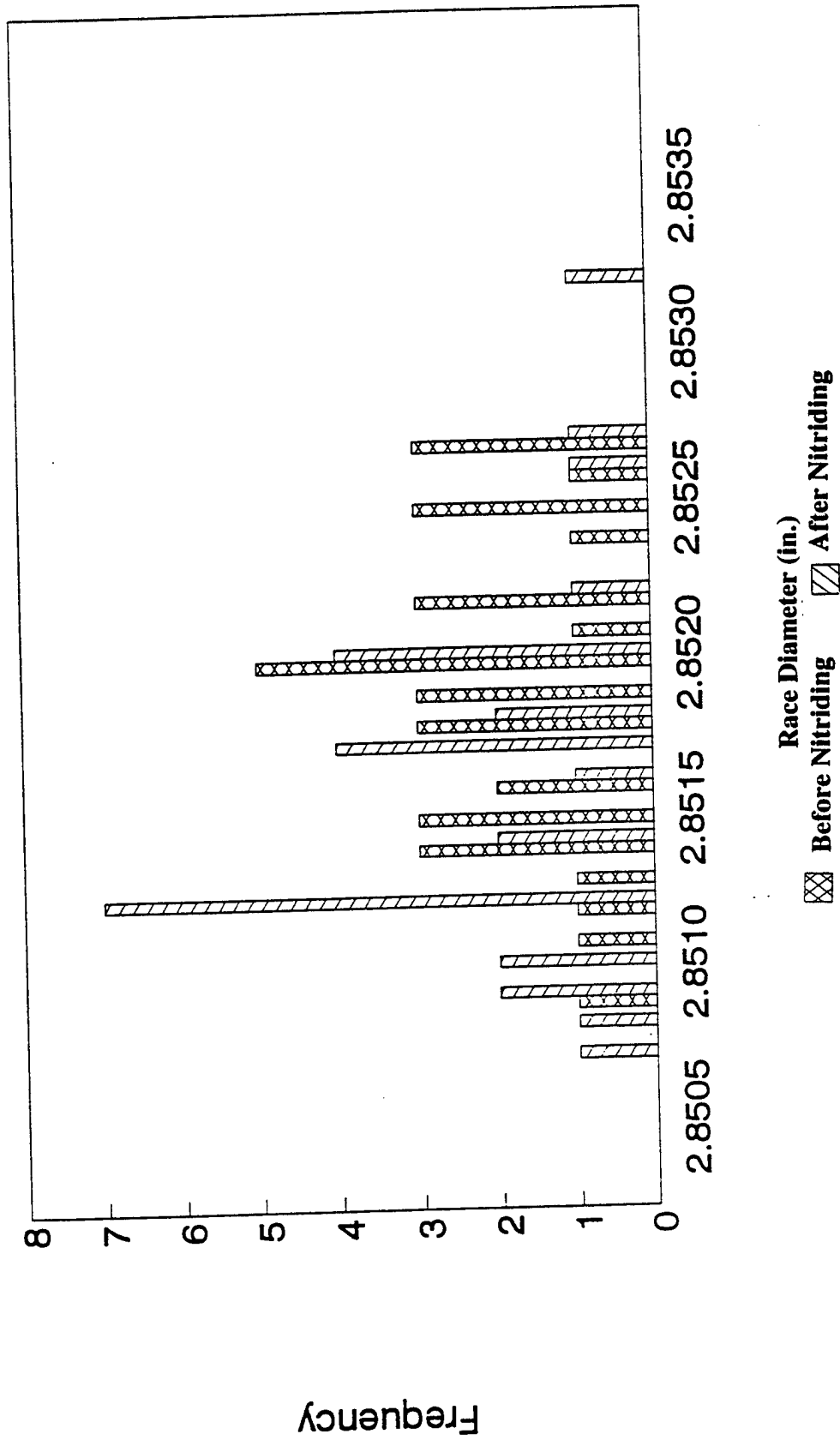
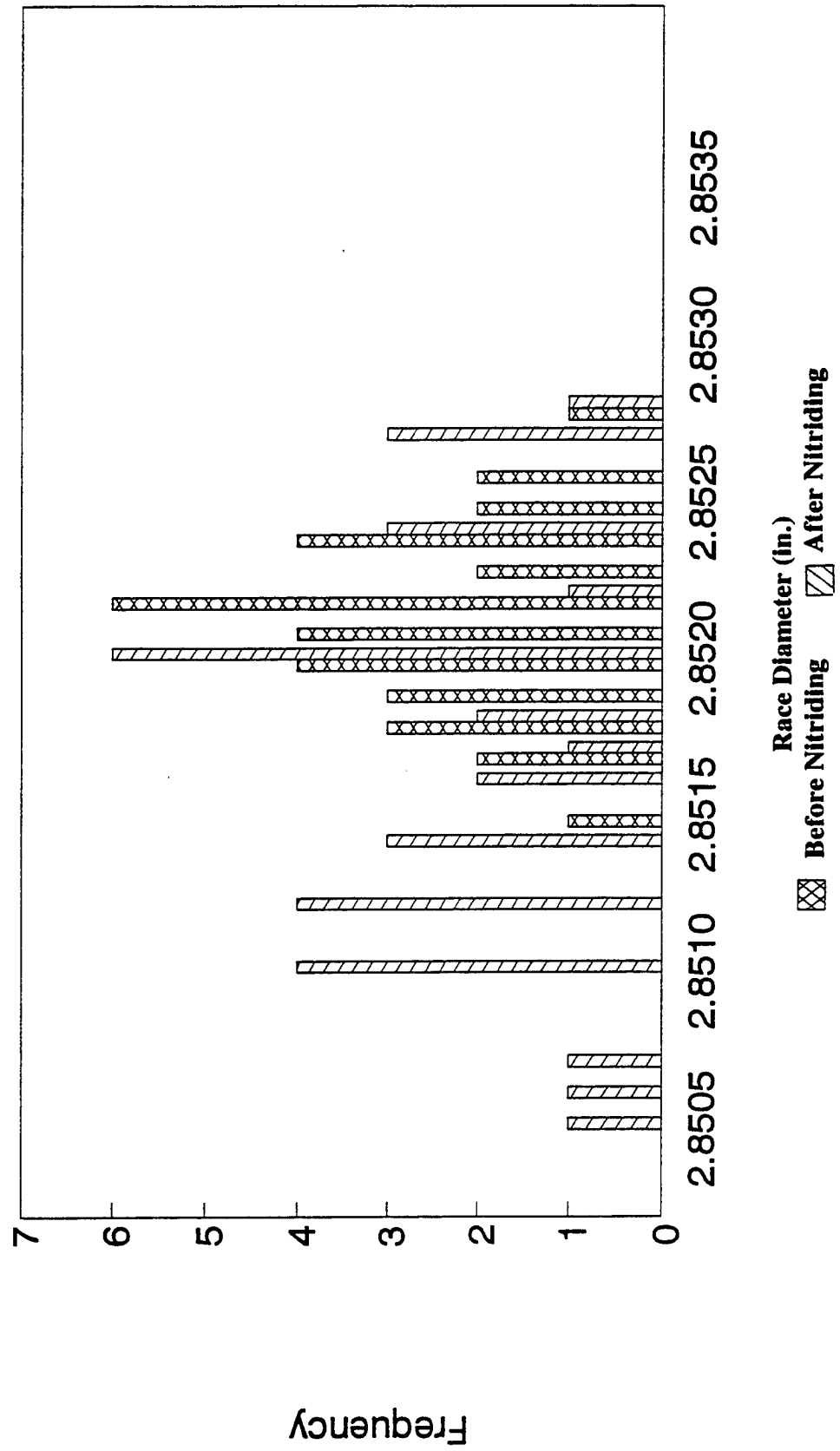


Figure 7.3-6 M50 208 Outers



**Figure 7.3-7 M50 NiL 208 Outers**

## 7.4 FINISHING AND ASSEMBLY

After the nitriding process was completed, the hardness and microstructure were examined to ensure the proper metallurgical properties. Initially, the high hardness of the nitrided case was thought to possibly make race grinding difficult. This turned out not to be the case. The nitrided surfaces of the rings were no more difficult to finish grind than standard M50 steel. Only the raceways and the bores of the bearings were finish ground after nitriding. The other surfaces are not dimensionally critical for bearing tests.

The task of ensuring the correct clearance and fit of the bearings was complicated by the fact that, in a normal bearing assembly operation, the raceways are finish ground and then the necessary ball sizes to yield the correct fit are assembled into the bearings. Because of the silicon nitride balls having been ordered in advance, the bearing rings for this contract had to be finish ground to match the size of the balls already in our possession, creating the correct fit of the bearing.

The specific finish grinding parameters were identical to the finish grinding parameters used for hardened M50 steel rings. The grinding wheels were aluminum oxide, 120 grain, medium hardness, with a friable bond. After nitriding, 0.127 mm (0.005 inches) was removed from the diameters of the raceway and the bore of the bearings, allowing the white layer to be completely removed. This was crucial to the performance of the bearings. Past rolling contact fatigue testing by The Torrington Company has shown the white layer to be detrimental the rolling contact fatigue performance. Finally, the raceways were polished to further improve the surface finish.

Metrology of the raceways was measured on a sample ring from each type of ring (M50 207 inner, M50 207 outer, M50 208 inner, etc...). A summary of the results is shown below in Table 7.4-1. All measurements showed good surface finishes for bearing raceways.

Table 7.4-1

Summary of Metrology Measurements, Bearing Raceways

Part Type	Ra μm (μin)	Peak to Valley μm (μin)	Brg. Ratio Depth @ 60% tp μm (μin)	Brg Ratio Depth vs tp % μm	Rk μm (μin)	Waviness Peak to Valley
M50 207 Inner	0.10 (3.95)	1.16 (45.66)	0.36/60% (14.2/60%)	0.52/89.1% (20.1/89.1%)	0.26 (10.41)	0.24 (9.41)
M50 207 Outer	0.11 (4.34)	1.33 (52.45)	0.27/60% (10.8/60%)	0.50/94.0% (19.9/94.0%)	0.27 (10.59)	0.19 (7.39)
M50 208 Outer	0.12 (4.64)	1.13 (44.61)	0.43/60% (17.0/60%)	0.51/75.7% (20.1/75.7%)	0.28 (11.05)	0.18 (7.20)
M50 208 Inner	0.082 (3.22)	1.01 (39.57)	0.25/60% (9.81/60%)	0.51/97% (20.0/97.0%)	0.19 (7.68)	0.21 (8.18)
M50 NiL 208 Outer	0.17 (6.62)	1.28 (50.22)	0.46/60% (18.08/60%)	0.51/68% (20.1/68.0%)	0.44 (17.30)	0.36 (14.22)
M50 NiL 207 Inner	0.084 (3.29)	0.81 (31.79)	0.29/60% (11.48/60%)	0.51/96.8% (20.0/96.8%)	0.23 (9.00)	0.24 (9.50)
M50 NiL 208 Inner	0.075 (2.96)	0.62 (24.31)	0.29/60% (11.48/60%)	0.51/99.0% (20.1/99.0%)	0.23 (9.01)	0.13 (5.26)

## 8.0 ROLLING CONTACT FATIGUE EVALUATION, 35 MM BORE, 207 RADIAL BEARINGS

The 207 bearing is a typical size used in the bearing industry for general fatigue evaluation. The bearing envelope is about 6.4 cm (2 3/4 inches) OD, 3.5 cm (1 3/8 inches) ID, with a width of about 2.5 cm (1 inch). The 207 bearing is a radial bearing and is designed for little thrust loading. There are nine 1.1 cm (7/16 inch) diameter balls in each bearing.

The test conditions are shown below:

*Stress: 3.65 GPa (530 ksi),  $S_{max}$*   
*Speed: 3000 rpm*  
*Lubricant: DTE Extra Heavy oil*

### 8.1 BASELINE DEFINITION

The format of the test is a sudden death test. Twenty-four bearings are used for each test. The bearings are tested in four groups of six bearings. Each group of six bearings is run until one of the bearings fails, then all six are removed from testing. This procedure is repeated for each of the four groups of bearings. Weibull analysis is then used on the data and an  $L_{10}$  life is calculated. Two comparisons can be made from a given 207 bearing test. First, the test  $L_{10}$  life can be compared to the theoretically calculated ABMA  $L_{10}$  life, which is based solely on the bearing geometry, maximum Hertzian contact stress, speed and lubrication. Second, the test  $L_{10}$  can also be compared to other test  $L_{10}$  lives to yield a comparison to other specific tests. Much of the Torrington Company's previous test data were produced at the following test conditions:

*Radial Load - 10,900 N (2450 pounds)*  
*Speed - 3000 rpm*  
*Lubrication - DTE Extra Heavy Oil*



In all steel bearings these conditions produce a maximum rolling contact stress of about 3.65 GPa (530 ksi). Weibull Analysis is used to interpret the results. The test  $L_{10}$  is compared to the ABMA calculated  $L_{10}$  and generally the ratio of the test  $L_{10}$  and the ABMA  $L_{10}$  is used to describe a test. The ABMA calculated  $L_{10}$  life for these conditions is 33.0 hours, which means at 33.0 hours, 10 percent of the population has failed.

The above discussion describes all-steel bearings. The modulus of elasticity of silicon nitride is different than steel. The modulus affects the maximum Hertzian rolling contact stress in the contact zone. The higher modulus of silicon nitride results in a higher Hertzian rolling contact stress for the same load applied to the bearing. Therefore, at the above described conditions the maximum contact stress for a bearing with silicon nitride balls would be much higher than the 3.65 GPa (530 ksi) for an all-steel bearing.

This makes direct comparison of all-steel bearings versus bearings with steel rings and silicon nitride balls a challenge. There are two avenues which can be evaluated. The first method would be based on the fact that rolling contact fatigue life is based mainly on the maximum rolling contact stress in the contact area. For this comparison, the load on the bearings for this contract would have to be lowered such that a maximum rolling contact stress of 3.65 GPa (530 ksi) is produced in the rolling contact zone (the same test stress as all-steel bearings).

The second school of thought says that the stress in the rolling contact zone is basically of no concern and the bearings should be tested at the same load, as design and application engineers are interested in what loads can be applied. Their perspective is that an all-steel bearing run at a certain set of conditions and a bearing with the same envelope size containing silicon nitride balls should perform equally as well if not better than the all steel bearings. For this comparison, the test conditions would remain equal to past 207 bearing tests.

The decision was made to reduce the load on the hybrid bearings and test at 3.65 GPa (530 ksi). 3.65 GPa (530 ksi) is a very high stress used in bearing testing to provide failure data. It is much higher than application stresses. An equivalent load on a hybrid bearing would cause an extremely high contact stress of 4.21 GPa (611 ksi).

The test conditions which produced the same rolling contact stress in the hybrid bearings were determined to be:

*Radial Load - 7050 N (1600 pounds)*

*Speed - 3000 rpm*

*Lubrication - DTE Extra Heavy Oil.*

It is important to note that the raceway curvature was not used to alter the rolling contact stress. All-steel test bearings and the hybrid test bearings for this contract had the same raceway curvature of 52%. The raceway curvature can be used to alter the contact stress. By opening up the raceway curvature (making the ball fit "loose" in the raceway) the stress can be raised. Conversely, the contact stress can be lowered by closing down the raceway curvature (making the ball fit "tighter" in the raceway). The "tighter" raceway provides a larger contact area, thereby reducing the rolling contact stress. The disadvantage of using the raceway curvature to alter the rolling contact stress is the raceway curvature dictates the ease of which lubricant can get into the contact area. "Tight" raceways can limit the amount of lubricant which enters the contact area, thereby reducing life.

## **8.2 SUMMARY OF FATIGUE TESTING, 207 RADIAL BEARINGS**

The following two sections summarize the 207 bearing testing for each inner ring steel type. The first section will discuss the nitrided M50 inner rings and the second section will discuss the nitrided M50 NiL inner rings.

### **8.2.1 SUMMARY OF FATIGUE TESTING, M50 STEEL**

As previously described, the 207 test is a sudden death test. The test results are analyzed and the test  $L_{10}$  is calculated using Weibull analysis. The test  $L_{10}$  life is then compared to a calculated  $L_{10}$  life to determine how the bearings performed relative to other groups of test bearings.

The results of the hybrid nitrided M50 207 bearing test are shown in Table 8.2.1-1.

**Table 8.2.1-1**  
**Hybrid Nitrided M50 207 Bearing Test Results**  
**(hours)**

<b>Group 1</b>	<b>2008 - Suspended</b>
<b>Group 2</b>	<b>1486 - Failed Inner Ring</b>
<b>Group 3</b>	<b>376 - Failed Inner Ring</b>
<b>Group 4</b>	<b>62 - Failed Ball/1384 - Failed Ball</b>

The results through the testing of group 3 were very good. The earliest failure was an inner ring at a time about 11 times the calculated  $L_{10}$  life. Group 4 was put on test and a ball failure occurred at 62 hours, which is still two times the calculated  $L_{10}$  life. But recent baseline testing of many different lots of 207 bearings show a 62-hour bearing failure to be shorter than most bearing failures in this test. The decision was made that another bearing would be replaced in the group and the group would continue to run. The advantage of this was twofold. First, more silicon nitride balls would be run on test, giving more fatigue data on the silicon nitride. And second, another inner ring would be run, hopefully producing an inner ring failure, since that is the test specimen in this test. After 1384 hours, one of the original five bearings had a ball failure. The data were analyzed using Weibull analysis. The test  $L_{10}$  life was 353 hours. The calculated  $L_{10}$  is 33 hours, producing a ratio of test  $L_{10}$  to calculated  $L_{10}$  of 10.7.

### **8.2.2 SUMMARY OF 207 FATIGUE TESTING, M50 NiL STEEL**

Similar to the M50 207 test, some relatively early ball failures lead to replacing the early failures with other bearings to improve the confidence in the overall test of the hybrid bearings.

The results of the hybrid nitrided M50 NiL 207 bearing test are shown below in Table 8.2.2-1.

**Table 8.2.2-1**  
**Hybrid Nitrided M50 NiL 207 Bearing Test Results**  
**(hours)**

<b>Group 1</b>	<b>87 - Failed Ball/172 - Failed Ball</b>
<b>Group 2</b>	<b>2002 - Suspended</b>
<b>Group 3</b>	<b>115 - Failed Ball/2004 - Suspended</b>
<b>Group 4</b>	<b>1194 - Failed Inner Ring</b>

The results showed a ball failure at 87 hours in the first group tested. This bearing was replaced with another bearing. One of the original bearings in group 1 then had another ball failure at 172 hours. Group 2 was then put on test and ran to suspension at 2002 hours. There was also a ball failure at 115 hours in group 3 and this bearing was also replaced with another bearing to produce more fatigue information about the fatigue behavior of the nitrided steel rings. Group 3 then ran to suspension at 2004 hours. Group 4 produced a inner ring failure at 1194 hours.

The data were analyzed using Weibull analysis which calculated a test  $L_{10}$  life of 380 hours. The calculated  $L_{10}$  life is 33 hours, which produces a ratio of the test  $L_{10}$  life to the calculated  $L_{10}$  life of 11.5.

### **8.3 FAILURE ANALYSIS, 207 BEARINGS**

Routinely, bearings are examined after failure for the cause or origin of the failed component. Spalling in the failed component can either be initiated subsurface or directly on the surface. Based on past failure analysis of test bearings, surface initiated failures occur more frequently than subsurface initiated failures. Surface initiated spalling of bearing rings is identified by a surface type defect generally at the nose of the spall (the leading edge of the spall, relative to the rolling direction of the balls). The surface type defects may be dents, grinding furrows, or microspalling in the contact zone of the bearing ring raceways. Spalling due to subsurface defects is more difficult to positively identify. If no clear surface defect is found, many times it is assumed that the spalling was subsurface initiated. This may or may not be the case because spalling **can sometimes travel**

backwards relative to the rolling direction of the balls, spalling out the surface initiated area of the raceway.

Ball failures are much more difficult to positively identify as to whether the initiation point on the ball occurred at the surface or subsurface. The random rotational action of the balls in the 207 test always spalls out relatively large amounts of material. The direction of the fatigue cracking can generally be seen back to an area where fatigue started, but evidence of a surface initiated ball spall is gone.

The failed 207 hybrid bearings examined from this testing revealed only one clear surface initiated inner ring spall. Figures 8.3-1 and 8.3-2 show the spall on the nitrided M50 207 bearing which failed at 1486 hours. The rolling direction of the balls is left to right in both figures. Figure 8.3-1 shows the whole spalled region of the raceway; note the symmetrical nature of this spall. The nose of the spall is on the left side of the photograph, and the initiation point can clearly be seen as an area of microspalling. Figure 8.3-2 shows this area of microspalling at a higher magnification.

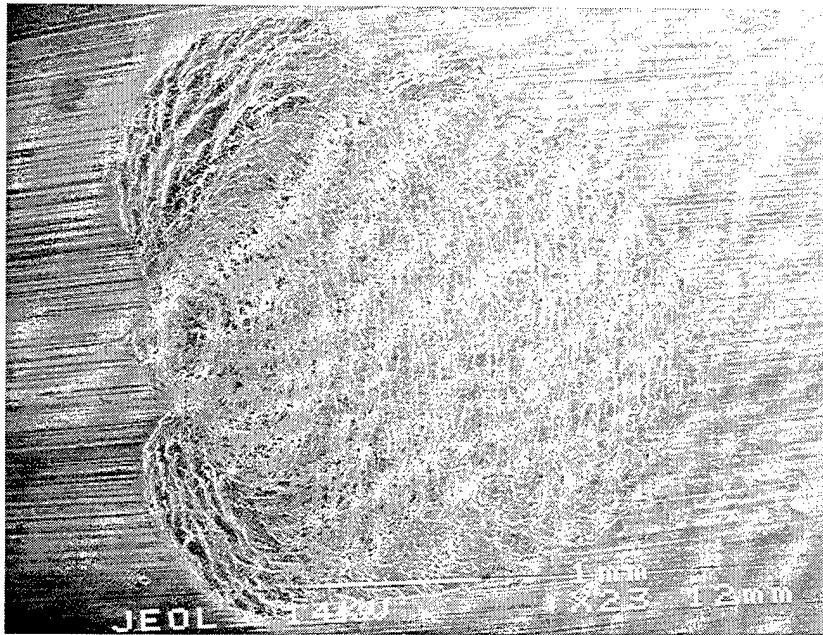


Figure 8.3-1, SEM photograph, 23X  
Spalled raceway, 1486 hours, Nitrided M50 Steel Inner Ring

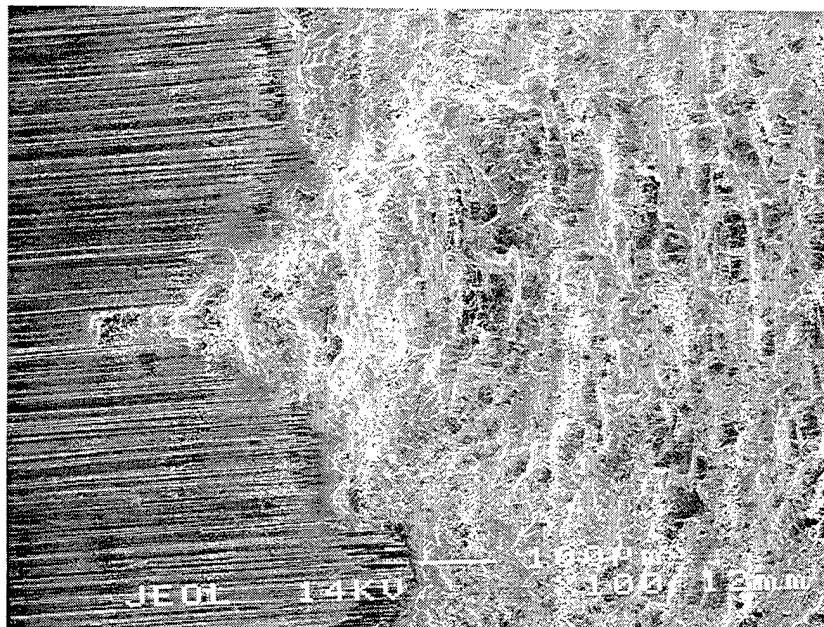


Figure 8.3-2, SEM photograph, 100X  
Microspalling at nose of spall of Figure 8.3-1

The other failed nitrided M50 steel inner ring did not have an obvious surface initiation point to the spall. This failure may have been subsurface initiated. Figure 8.3-3 shows the spall. The rolling direction of the balls is from left to right.

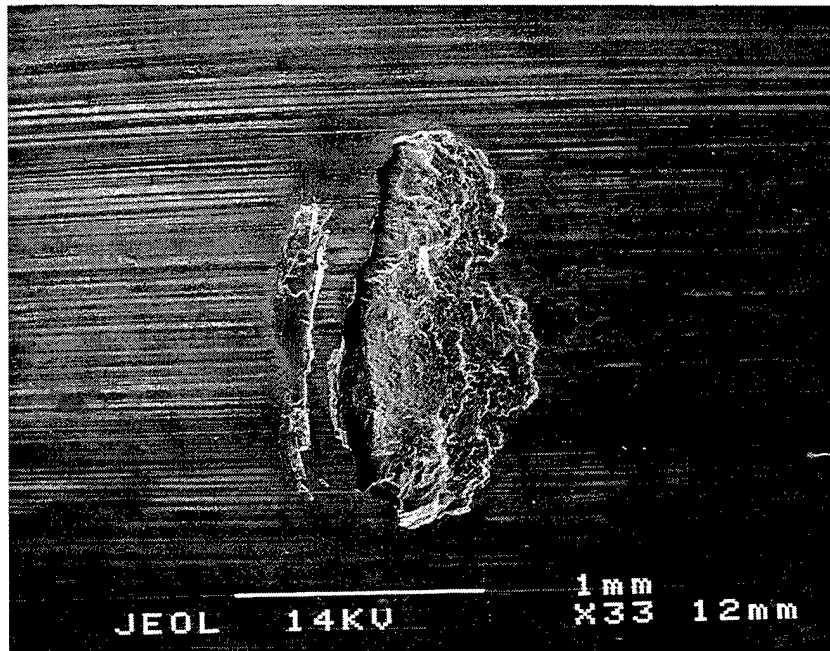


Figure 8.3-3, SEM photograph, 33X  
Spalled raceway, 376 hours, Nitrided M50 Steel Inner Ring

The nitrided M50 NiL inner ring failure also did not have a clear surface initiated failure. This spall is shown in Figures 8.3-4 and 8.3-5. The ball rolling direction is again from the left to the right. This spall shows the most evidence of being subsurface initiated. Note the major crack running vertically through the photograph; this crack runs across the raceway, perpendicular to the rolling direction. Also note the fatigue crack growth away from the crack both with and against the rolling direction of the balls.

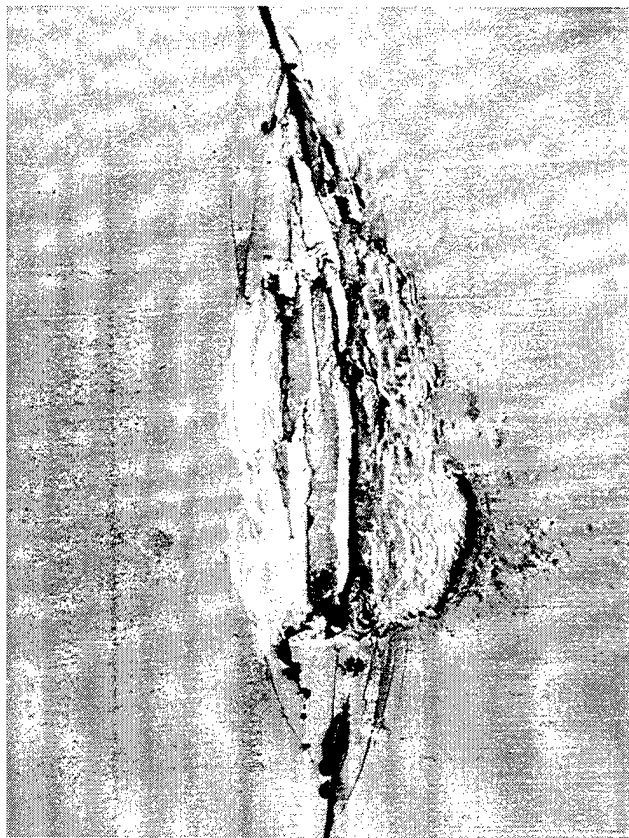


Figure 8.3-4, SEM photograph, 18X  
Spalled raceway, 1194 hours, Nitrided M50 NiL Steel Inner Ring



Figure 8.3-5, SEM photograph, 50X  
Closer view of evidence of fatigue crack propagation with and against ball rolling direction



Closer view of evidence of fatigue crack propagation with and against ball rolling direction

As stated earlier in this section, it is difficult to determine the exact cause and location of the initiation point in the spalling in ball failures. Generally the initiation point of a ball failure is near the center of the spalled region. This is due to the random rotational action of the balls during the operation of a radial bearing. Several SEM photographs have been included to show some of the ball failures. The approximate initiation points have been marked using arrows, and in all cases fatigue striations can clearly be seen radiating away from the initiation areas. Figures 8.3-6, 8.3-7, and 8.3-8 show three spalled regions on some of the silicon nitride balls. Figures 8.3-7 and 8.3-8 were taken by Dr. J. J. Mecholsky, University of Florida, Dept. of Materials Science and Engineering. Note in Figure 8.3-8 that there may have been two spall fatigue origins in this spall.



Figure 8.3-6, SEM photograph, 17X  
Spalled ball, 115 hours, Hybrid M50 NiL Bearing

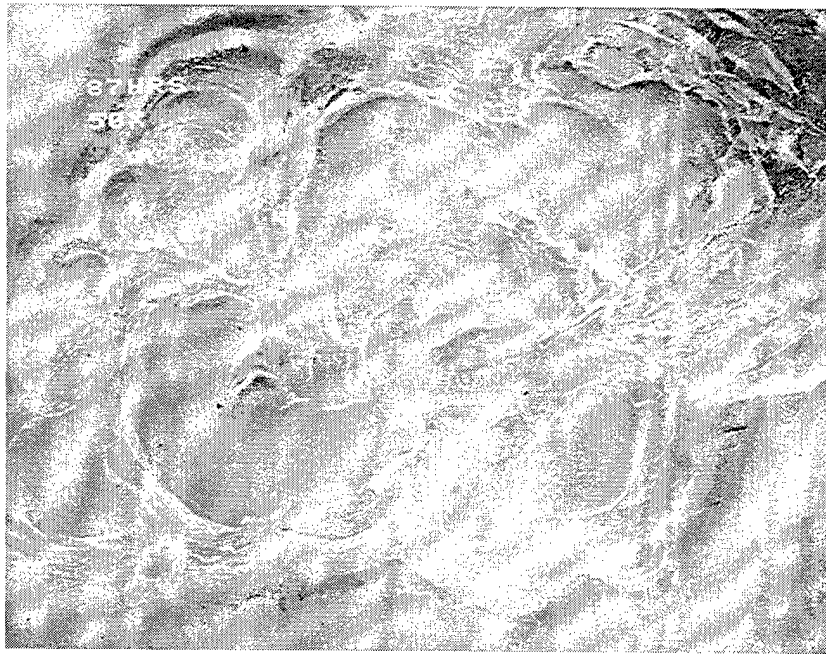


Figure 8.3-7, SEM photograph, 50X (Mecholsky)  
Spalled ball, 87 hours, Hybrid M50 NiL Bearing



Figure 8.3-8, SEM photograph, 35X (Mecholsky)  
Spalled ball, 172 hours, Hybrid M50 NiL Bearing

## 8.4 207 BEARING TEST CONCLUSIONS

The  $L_{10}$  lives of the hybrid bearings in this test were 353 and 380 hours for M50 and M50 NiL, respectively, with equivalent life factors of 10.7 and 11.5. These results are entirely satisfactory but not extraordinary. Life factors of 10 to 12 are common for good quality standard bearings in this test, however, the best steels combined with the best raceway surface finishes have had much longer lives.

Ball failures prevented the life results of this test from being exceptionally high. The few early ball failures experienced here are consistent with other testing of silicon nitride balls at the high stress levels of bearing life testing. This needs to be kept in perspective. Many thousands of silicon nitride balls have been used in bearing applications with no failure problems. Normal bearing applications operate at much lower contact stress levels, typically 690 to 2050 MPa (100 to 300 ksi). Apparently a very small percentage of silicon nitride balls have small flaws, too small to identify in our work, that are of a critical size to initiate failure at high contact stresses of bearing life tests, but are below the threshold size to initiate failure at application stresses.

Nitrided ring failures were too few (only two) to make a valid statistical estimate of the lives of the bearing raceways. Indications are that without the ball failures the life factors would be very much higher.

The high 3.65 GPa (530 ksi) maximum contact stress of the bearing life test and to a much greater extent the very high 4.8 - 6.2 GPa (700-900 ksi) used for various RCF rig tests are capable of failing materials that may perform well in service. For example, M50 steel which has been adopted for many important aerospace applications often gives unfavorable results on rig tests. The carbides in M50 act as significant stress raisers for crack initiation at very high stresses, but it is obvious from the great number of M50 bearings in service for many years that M50 carbides do not have an adverse effect under normal operating conditions. High stress RCF rigs are for screening materials and heat treatments. Those that do well have merit and are worthy of further investigation with full scale bearing testing. Those that do not are not necessarily unsatisfactory; and results must

be considered in this context. High stress bearing life tests are usually run to produce data that can be used by bearing engineers in their life predictions. The authors believe that tests simulating applications conditions, as in the 208 test described in the next section (9.0), are the preferred way to evaluate materials and predict what bearing performance will be.

## **9.0 ROLLING CONTACT EVALUATION, 40 MM BORE 208 THRUST BEARINGS**

The 208 bearing test was designed to test materials and processes under the conditions of gas turbine engine main shaft bearings. The bearing is an angular contact design manufactured with the dimensional tolerances and quality control procedures of main shaft bearings. The test is run at 10,000 rpm under thrust loads that produce maximum contact stresses up to 2.62 GPa (380 ksi). The lubricating oil corresponds to MIL-L-7808J and the test temperature is 150°C (300°F), giving a calculated elastohydrodynamic (EHD) film thickness of 0.076  $\mu\text{m}$  (3  $\mu\text{in}$ ).

The test procedure used in the present project was developed for Air Force Contract F33615-84-2430, Improved Fatigue Life Bearing Development (5). In the past, efforts to extend bearing life had emphasized improvements in surface roughness and topography and maintenance of clean oil systems. One result of this was that the M50 steel bearing in common use had an  $L_{10}$  life well in excess of 2000 hours in the clean and controlled conditions of the 208 test, making testing time to demonstrate further improvement prohibitive. The approach was taken that actual failures in service take place when the oils and surfaces are not ideal, and life improvement comes from resistance to propagation from surface defects. From this the present test procedure was adopted. The bearings are first run for 15 minutes in oil contaminated with 2.5 ppm of 20  $\mu\text{m}$  (786  $\mu\text{in}$ ) aluminum oxide particles. They are then disassembled, washed, examined for surface damage, reassembled, and run in different rigs with clean oil. Bearings are run for 24 hours, taken apart, reinspected for surface condition, and put back on test. Reinspection takes place again after 250 hours, after which the bearings are run to failure or to 2000 hour suspension time.

### **9.1 BASELINE TESTS AND CONTACT STRESSING**

The results for the hybrid bearings were compared to the results of previous tests of all- steel bearings. The all-steel bearings were M50 steel, M50 NiL, and M50 NiL with thin dense chromium (TDC) coating. The latter was the Improved Fatigue Life Development of the Air Force contract work (5). Low alloy steels such as 52100 are not run on this 150°C (300°F) test. The hybrid bearings were run under a thrust load of 7500 N (1700 lbs) to have a maximum contact

stress of 2.62 GPa (380 ksi), the highest stress used for all steel bearings. All-steel bearings have 11,880 N (2700 lbs) thrust load to produce 2.62 GPa (380 ksi) contact stress. We were fortunate in also having results for all-steel bearings tested under 7500 N (1700 lbs) thrust. We were thus able to compare the hybrid and all-steel bearings under both equivalent stress and equivalent load conditions. Table 9.1-1 summarizes this comparison.

<u>Past Steel</u> <u>Bearings</u>	<u>Nitrided Hybrid</u> <u>Bearings</u>	<u>Past Steel</u> <u>Bearings</u>
7500 N -----	7500 N	11,880 N
2.28 GPa	2.62 Gpa -----	2.62 GPa
1700 Lbs.-----	1700 lbs.	2700 lbs.
330 ksi	380 ksi -----	380 ksi

Table 9.1-1  
Summary of Stress/Load Baseline Comparison, 208 Bearing Test

## 9.2 SUMMARY OF FATIGUE TESTING, 208 BEARINGS

The discussion of the results and analysis of the 208 bearing testing is in two sections. The first compares results for equivalent stressing; the second for equivalent loading. Each section will discuss both nitrided M50 and nitrided M50 NiL steel.

### 9.2.1 DISCUSSION OF EQUAL STRESS TESTING

The two hybrid bearing tests completed under this contract were compared to two past tests done at approximately the same maximum Hertzian contact stress of about 380 ksi. Past testing included all M50 steel components, and M50 NiL races with TDC coating coupled with M50 steel balls. The results are listed in Table 9.2.1-1 and summarized using Weibull Analysis in Table 9.2.1-2

Table 9.2.1-1  
Summary of Results for 208 Bearing Tests, Hours  
Maximum Contact Stress 2.62 GPa (380 ksi)

<i>Hybrid Nitrided M50</i>	<i>Hybrid Nitrided M50 NiL</i>	<i>M50</i>	<i>M50 NiL With TDC</i>
2034 (S)	797 (FI)	68 (FI)	434 (FI)
2034 (S)	1299 (FI)	147 (FI)	486 (FI)
2038 (S)	1882 (FI)	310 (FI)	722 (FI)
2038 (S)	2001 (S)	316 (FI)	695 (FB)
2020 (S)	2016 (S)	334 (FI)	1100 (FB)
2020 (S)	2022 (S)	746 (FI)	1504 (S)
2006 (S)	2032 (S)	1127 (FI)	1535 (S)
2038 (S)	2032 (S)	1500 (S)	1535 (S)
2004 (S)	2001 (S)	1500 (S)	1544 (S)
2004 (S)	2174 (S)	1500 (S)	1587 (S)
			1684 (S)

(FI) Failed Inner Ring  
(FB) Failed Ball  
(S) Suspended Bearing

Table 9.2.1-2  
Summary of Weibull Analysis for 208 Bearing Tests  
Maximum Contact Stress 2.62 GPa (380 ksi)

<i>Bearing Material</i>	<i>L<sub>10</sub>, hours</i>	<i>90% Lower Confidence L<sub>10</sub>, hours</i>	<i>Weibull Slope</i>
<i>Hybrid Nitrided M50</i>	<i>*</i> —	1187	1.5 (estimated)
<i>Hybrid Nitrided M50 NiL</i>	998	444	1.72
<i>M50 NiL &amp; TDC Rings (M50 Balls)</i>	478	254	2.47
<i>M50</i>	93	25	1.02

\* No Failures, therefore an L<sub>10</sub> life could not be determined

There were no hybrid nitrided M50 failures; therefore, the 90% confidence band (L90CB) was used to compare test results. There were three hybrid nitrided M50 NiL bearing failures, so that data did allow a calculation of an  $L_{10}$  life, which can be compared to the previous tests  $L_{10}$  lives. Note the L90CB of the hybrid M50 bearings is four times that value for the M50 NiL & TDC bearings. This is very significant because the development of M50 NiL with TDC coated raceways was itself a step in improving the reliability of high performance bearings. M50 steel has long been used in the most demanding high performance applications where fracture toughness was not critical. M50 has worked very well in these applications. Carburized M50 NiL with TDC coated raceways was the next development, providing increased fatigue life along with fracture toughness. The bearing testing under this contract has now shown even further improvements in fatigue life are possible with both through hardening and fracture tough, carburizing steels.

### **9.2.2 DISCUSSION OF EQUAL LOAD TESTING**

The two hybrid bearing tests completed under this contract were compared to three past tests performed at approximately the same load, 7500 N (1700 lbs) thrust. The higher Modulus of Elasticity of the NBD-200 silicon nitride results in the hybrid bearings having a higher maximum contact stress in the rolling contact zone. The maximum contact stress in the hybrid bearings was 2.62 GPa (380 ksi); the maximum contact stress in the all-steel bearing tests was 2.27 GPa (330 ksi). The results are listed in Table 9.2.2-1 and summarized using Weibull Analysis in Table 9.2.2-2.



Table 9.2.2-1  
Summary of Results for 208 Bearing Tests, Hours  
Approximately 7500 N (1700 Pounds) Thrust Load

<i>Hybrid Nitrided M50</i>	<i>Hybrid Nitrided M50 NiL</i>	<i>M50</i>	<i>M50 NiL</i>	<i>M50 NiL With TDC</i>
2034 (S)	797 (FI)	429 (FI)	270 (FI)	374 (FI)
2034 (S)	1299 (FI)	445 (FI)	317 (FI)	901 (FI)
2038 (S)	1882 (FI)	502 (FI)	326 (FI)	1082 (FI)
2038 (S)	2001 (S)	635 (FI)	677 (FI)	2213 (S)
2020 (S)	2016 (S)	666 (FI)	779 (FI)	2213 (S)
2020 (S)	2022 (S)	1390 (FI)	998 (FI)	2278 (S)
2006 (S)	2032 (S)	1916 (FI)	1372 (FI)	2278 (S)
2038 (S)	2032 (S)	2010 (FI)	1500 (FI)	2395 (S)
2004 (S)	2001 (S)	2095 (S)	2715 (S)	3571 (S)
2004 (S)	2174 (S)	2095 (S)	2890 (S)	3571 (S)

(FI) Failed Inner Ring

(FB) Failed Ball

(S) Suspended Bearing

Table 9.2.2-2  
Summary of Weibull Analysis for 208 Bearing Tests  
Approximately 7500 N (1700 Pounds) Thrust Load

<i>Bearing Material</i>	<i>L<sub>10</sub>, hours</i>	<i>90% Lower Confidence L<sub>10</sub>, hours</i>	<i>Weibull Slope</i>
<i>Hybrid Nitrided M50</i>	- *	1187	1.5 (estimate)
<i>Hybrid Nitrided M50 NiL</i>	998	444	1.72
<i>M50</i>	368	172	1.73
<i>M50 NiL (M50 Balls)</i>	232	112	1.53
<i>M50 NiL &amp; TDC Rings (M50 Balls)</i>	533	152	1.33

\* No Failures, therefore an L<sub>10</sub> life could not be determined

As with the equal stress comparison, the lower 90% confidence  $L_{10}$  must be compared between the different groups of bearings because of the excellent performance of the hybrid nitrided M50 steel bearings. The hybrid nitrided M50 bearings outperformed the rest of the bearing tests by a wide margin. The hybrid nitrided M50 NiL bearings increased the rolling contact fatigue life by about a factor of three over the past three bearing tests of all steel bearings. This is very significant to the future of rolling element bearings because the hybrid bearings tested as part of this contract well outperformed past all-steel bearings at the same loading conditions, while at the same time withstanding the higher contact stress resulting from the silicon nitride balls. This test suggests that perhaps in the future, hybrid bearings with nitrided steel bearing rings may be able to be either designed smaller, reducing necessary space and weight requirements, or bearing positions can be loaded higher with no sacrifice in useful bearing life. The two hybrid nitrided steel bearing tests were the best performing sets of bearings in the history of The Torrington Company's contaminated 208 bearing test.

### **9.3 FAILURE ANALYSIS, 208 BEARINGS**

Aluminum oxide is a very hard, abrasive material, and when mixed into the oil in very small concentrations has a very large effect on the rolling contact surfaces. Past testing has shown that after only 15 minutes running in the contaminated oil, the steel raceways and steel balls become pitted over the entire contact area within the bearing.

The test procedure for the 208 bearings includes periodic stops in the bearing test for inspection of the raceways to determine the effect of the pitted raceways over time. The failure analysis for these bearings runs parallel along with the testing.

The first step is to examine the bearings directly after the contamination run. The first observation which was made, after the first few contaminated bearings were examined, was that the NBD-200 silicon nitride balls were completely unharmed by the 15-minute run in contaminated oil. It was expected they would resist damage better than the balls from past all- steel tests, but not

come away with no damage at all. The nitrided steel races did show pitting resulting from the 15-minute contamination run because the aluminum oxide is harder than the nitrided steel. Figure 9.3-1 and 9.3-2 show an optical photograph of the raceway surface of a nitrided M50 and a nitrided M50 NiL raceway after the 15-minute contamination run. The photos are of an "average" area.



Figure 9.3-1  
Optical photograph of nitrided M50 raceway after 15 minute contamination, 100X



Figure 9.3-2

Optical photograph of nitrided M50 NiL raceway after 15 minute contamination, 100X

After the 15 minutes running in contaminated oil, the bearings were then carefully cleaned, removing all aluminum oxide, and run under the same conditions in clean oil. After 24 hours, they were stopped, taken apart and examined again for any signs of fatigue propagation resulting from the contamination pits. In all cases for both nitrided steels, there were no signs of any form of propagation. Figures 9.3-3 and 9.3-4 show typical raceway surfaces for M50 and M50 NiL, respectively. Note that these are not the same exact locations on the raceway as the photographs in Figures 9.3-1 and 9.3-2. There were no major differences in the characteristics of the contamination damage through this point in the bearing tests.



Figure 9.3-3  
Optical photograph of nitrided M50 raceway after 15 minute contamination  
and 24 hours running in clean oil, 100X

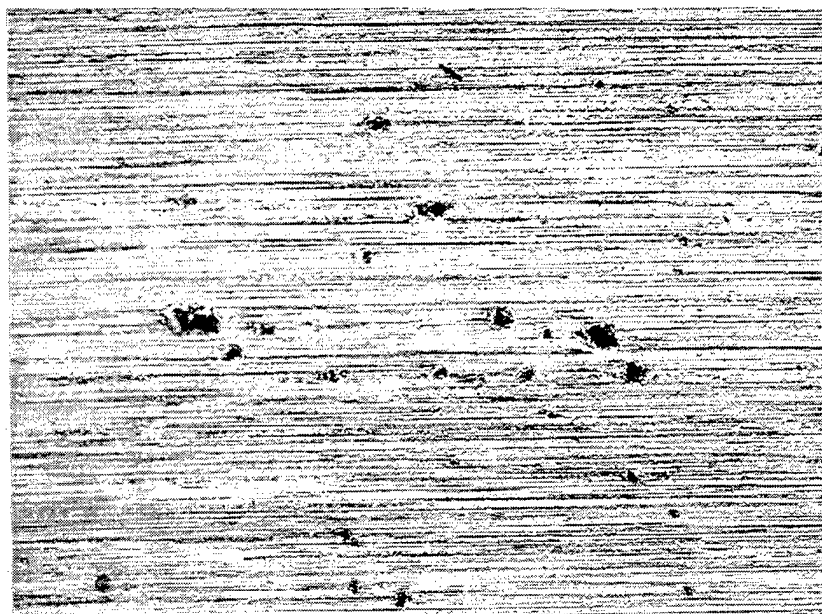


Figure 9.3-4  
Optical photograph of nitrided M50 NiL raceway after 15 minute contamination  
and 24 hours running in clean oil, 100X

The bearings were then run for about 200 hours and stopped and examined for a final time before they are allowed to run to failure or suspension. Figures 9.3-5 and 9.3-6 show the raceway surfaces of M50 and M50 NiL respectively. Again, these are not the same exact areas as the previous photos, but it can be clearly seen that there are basically no changes going on in the vast majority of the pits caused by the original contamination run.

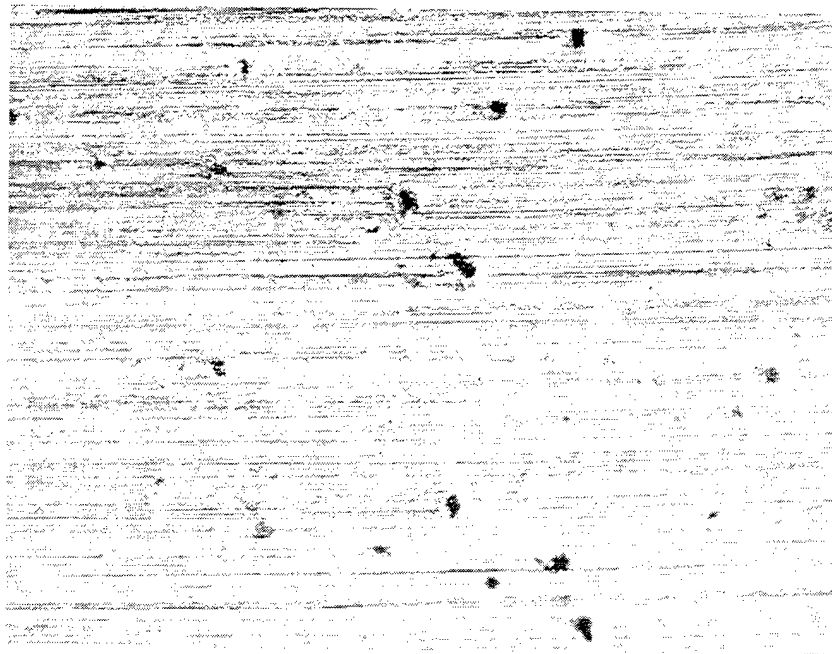


Figure 9.3-5  
Optical photograph of nitrided M50 raceway after 15 minute contamination  
and 208 hours running in clean oil, 100X

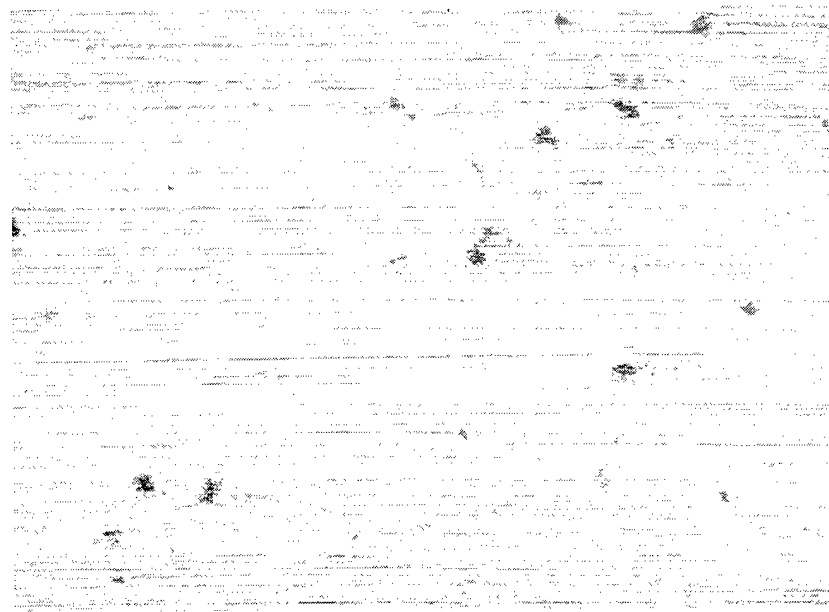


Figure 9.3-6  
Optical photograph of nitrided M50 NiL raceway after 15 minute contamination  
and 212 hours running in clean oil, 100X

After failure, the bearings were examined for the origin of the spalling fatigue. The pits in the raceway surface from aluminum oxide contamination usually serve as the initiation points for the spalling to develop. This was the case with two out of the three 208 bearing failures. All the bearings which failed were manufactured from nitrided M50 NiL steel. No nitrided M50 steel bearings failed; every bearing test was suspended out at 2000 hours. The earliest 208 bearing failure occurred at 797 hours. The spall is shown in Figure 9.3-7. The rolling direction of the balls is from the left to the right. The spall is very consistent with past experience in 208 bearing failures. Spalling in the 208 bearing test is initiated on the raceway surface and continues with fatigue crack propagation in the rolling direction of the balls. The spall shown in Figure 9.3-7 was initiated on the very left side (at the point or nose) of the photograph, and grew towards the right side of the photograph. Figure 9.3-8 shows a closer view of the nose of the spall in Figure 9.3-7. The arrow shows what is an original contamination pit. The spalling is initiated and propagates from just behind surface defects.

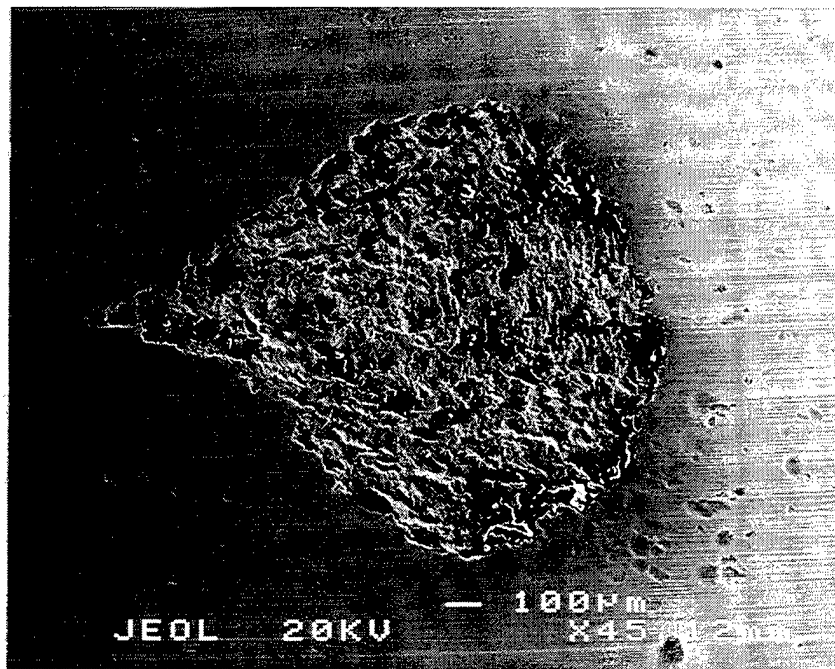


Figure 9.3-7

SEM photograph showing raceway spall of nitrided M50 NiL 208 inner ring after failure at 797 hours, ball rolling direction is from the left to the right, 45X

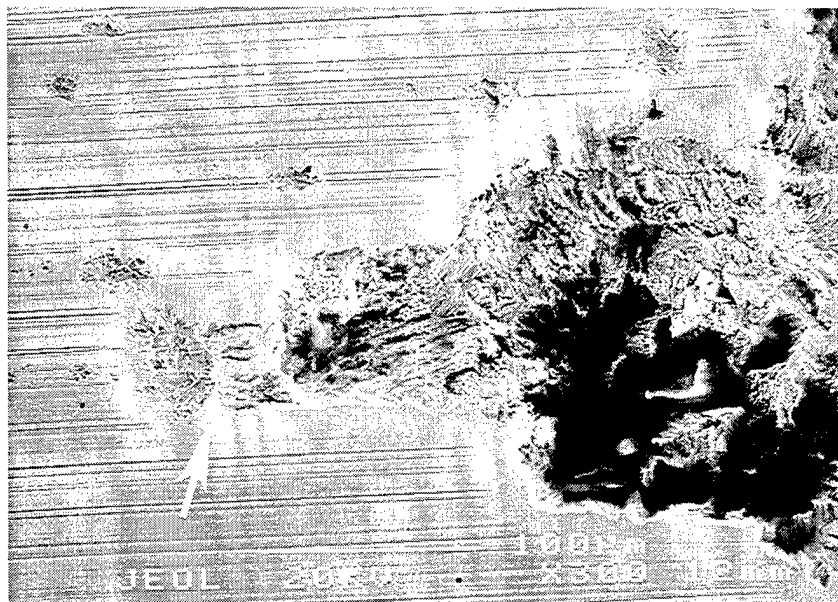


Figure 9.3-8

SEM photograph showing the nose of the spall, note arrow showing an original contamination pit and subsequent spall propagation in the ball rolling direction, 300X



Figures 9.3-9 and 9.3-10 show the same type of pictures of the spall as the previous two Figures, 9.3-7 and 9.3-8. Again this spall has propagated from an initial defect from the contamination run. Figure 9.3-9 shows the whole spall. The rolling direction of the balls in this picture is from the right to the left. Figure 9.3-10 shows the triangular shaped pit from which the spall propagated. The first two failed 208 bearings clearly had surface initiated spalling in the raceways. This mode of failure is the normal mode for the contaminated 208 bearing test.

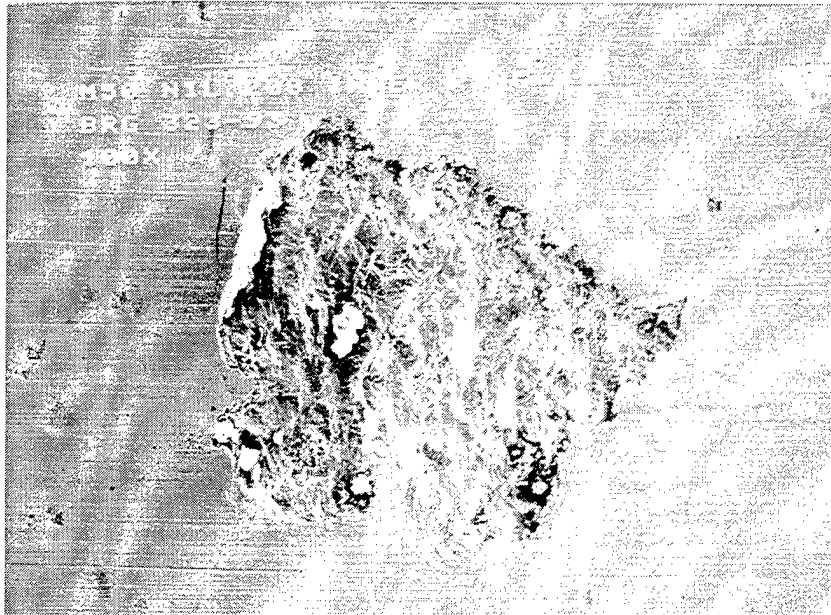


Figure 9.3-9

SEM Photograph showing raceway spall of nitrided M50 NiL 208 inner ring after failure at 1299.8 hours, ball rolling direction is from the right to the left, 100X



Figure 9.3-10

SEM photograph showing the nose of the spall; note arrow showing the original contamination pit and subsequent spall propagation in the ball rolling direction, 500X

The final 208 bearing failure was a nitrided M50 NiL inner ring which failed at 1882.1 hours. Unlike the other two bearing failures already discussed, this failure did not seem to be directly related to the contamination pits. There was no clear initiation point. Figure 9.3-11 shows the whole spall. Figure 9.3-12 shows the nose of the spall. The rolling direction for both figures is left to right. Figure 9.3-12 does not have any shallow surface defect at the beginning of the spall. This fatigue failure may have been subsurface initiated, but this is impossible to prove.

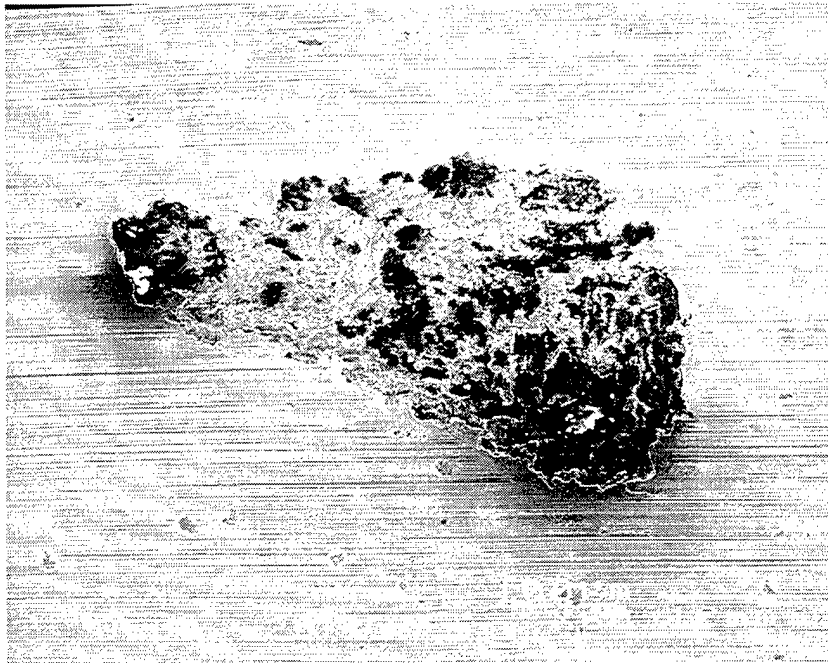


Figure 9.3-11  
SEM photograph showing raceway spall of nitrided M50 NiL 208 inner ring after failure at 1882.1 hours; ball rolling direction is from the left to the right, 60X

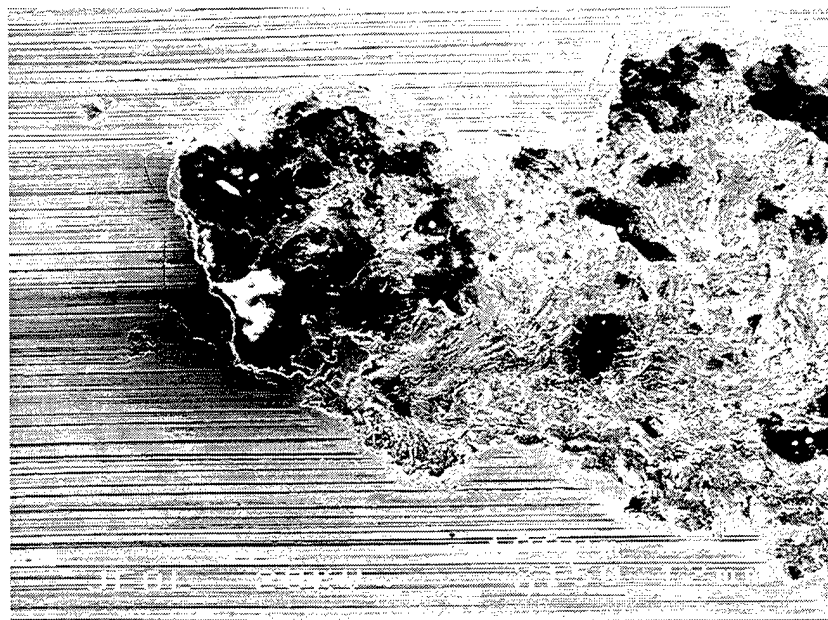


Figure 9.3-12  
SEM photograph showing the nose of the spall; note that there is no shallow contamination pit around the nose of this spall, 150X

The residual stress profiles resulting from nitriding and grinding were examined on both types of steels both after finishing and after the bearing testing was completed. Figure 9.3-13 shows the residual stress profiles obtained on nitrided M50 steel inner rings (207 and 208 size) before and after the bearing testing. Figure 9.3-14 shows the same type of results obtained on nitrided M50 NiL steel. The results for both materials are the same. The compressive residual stress field did not change appreciably during the bearing operation.

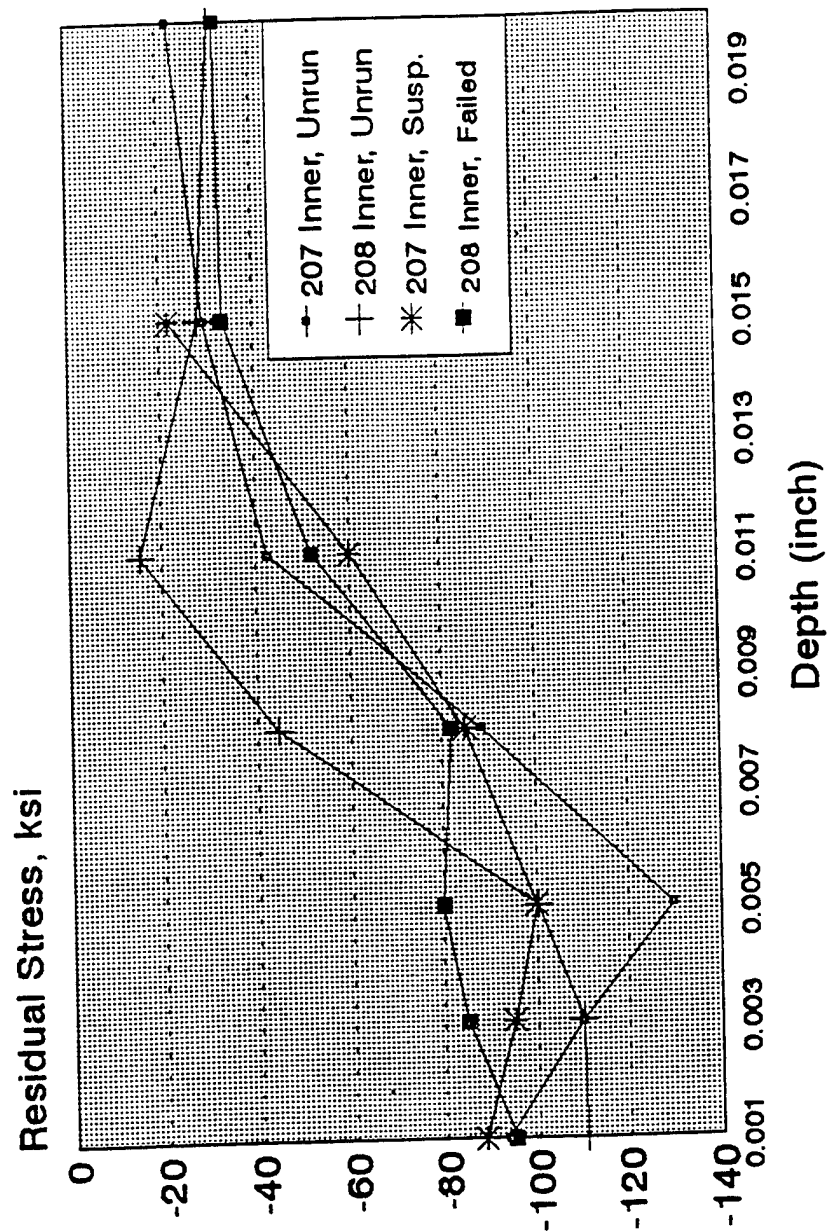
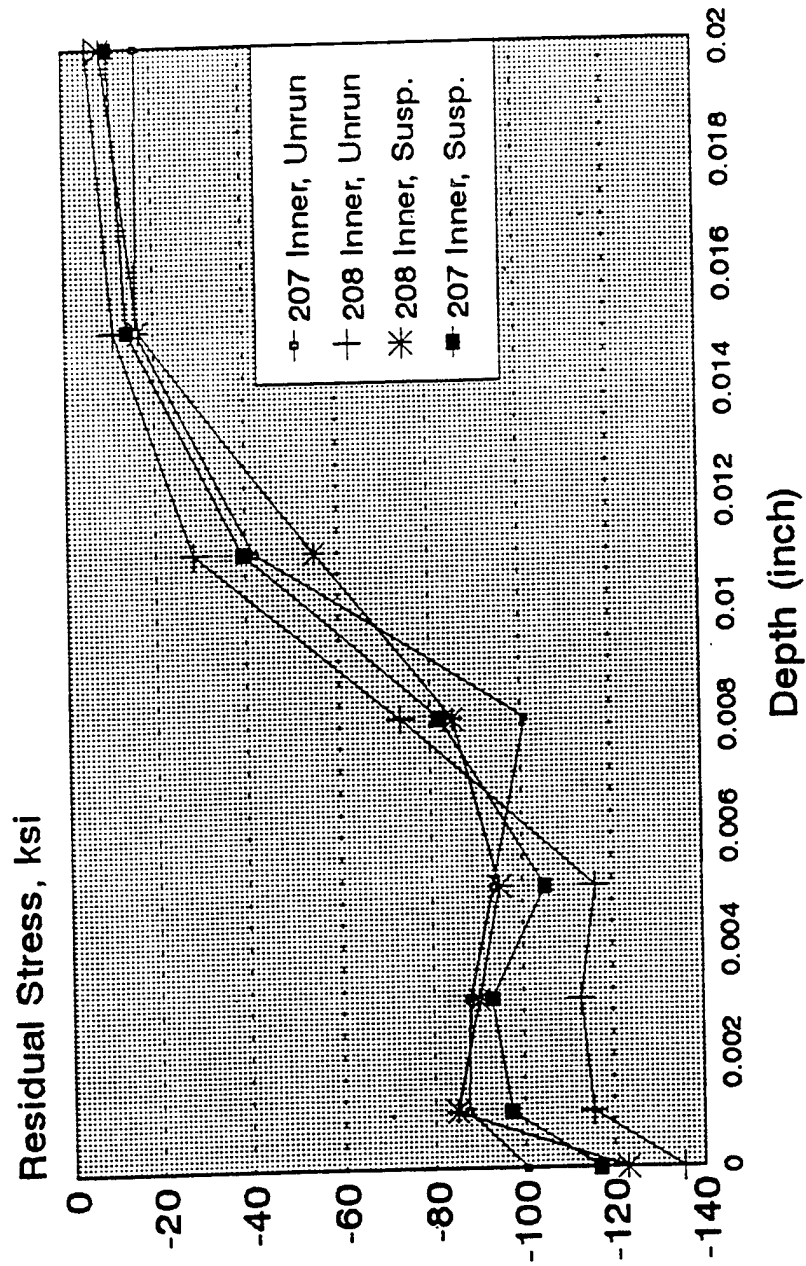


Figure 9.3-13 Residual Stress Profiles, Nitrided M50 Steel  
Unrun 207 and 208 Inner Rings vs Run 207 and 208 Inner Rings



**Figure 9.3-14** Residual Stress Profiles, Nitrided M50 NiL Steel  
Unrun 207 and 208 Inner Rings vs Run 207 and 208 Inner Rings

#### 9.4 208 BEARING TEST CONCLUSIONS AND DISCUSSION

Both the nitrided M50 and M50 NiL hybrid bearings performed extremely well, better than any all-steel bearings run under these conditions. The rolling contact action of silicon nitride balls on the very hard steel surfaces, with high compressive residual stresses in the surface and near surface regions, is very favorable for avoiding failures under poor lubrication or contamination conditions.

The authors consider this a most important test result. With the improvements in bearing steels and processing over several years, subsurface initiated rolling contact fatigue failures are now rare in all types of bearings and applications. Bearing life depends upon surface conditions. The aluminum oxide contamination used in the 208 test was derived from actual conditions found in service. It is, of course, but one of a great many different possible types of contamination-surface interactions. But considering that the contamination particles are very hard and that the test is run with a thin oil film in the boundary lubrication regime, the 208 bearings are tested in very adverse surface conditions. The hybrid bearings that excelled in this test will benefit in other situations where contamination, poor lubrication, or partial EHD conditions limit performance.

The very hard nitrided surfaces did not prevent damage by the even harder aluminum oxide particles. The hybrid bearings ran well in spite of extensive surface damage, indicating resistance to propagation to failure. In tests of all steel bearings described in the references (5,7,8), the failure process was one of initial indentation damage followed by shallow surface peeling from the indentations, eventually leading to macro spalling failures from the peeled areas. The hybrid bearings had no evidence of peeling despite many surface indentations, further evidence of resistance to propagation. The strengthened surfaces and compressive residual stresses in the nitrided raceways are likely causes of resistance to propagation, but we must also consider that silicon nitride balls may be contributing to a more favorable rolling contact action as compared to steel on steel.

The difference between M50 over M50 NiL in these tests could be only statistical or could indicate an advantage for M50. The carbide morphology in M50 gives it better wear resistance. Partial EHD conditions exist, especially at the edges of the damage indentations. Better wear resistance could be of benefit here.

No ball failures occurred in this test. The silicon nitride balls were not damaged by the aluminum oxide because the silicon nitride is harder than the alumina. These suggest that an all silicon nitride bearing could be extraordinarily good when conditions warrant its application.

In conclusion, many hybrid bearings are used today, but mostly in machine tool applications that benefit from the hybrid's cooler operation and higher speed capabilities. These are otherwise benign environments, and the bearings use low alloy 52100 steel rings. The goal of the present project was to improve the bearing rings for more difficult applications, to take advantage of the superior properties of the silicon nitride rolling elements, and to permit wider application of hybrid bearings. The 208 bearing test, with its high speed, higher temperature, thin lubrication film, and contamination conditions, represents many of the conditions for which better bearings are needed. The success of the improved hybrid bearings in this test demonstrates that the goal of this project has been reached.



## 10.0 REFERENCES

1. Braza, J. F., "Rolling Contact and Sliding Wear Performance of Ferritic Nitrocarburized M50 Steel," Tribology Transactions, Vol. 35,1, pp.89-97, 1992.
2. Braza, J. F. and Pearson, P. K., "Tribological and Metallurgical Evaluation of Ferritic Nitrocarburized M50 and M50 NiL Steels," Creative Use of Materials for Rolling Contact Bearings, J.J.C.Hoo, Ed., ASTM STP1195, pp.49-60, 1993.
3. Pearson, P. K. and Dezzani, M. M., "Rolling Contact Fatigue Behavior of Nitrided Surfaces," Advanced Materials and Processes for Aerospace Transmissions, Institute of Mechanical Engineers, London, March 1993.
4. Glover, D., "A Ball-Rod Rolling Contact Fatigue Tester," Rolling Contact Fatigue Testing of Bearing Steels, J.J.C.Hoo, Ed., ASTM STP771, pp. 107-124, 1982.
5. Bamberger, E. N., Averbach, B. L., Pearson, P. K., VanPelt, S., and Price, M. J., Improved Fatigue Life Bearing Development, Final Report for the Period Sept.1984-Dec.1988, AFWL-TR-89-2012, R89AEB259, June 1989.
6. Averbach, B.L., and Bamberger, E.N., "Analysis of Incidents in Aircraft Gas Turbine Bearings," STLE Tribology Trans., Vol.34 (1991), 2, pp.241-247.
7. Averbach, B. L., VanPelt, S. G., Pearson, P. K., and Bamberger, E. N., "Surface Initiated Spalling Fatigue in M50 and M50 NiL Bearings," Lubrication Engineering, Vol.47, 10, p.837-843, 1991.
8. Averbach, B. L., VanPelt, S. G., and Pearson, P. K., "Initiation of Spalling in Aircraft Gas Turbine Bearings," paper 90-2291, AIAA Joint Propulsion Conference, July 1990.